THE ROLE OF CALCIUM IN THE DESTRUCTION OF TARGET CELLS BY CYTOTOXIC T CELLS

by

Nancy L. Allbritton

B.S., Physics
Louisiana State University, Baton Rouge
(1979)

M.D.
Johns Hopkins University School of Medicine
(1985)

Submitted to the Harvard MIT Division of Health Sciences and Technology in partial fulfillment of the requirements for the degree of Doctor of Philiosophy

at the

Massachusetts Institute of Technology

May 1987

Signature of Author_____
Dept. of Health Sciences and Tech.
May, 1987

Certified by_____
Herman N. Eisen
Professor, Dept. of Biology
Thesis Supervisor

Accepted by_____
Roger G. Mark
Chairman, Graduate Committee

THE ROLE OF CALCIUM IN THE DESTRUCTION OF TARGET CELLS BY CYTOTOXIC T CELLS

by

Nancy L. Allbritton

Submitted to the Harvard MIT Division of Health Sciences and Technology on April 28, 1987 in partial fulfillment of the requirements for the degree of Doctor of Philosophy in Medical Physics

ABSTRACT

The immune system has evolved elaborate molecular and cellular mechanisms to defend the body against invasion by pathogens (viruses, bacteria, and protozoal parasites). One immune mechanism involves the cytotoxic T lymphocyte (CTL) that can specifically recognize and destroy cells bearing foreign proteins (target cells). Virus-infected cells, transplanted tissue, and some tumor cells are examples of target cells. To learn more about the mechanism by which CTLs destroy target cells, this work investigates the possibility that a CTL-mediated calcium influx into target cells may be an essential event in the sequence of reactions that lead to the death of these cells.

Target cell death was studied by following the intracellular free calcium (ICF) calcium level, DNA fragmentation, and lysis of cells in response to intact CTLs, cytolytic granules of CTLs, and Na+, K+, and Ca++ ionophores. ICF Ca++ measurements were made in a flow cytometer with the fluorescent dye, indo-1.

The results of these experiments suggest that a marked and sustained elevation of the calcium ion concentration in target cells is a proximal cause of their death. Targets exposed to CTLs or their lytic granules undergo a rapid rise in ICF calcium. Analysis of selective ionophores for Ca++, K+, Na+ suggests that while elevated calcium concentrations are lethal, the DNA fragmentation observed in the target cell on killing by CTLs can be duplicated with a K+ ionophore (valinomycin) and not with a calcium ionophore (ionomycin).

Thesis Supervisor: Dr. Herman N. Eisen
Title: Professor of Biology

Acknowledgements

I would like to express my appreciation to Herman Eisen and the members of his lab for their support and guidance. I would like to thank Peter Hansen, Robert Wolley, and the staff of the Cambridge Research Laboratory for their technical assistance and the use of their facilities. In addition, I thank my parents, Irene and Allan Allbritton, for the support and motivation to stay in school.

But most of all, I would like to express my gratitude to my husband, Chris Sims, for his unlimited understanding and support for all my endeavors.

Table of Contents

Abbreviations

CTL = cytotoxic T lymphocyte

PE = phycoerythrin

PHA = phytohemaglutinin

DMSO = dimethyl sulfoxide

IL 2 = interleukin 2

COF = carboxyfluorescein

FITC = fluorescein isothiocyanate

kDa = kilodalton

EBV = Epstein Barr virus

ICF = intracellular free

ECBS = extracellular buffered salt solution

ICBS = intracellular buffered salt solution

TCR = T cell antigen receptor

APC = allophycocyanine

BSA = bovine serum albumin

HBS = hepes buffered saline

E:T = effector : target ratio

MHC = major histocompatibility complex

IP_3 = inositol triphosphate

LAK = lymphokine activated killer

PFP = pore forming protein

ADCC = antibody dependent cell-mediated cytotoxicity

uM = micromolar

nM = nanomolar

um = micron

mM = millimolar

ml = milliliter

BLT = N-alpha benzyloxycarbonyl L-lysine-thiobenzyl ester

FCS = fetal calf serum

PMT = photomultiplier tube

SRBC = sheep red blood cells

Figures

page

Tables

I. Introduction and Background

A. Introduction

A large body of evidence indicates that the destruction of target cells by murine cytolytic lymphocytes (CTLs), and other lymphocytes termed "natural killer" (NK) cells, is brought about by the release from these cells of toxic granules[3,133]. One of the granule proteins, called perforin (cytolysin or pore-forming protein (PFP)) resembles complement factor 9 and like C9 forms transmembrane ion-channels that are presumed to cause target cell lysis[42,44-46,70-72,132]. The granules also contain one or more neutral serine esterases, at least one of which has some sequence homology with a complement component[43,47,48]. Hence there are reasons for believing that target cell lysis by antigen-activated T cells and by antibody (or immune complex)-activated complement are fundamentally the same. However, there are some differences: e.g. DNA fragmentation occurs as an early event in immune target cells when they are lysed by CTLs but not when lysed by complement[83,91-93,140]. Another difference is that CTLs themselves are resistant to lysis by the toxic granules but not to lysis by complement[67,68].

To learn more about the mechanism by which CTLs destroy target cells, this work investigates the

possibility that a CTL-mediated calcium influx into target cells may be an essential event in the sequence of reactions that lead to death of these cells. We have focussed in this study on the intracellular calcium ion concentration in target cells for several reasons. First, much evidence indicates that ion channels play an essential part in the cytolytic process hence changes in intracellular calcium ion might be expected because the cells normally exclude extracellular calcium ions efficiently. The intracellular calcium ion concentration is normally 1/1000 - 1/10,000 that of the normal extracellular medium[80,85,159]. In addition calcium ions regulate a variety of intracellular processes and a large change in calcium level can have drastic effect on cell function and survival[33-35,58,95-97]. Finally, the development of calcium-sensitive, fluorescent probes and advances in flow cytometry, now make it possible to monitor with precision and sensitivity changes in calcium ion concentration in individual cells. We have studied target cell death by following the ICF Ca++, DNA fragmentation, and cell lysis of cells exposed to intact CTLs, cytolytic granules of CTLs and Na+, K+, and Ca++ selective ionophores.

Our results suggest that a marked and sustained elevation of calcium ion concentration in target cells is a proximal cause of their death. Target cells exposed to

CTLs or their lytic granules undergo a rapid rise in ICF Ca++. Analysis of selective ionophores for Ca++, K+, Na+ suggests that while elevated calcium concentrations are lethal, the DNA fragmentation observed in the target cell on killing by CTLs can be duplicated with a K+ ionophore (valinomycin) and not with a calcium ionophore (ionomycin).

B. Background

The destruction of target cells by CTLs is one of many elaborate mechanisms the immune system has evolved for defense against invasion of the body by pathogenic microbes (e.g. viruses, bacteria, and protozoal parasites)[163,164]. In the humoral part of the immune system, antibody serves as the sensor for antigen and triggers antigen destruction by activating either a set of 14 complement proteins or various cytotoxic cells (macrophages, large granular lymphocytes, granulocytes) with a surface receptor for the invariant domain (F_C) of antibody molecules[163,164]. In the T cell compartment, antigen recognition is due to an immunoglobulin-like antigen-specific T cell receptor (TCR). Antigen binding to the TCR triggers the cytolytic activity of cytotoxic T cells (CTLs) and the release of a lymphokine (gamma-interferon) which activates macrophages to kill cells[163,164]. It is the cytolytic activity of the T cells that forms the subject of this thesis.

There are two broad groups of T cells called CD4 and CD8 cells[163,164]. They differ in surface glycoproteins and function. CD8 cells are $L3T4^-$, $Lyt\text{-}2^+$ (in the mouse) or $T4^-$, $T8^+$ (in the human) and most of them are cytolytic i.e. they are CTLs (some CD8 cells may function as suppressor cells). CD4 cells are $L3T4^+$, $Lyt\text{-}2^-$ (in the mouse) or $T4^+$, $T8^-$ (in the human). When activated they

produce lymphokines such as interleukin-2 and interleukin-4 that promote growth and differentiation of B cells and other T cells. Hence CD4 cells are generally called T helper cells (T_h). However many CD4 cells are also cytolytic and there is considerable evidence to suggest that they and CD8 cells kill by the same mechanism. Hence in this thesis all T cells that lyse target cells will be referred to as CTLs whether they are CD8 or CD4 cells.

Oportunities to study the mechanism by which CTLs lyse targets has been greatly enhanced by the development of clonal cell lines of cytotoxic T lymphocytes. The observation that supernatants of PHA-stimulated lymphocytes could sustain T lymphocytes led to the discovery of T cell growth factor or interleukin 2 (Il 2)[1,2]. The use of recombinant Il 2 or supernatants of lectin-stimulated lymphocytes has led to the long term culture and cloning of CTLs[1,2]. The use of serial antigenic stimulation in growing CTLs in combination with the growth factor(s) has also contributed to the preservation of lytic specificity[1,2].

CTL lysis of targets has traditionally been considered to take place in 3 stages; a. binding of a CTL to a target cell, b. programming of the target cell for lysis or the lethal hit, c. lysis of the programmed target cell after the CTL disengages (killer cell-independant lysis (figure 1))[3-7]. Adhesion of a CTL to a

FIGURE 1

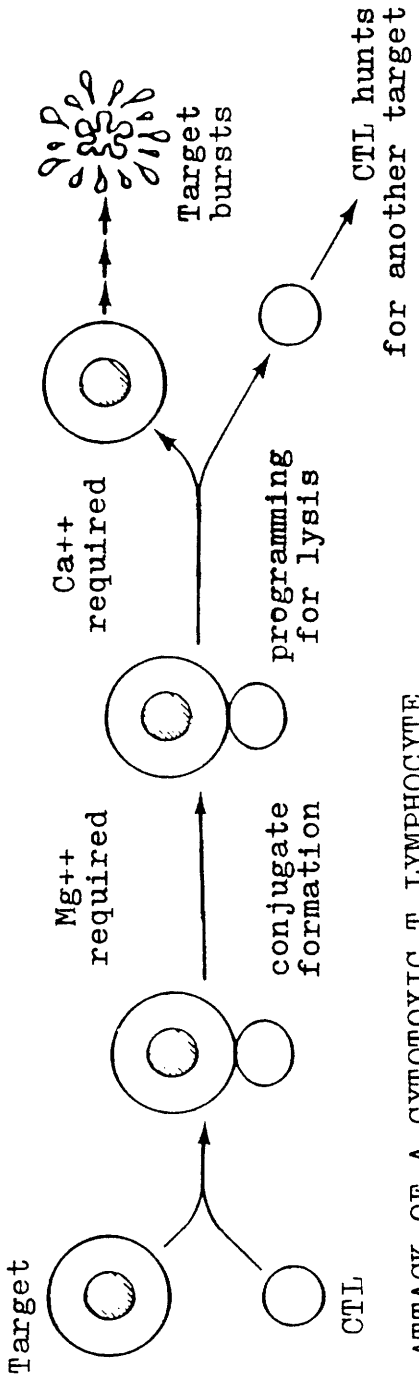

ATTACK OF A CYTOTOXIC T LYMPHOCYTE ON A TARGET CELL

Figure 1

Figure 1 displays the steps in the attack of a CTL on a target cell.

target cell is mediated by both antigen dependent and independent pathways[8-16]. Cell-cell adhesion occurs almost as efficiently between CTLs and target cells that have or do not have the antigen[17,18]. Antibody blocking studies of CTL mediated cytolysis have shown that the molecules LFA-1, T8, T4, LFA-2, LFA-3, and ICAM-1 are involved in adhesion[9,10,11,13,14]. LFA-1 is an antigen found on most bone marrow derived cells[9]. Adhesion via LFA-1 (possibly to ICAM-1 on the target cell) requires divalent cations and is temperature sensitive[10,11]. Intercellular adhesion molecule 1 (ICAM-1), a molecule distinct from LFA-1, inhibits phorbol ester stimulated aggregation of LFA-1+ EBV lines[10]. LFA-2 is a surface protein (also called T11) that fortuitously binds sheep red blood cells[9]. It is expressed by all T but not B lymphocytes. LFA-2 adhesion (possibly to LFA-3 on the target) is independent of divalent cations and is temperature insensitive[11]. LFA-3 is an antigen found on most cells, lymphoid and others. T8 is an immunoglobulin-like glycoprotein found on the surface of T cells with cytotoxic or supressor functions; it is thought to bind the invariant domain of class I major histocmpatibility molecules. T4 is an immunoglobulin-like glycoprotein found on some cytolytic T cells that do not express T8. T4 is thought to bind the invariant domain of class II major histocmpatibility molecules. While these molecules

support CTL adhesion to targets, they are not necessary for target cell lysis. Linking antibodies against the T cell antigen receptor to target cells can overcome the lytic inhibition induced by anti-Lyt2 (T8) and anti-LFA-1 antibodies[8].

The signal that initiates T lymphocyte activation and proliferation occurs through the T cell antigen receptor[19-25]. The antigen-specific T cell receptor (TCR) is an immunoglobulin-like glycoprotein composed of a disulfide linked dimer. Its alpha and beta chains (42-44 kDa, mouse and 50-40 kDa, human) are noncovalently linked to the T3 complex. The T3 complex is composed of four polypeptide chains (gamma, delta, epsilon and zeta) in humans and mice[19,26]. Each subunit is between 20 and 30 kDa. In cells with surface T8 (or Lyt-2), the TCR recognizes antigen in association with class I major histocompatibility molecules while cells with surface T4 or L3T4 recognize antigen with class II MHC molecules[2]. Evidence suggests that the T3 molecule may act as a signal transducer between the TCR and the cell interior[21,23,27,28,29]. Antigens, anti-TCR antibody, lectins, and anti-T3 antibody can stimulate increases in intracellular free (ICF) calcium, phosphorylation of intracellular proteins, and production of inositol triphosphate (IP_3) and its breakdown products in T lymphocytes[21,23,27,28,30,31,32]. The implication is that

perturbation of the T cell antigen receptor activates a phosphodiesterase which leads to the production of IP_3 and diacylglycerol[33-35]. Diacylglycerol activates protein kinase C and IP_3 releases calcium from intracellular stores. Increases in the intracellular free calcium may also be due to the opening of plasma membrane calcium channels. Increased ICF Ca^{++} may activate Ca^{++}-dependent protein kinases resulting in protein phosphorylation. The exact mechanism by which these secondary events result in cellular activation and proliferation is not known.

It is clear that activation of the CTL for lysis occurs through the T cell antigen receptor although it is not clear which if any of the above steps leading to cellular proliferation and activation are also necessary for target cell lysis[36]. Preincubation of CTLs with anti-T3 or anti-TCR antibody will inhibit target cell lysis[8,16]. However CTLs are capable of lysis of cells which are not normally targets when anti-T3 or anti-TCR is bound to the target cell surface[8,15,16]. Increases in ICF Ca++ of CTLs has been observed upon addition of target cells[25].

Most cytotoxic lymphocytes and possibly all possess cytoplasmic granules visible by light or electron microscopy[3]. The presence of granules correlates well although not perfectly with cytolytic activity[3]. By microscopy and histochemical staining these granules are

membrane bound and contain lysosomal enzymes[3]. Membrane bound granules have been isolated from the cytoplasm of murine CTL, natural killer (NK) and lymphokine activated killer (LAK) cells[3,37-41]. These granules are capable of lysing red blood and tumor cells in the presence of calcium in an MHC-independent fashion. Addition of granules to red blood or tumor cells results in the depolarization of the plasma membrane and formation of circular membrane lesions up to 16 nm in diameter[38,41,42]. When added to planar bilayers, the granules create functional ion channels permeable to mono- and divalent ions and larger molecules (COF, EGTA, Tris)[38,41,42]. Incubation of the granules alone in the presence of calcium results in ring like structures of 16 nm. The granules contain mainly protein with five major bands on SDS polyacrylimide gels[41]. The granules contain a variety of lysosomal enzymes, including acid phosphatase and B-glucuronidase[38,41]. A serine esterase and a lytic molecule (perforin, cytolysin or PFP) have also been localized to these granules[42-47]. The serine esterase is a membrane-associated, disulfide-linked dimer of ~30 kDa which cleaves a synthetic substrate (BLT) but not I^{125}-casein. Hence its natural substrate may be limited to very few substances (like the complement proteins that are serine esterases)[47,48]. Its function in the granules is not yet known. Perforin is a 70 kDa protein[42-46,49]. In

the presence of calcium it is capable of inserting into lipid bilayers and polymerizing to form tubular structures with inner diameter up to 16 nm. Purified perforin is capable of lysing tumor and red blood cells and depolarizing their membranes[42,46]. Insertion of perforin into lipid bilayers results in the flow of mono- and divalent ions[42]. Patch clamp recordings of tumor cells exposed to perforin results in an inward current flow that appears to be the summation of discrete events[42,46]. This is indicative of functional channel formation by a polyperforin complex.

Morphologic studies of CTLs in contact with targets show a pronounced cytoplasmic polarization after target cell binding[3-6,51,150]. Studies have shown that the cytoplasmic granules are generally located in the trailing end of the CTL as it moves[51]. Upon contact with an appropriate target cell but not with an inappropriate one, the granules are transported to the area of membrane in contact with the target[51,52]. The golgi apparatus reorients in a similar fashion[53]. Tubulin and actin fibers also become assymetrically oriented following target cell binding[3,5,6,54,55,150]. The CTL and target cell membranes become interdigitated following contact[3,5,6]. CTL conjugation with a target cell whose antigen is recognized is approximately ten times stronger than with an inappropriate target cell (as measured by the

force required to separate the cells)[12].

There is strong evidence that CTL lysis of targets invloves a secretory process[3]. Acid phosphatase, which is found in lysosomal granules, is deposited on the surface of the target cell and into the intercellular space[3,52,56]. Fluorescent studies have demonstrated the presence of granule antigens on the surface of target cells in contact with CTLs[41]. Chloroquine, which raises the pH of lysosomal granules, inhibits CTL killing[57]. Serine esterase can be measured in the supernatant of CTLs after addition of target cells[47]. Increases in cytoplasmic calcium concentration appear to activate many secretory phenomena such as the release of neurotransmitters, hormones and digestive enzymes[58]. As discussed earlier increases in ICF Ca++ appear to play a prominent role in T lymphocyte activation. The calcium ionophore, A23817, causes release of the granule contents, serine esterase and perforin[43,59]. This triggering by an increase in ICF Ca++ strongly suggests a process of exocytosis. In addition the "programming for lysis" stage of CTLs is dependent on the presence of extracellular calcium[5,6].

Tubular structures similar to those formed by granules and perforin have been identified on target cells exposed to some but not all CTLs[41,62]. Marker release from resealed red blood cell ghosts used as targets for

antibody dependent cytotoxic cell (ADCC) targets provides evidence for pore formation with a maximal size of 15 nm[69].

The evidence for the exocytosis of granule components, especially perforin, onto the target cell is quite strong. There are, however, alternative mechanisms for CTL mediated lysis of target cells, although less well supported[4,60-62]. Since perforin has not yet been isolated from human T8+ lymphocytes and granules not visualized in a few types of lymphocytes, it is worth considering these alternative theories[44,62].

A variety of toxic molecules e.g. CTL toxin, lymphotoxin, and NK cytotoxic factor, are secreted into the media by activated CTLs[63-66]. These factors require a long period of time (24 hours) to be cytocidal. They have not been localized to lymphocyte granules. The primary difficulty in attributing target cell lysis to these toxins is that they kill cells very slowly ($t^{1/2}=\sim 24$ hours). In contrast target cell death can be detected within an hour after addition of CTLs. If cells are forced to take up lymphotoxin by incubating them in a hypertonic solution with 10% PEG, which stimulates pinocytosis, a maximum of 35% Cr^{51} specific release occurs at 4 hours[65]. Since this is an artificial situation which only causes a maximal killing of 35%, it does not seem that lymphotoxin could be the major cytolytic component of

CTLs. Also arguing against a major role for lymphotoxin is its ability to lyse cloned CTL cell lines[65]. These cell lines have been shown to be resistant to being lysed by CTLs and cytotoxic granules isolated from CTLs[65,67,68].

Other proposed mechanisms for target cell destruction include release of reactive oxygen intermediates by CTLs and shearing of the target cell membrane by CTLs[3,4,61]. There is very little evidence to support either of these mechanisms[3].

The tubular structures formed by CTLs, granules and perforin are remarkably similar to the structures formed by the C5b-9 complex of the complement system. In addtion perforin is related antigenically and structurally to c9 [70,71,132]. The serine esterases contained in granules are reminiscent of the enzymes involved in the complement cascade[41,43,48,71,72]. It has been proposed therefore that CTL and complement destroy target cells the same way.

Complement, activated by antibody, causes colloid osmotic lysis of cells[73-75]. Transmembrane channels are formed when hydrophobic regions of C5-9 are exposed by fusion of the five proteins. The complex then inserts itself into lipid membranes and forms transmembrane channels. The largest of these channels is formed by poly-C9 structures (inner diameter = 11 nm). Osmotic lysis permits small ions to equilibrate across the membrane and an unbalanced osmotic pressure occurs as a

result of the cellular macromolecules. Water, which freely crosses the cell membrane, flows into the cell in response to the osmotic pressure differential resulting in cellular swelling and membrane rupture. Increasing the osmotic pressure of the extracellular media can prevent complement-mediated lysis.

There are enough differences between complement and CTL mediated cytotoxicity to suggest that the two processes are significantly different. Target cells of CTLs have not been shown convincingly to be protected by hyperosmotic media[3,76-78]. Unlike osmotic death target cells undergo cytoplasmic blebbing (zeiosis) and DNA breakdown before membrane rupture with subsequent fragmentation of the cell and nucleus[79-83]. This type of morphologic death is called apotosis by pathologists and is not seen in osmotic lysis which leaves the cells morphologically intact as a ghost[84-86]. This apototic death or cellular fragmentation is seen with death due to Il-2 withdrawal (T cells), steroids acting on T cells, endocrine changes, and embryogenesis[80,86-90]. It often requires active metabolism of the cell[80,86-90]. DNA fragmentation into multiples of 200 base pairs can be quantitatively measured and has been shown to be detectable within five minutes after addition of CTLs to targets[91-93]. Even if the amount of antibody or complement is varied to mimic the time course of CTL

mediated Cr^{51} release, DNA fragmentation does not occur in complement lysis[83]. These features of target cell death imply that CTLs mediate cell lysis in a way quite different from complement.

Some evidence suggests that CTL mediated cytotoxicity may operate through the activation of intracellular enzymes. Both steroid and CTL lysis are accompanied by DNA fragmentation which suggests the activation of an endogenous endonuclease. There is evidence that phospholipase A may be active during target cell death[50]. These results imply that the activation of a number of intracellular enzymes may constitute the "death program" of these cells.

Free calcium is responsible for the activation of many intracellular enzymes and is maintained at a very low intracellular concentration despite an enormous gradient across the plasma membrane (intracellular/extracellular Ca++ = 10^{-4})[80,85,159]. ICF Ca++ levels regulate many critical cell functions such as cell cycle, cell transport, regulatory proteins, exocytosis and many enzymes[33-35,58,95-97]. Destructive enzymes, such as phospholipases and endonucleases, can be calcium activated[84,85,98,99]. It has been proposed by Berke and others that an influx of calcium may be responsible for target cell death[81,82,100,101]. The cytoplasmic blebbing may be the result of Ca++ activated cytoskeletal proteins

while DNA fragmentation would occur by activation of a calcium-dependent endonuclease. Cell death could result from ATP depletion (from activation of ATPases) and from membrane damage caused by activation of phospholipases. Evidence supporting these possibilities has come from studies of cell death in other systems[75,84,85,98,99,102-104]. Steroid lysis, which duplicates many features of CTL-mediated target cell death, is dependent on the presence of extracellular calcium. Membrane altering agents such as mellitin, silica, lysolethicin, and others have also been shown to exhibit a calcium dependent toxicity in rat liver cells[98]. The calcium ionophore, A23817, is a potent cytocidal agent in all cells and is dependent on extracellular calcium for its toxicity[81,101,105]. These data indicate that maintenance of the extracellular/intracellular calcium gradient is critical for cell viability.

However, evidence supporting a connection between target cell intracellular calcium levels and the destruction of the cell by a CTL is sparse primarily due to the inability to dissociate the CTL activation process from subsequent target cell lysis[4,81,82]. Agents used to alter the target cell response also effect the CTL activation process. By taking advantage of recently developed fluorescent molecules it is feasible to monitor the ICF Ca++ of individual cells by flow cytometry. This

thesis investigates the possibility that a calcium influx into target cells may be the primary mechanism of CTL induced target cell death. This was investigated by following the ICF Ca++ of cells exposed to intact CTLs or isolated CTL granules. In addition, the effects of the granules and of K^+, K^+-Na^+, Ca^{++}-Mg^{++}, and Ca^{++} selective ionophores on DNA degradation and cell lysis were examined.

II. Materials and Methods

A. Reagents

Ionomycin (free acid), valinomycin, A23817, quin-2 AM and gramicidin D were obtained from Calbiochem and stock solutions were made in DMSO. The acetoxymethylester and potassium salt of indo-1 were obtained from Molecular Probes and stock solutions kept in DMSO and distilled water, respectively. Phycoerythrin-avidin was purchased from Becton Dickinson and chromium^{51} and iodine^{125}-deoxyuridine from New England Nuclear. Dithiothreitol, cyanide, and azide were dissolved in distilled water and obtained from Sigma, Coleman and Bell, and Fluka, respectively. N-OH-succinimidobiotin was from Sigma and dissolved in DMSO, while N-succinimidyl-3-(2-pyridyldithio)proprionate was purchased from Pierce Chemical Company, Rockford, IL and kept in ethanol. EGTA and HEPES were Fluka Puriss. Reticulocyte beads were from Ortho, Westwood, MA. Fluorescein isothiocyanate (FITC) was from Kodak and dissolved in ethanol. Allophycocyanine-avidin was from Biomedia, Foster City, CA. Percoll was from Pharmacia, sheep red blood cells from Colorado Serum Co., Denver, and $CaCO_3$ from Mallinckrodt. The 1 N standard NaOH was Acculute by Anachemia Chemical Inc, Champlain.

B. Cells and Solutions

2C, 3H2, 3C11, G4, 2.1.1 are murine cytotoxic T lymphocyte clones (CTL) that are directed against D^d. They are maintained in K media with 20-30 U/ml human recombinant interleukin 2, and irradiated feeder cells expressing D^d (P815 or Balb C spleen cells). D10 and TDH-1 are murine T helper lymphocyte clones that do not kill while 5.5 is a murine T helper lymphocyte clone that does kill with lectin. The T helper cells are also maintained in K, recombinant human interleukin 2, and irradiated stimulator cells bearing the appropriate antigen. RDM4, and S49 are murine T lymphomas. Yac-1 is a murine undifferentiated lymphoma and P815 is a murine mastocytoma. P815 and Yac-1 express D^d but EL4 does not.

Relaxation buffer contains 100 mM KCl, 3 mM NaCl, 3 mM $MgCl_2$, 1.25 mM EGTA, 10 mM PIPES, 0.5 mM ATP and is pH 6.78. Extracellular buffered salt solution (ECBS) contains 145 mM $NaCl_2$, 5 mM KCl, 0.5 mM $MgSO_4$, 10 mM HEPES, 1 mM NaH_2PO_4, 5 mM glucose and is pH 7.2. Intracellular buffered salt solution (ICBS) contains 100 M KCl, 20 mM NaCl, 1 mM $MgCl_2$, 10 mM HEPES, pH 7.2. In addition the ECBS and ICBS contain either $CaCl_2$ or EGTA usually at 1 mM or 5 mM respectively. K medium contains RPMI, 10% heat inactivated fetal calf serum, 4.5 mM HEPES, 1.2 mM L-glutamine, 90 U/ml penicillin, 90 mg/ml streptomycin, and 44 uM B-mercaptoethanol. RPMI + HEPES

is RPMI with 4.5 mM HEPES. TEA is 40 mM Tris acetate, 1 mM EDTA, pH 8 while TE is 10 mM TrisCl, 1 mM EDTA, pH 8. PBS and HBSS were made as described in Mishell and Shiigi[129].

C. Monoclonal Antibody and Cell Coupling

1B2 is a monoclonal antibody directed against the T cell antigen receptor of the CTL clone, 2C[106]. Hybridoma cells producing 1B2 were injected into the peritoneum of pristine-primed Balb C mice. Ascites was collected and lipoproteins removed by precipitation with 0.25% Nadextran Sulfate and 1.5% $CaCl_2$ [129]. IgG was then purified by precipitation with 50% saturated ammonium sulfate two times, dialysis against 50 mM $KHPO_4$, pH 8.0 and passage over a DEAE-cellulose column[129]. The purified IgG was dialyzed against PBS and the protein concentration determined by the absorbance at 280 nm[129].

The 1B2 antibody was linked to N-succinimidyl-3-(2-pyridyldithio)proprionate (SPDP) for cell coupling by incubation of 1 mg/ml 1B2 with 0.3 mg SPDP/ml for 30 minutes at room temperature[8]. The 1B2-SPDP was then dialyzed against PBS overnight and stored at 4°C for future use.

Cells were coupled to 1B2-SPDP by washing twice in PBS followed by incubation of 10^6 cells/ml with 50 uM dithiothreitol (DTT) at room temperature for 45 minutes[8].

After washing twice in PBS, 10^7 cells/ul were incubated with 1B2-SPDP (0.5 mg/ml) for 45 minutes at room temperature. The cells were then washed twice in PBS and once in K medium.

D. Phycoerythrin, Allophycocyanin and FITC Labelling

Phycoerythrin (PE) is a fluorescent phycobiliprotein of algal origin with a high extinction coefficient and quantum number[108]. It has an excitation maximum at 495 and 545 nm and an emission maximum at 576 nm. PE was attached to cells by an avidin-biotin system. Cells were washed twice in PBS, pH 8.0 and resuspended at $2X10^6$/ml in PBS, pH 8.0 with 0.1% N-OH succinimidobiotin (volume/volume from a 1 mg/ml stock) for 45 minutes at room temperature. Cells were then washed twice in PBS pH 7.2 and resuspended at 10^6 cells/100ul to which PE-avidin was added at a 1/10 dilution. After 45 minutes at room temperature the cells were washed once in PBS and resuspended in K medium.

APC-avidin was attached in a manner similar to PE-avidin. Cells to be labelled with FITC were suspended in PBS, pH 7.2, 10 uM FITC for 10 minutes at 37 ^oC and then washed.

E. Chromium51 Release Assays

Cells were loaded with chromium 51 (Cr^{51}) by washing

twice in K medium and resuspending to a final concentration of $2X10^7$ cells and 200 uCi Cr^{51} in 400 ul of K medium[107]. The cells were then incubated for one hour in a 37°C, 5% CO_2 incubator with frequent mixing. Cells were washed three times with the desired assay medium.

CTL killing assays were done in 200 ul K medium with 10^4 target cells per sample point for 4 hours in a 37°C, 5% CO_2 incubator. Granule killing assays were done in the extracellular buffered salt solution with 1 mM $CaCl_2$ for one hour in a 37°C water bath using $5X10^4$ target cells in 100 ul for each sample point. Ionophore toxicity assays were done in the extracellular buffered salt solution with the indicated calcium concentration for one hour in a 37°C water bath using $5X10^4$ target cells in a 100 ul for each sample point.

At the completion of the assay times, the samples were spun at 1500 rpm (300 g) for 5 minutes and aliquots of supernatant removed. The specific release was calculated from the formula:

$$\text{Specific release} = \frac{\text{test release - nonspecific release}}{\text{total release - nonspecific release}}$$

Samples with 0.5% NP40 were used for the total release and samples with aliquots of K medium, relaxation buffer, or DMSO, equivalent to that of the test samples were used as the nonspecific release. CTL killing and ionophore toxicity assays were done with each point in triplicate

and granule killing assays with each point duplicated.

F. Granule Preparations

Cytolytic granules were prepared from mouse cytolytic T cell clones (3C11, 3H2, or G4)[67]. Adherent and nonadherent CTL clones were harvested. Adherent cells were freed by incubation with a 1:1 ratio of PBS with 10mM EDTA and K medium at room temperature for 5 minutes. Adherent and nonadherent cells were pooled and washed twice in Hanks balanced salt solution and twice in relaxation buffer. Cells were cavitated with 350 psi of nitrogen. The nuclei were removed by spinning at 1000 rpm (140 g) for 5 minutes. The nuclei-free cellular suspension was then layered on a percoll gradient composed of 39%-60%-90% (volume ratio 2:1:1.75) percoll in relaxation buffer and centrifuged at 20,000 rpm (52,000 g) for 30 minutes. Fractions were then collected from the gradient and tested for lytic activity against sheep red blood cells (SRBC). SRBC were washed twice in HEPES buffered saline (HBS) and resuspended at a 1/10 dilution in HBS with 0.4 mg/ml BSA, 5 mM $CaCl_2$. Granules fractions were then assayed by adding 2 ul aliquots of each fraction to 100 ul SRBC (10^8 cells) and incubating at 37^oC for 15 minutes. The volume of each sample was then brought to 1 ml with PBS. Samples to be used as the total release

received 1 ml of distilled water instead of PBS. Samples were spun 15 seconds in a microfuge. Aliquots (180 ul) of the supernatant were removed and the absorbance at 414 nm measured using a Dynatech 96 well plate reader. The most lytic fractions were pooled ($\sim$50% and greater.) Percoll was removed by pelleting at 40,000 rpm (100,000 g) for 90 minutes. The granule layer was collected from above the percoll pellet, retested for sheep red blood cell lysis, and frozen for later use at -70°C.

G. DNA Fragmentation

$5X10^6$ cells were incubated with 50 uCi of I^{125}-deoxyuridine in 10 mls of K medium, overnight (15 hours) in a 37°C, 5% CO_2 incubator[91]. The cells were washed twice in PBS. Targets to be added to CTLs were resuspended in K medium, while those receiving either CTL granules or ionophores were resuspended in ECBS with 1 mM calcium. CTLs, CTL granules, or ionophores were added to $4X10^4$ (I^{125}) targets with a final volume of 100 ul. The samples were incubated at 37°C for 1 hour. The cells were then lysed by addition of PBS with SDS and EDTA (final concentration of 2% and 3 mM respectively). The DNA was ethanol precipitated with two times the volume of ethanol and resuspended in TE with gel loading buffer[109]. The samples were loaded onto a 0.8% agarose gel with TEA buffer and electrophoresed overnight at 40 mV[109]. The gel was dried and exposed to Kodak X-Omat AR film.

H. Indo-1 and Quin-2 Loading

The acetoxymethylester of indo-1 (indo-1 AM) was stored as a 1 mM stock solution in DMSO, dessicated at -20°C. Cells were washed twice and resuspended in RPMI with 45 mM HEPES. Indo-1 AM was added at the indicated concentration to $2X10^5$ cells/ml. Cells were incubated for 1-1.5 hours in a 37°C, 5% CO_2 incubator. The cells were then washed once into K medium and placed in a 37°C, 5% CO_2 incubator for 0.5-1.5 hours (shorter times were used for cells that were to be preconjugated). Cells were washed with the desired solution (K or extracellular buffered salt solution) immediately prior to use. Spectrofluorimetric measurements were made in the extracellular buffered salt solution with either 1 mM $CaCl_2$ or 5 mM EGTA and used done in LS-5 Perkin Elmer or a Aminco-Bowman (#4-8202) spectrofluorimeter.

The amount of intracellular dye in the cells after loading was measured by lysing the cells with 0.02% triton. The intensity of fluorescence of the released dye was then compared to standards made using indo-1, the deesterified dye. Emission spectra of the released dye in extracellular buffered salt solution with 1 mM $CaCl_2$ or 5 mM EGTA were taken to insure that the indo-1 AM was being properly deesterified by the cells (excitation, 350 nm.)

The acetoxymethylester of quin-2 (quin-2 AM) was stored as a 4 mM stock solution in DMSO, dessicated at -20°C. Cells were washed twice and resuspended in RPMI with 45 mM HEPES. Quin-2 AM was added at the indicated concentration to $2X10^6$ cells/ml. Cells were incubated for 0.5 hours in a 37°C, 5% CO_2 incubator, washed twice with extracellular buffered salt solution with 1 mM $CaCl_2$ and used immediately[110].

I. Conjugation

CTLs for conjugation were labelled with biotin-avidin-PE, and target cells with or without 1B2 attached were loaded with indo-1 AM. Conjugates were formed by mixing targets ($5X10^5$/ml) with CTLs ($15X10^5$/ml) in K medium at room temperature. Cells were allowed to sit undisturbed for 40-60 minutes at room temperature. A separate sample containing 1 ml of cell conjugates was made for each time point. At time zero the conjugates were placed at 37°C. No tubes were mixed until just prior to being run on the flow cytometer.

J. Flow Cytometry

The hardware, data collection, and controls used with flow cytometry are described in the results section on flow cytometry.

Cells were analyzed at 37°C at flow rates of 100-200 cells/second. Time courses done for 10 minutes or less were done by running the sample continuously and storing the data on a 15 Mb hard disc. At a later time the data was analyzed and broken into 1 minute intervals. Test sample time courses were done by addition of the stimulus, brief mixing, and then starting the sample flow. Approximately 30 seconds occurred between stimulus addition and appearance of the cells before the laser beam. Control samples (those not challenged with a stimulus) were run for the same length of time immediately after or before the test sample.

For time courses greater than 10 minutes, 10,000 cells were collected on the ratio graph for each time point. The cells were maintained at 37°C during and between sampling. Test sample and control sample time courses were run at the same time with one time course starting approximately 2-3 minutes after the other.

K. Titrations

For EGTA:NaOH titrations, EGTA was weighed in a Mettler Balance, model H30. The EGTA was dissolved in distilled water and the pH brought to 2.8 (the pK for $EGTAH_3 = EGTAH_2 + H$ is 2.7)[111]. The solution was then brought to a measured volume with distilled water in a volumetric flask. A standard 1 N NaOH solution was added

in aliquots to the EGTA using a 10 ml buret. The pH was determined after each addition of NaOH using a Radiometer, model PHM63, digital pH meter. The equivalence point for the EGTA was determined graphically by plotting the pH versus the volume of NaOH added. The volume of base at the equivalence point was then used to determine the EGTA concentration (i.e. 1 mole EGTA: 2 moles NaOH.)

The EGTA-calcium titrations were performed in a similar fashion[112]. $CaCO_3$ was baked in an oven at 500°F for 3 hours. A stock solution of calcium was made by weighing the dried $CaCO_3$, dissolving it in concentrated HCl, increasing the pH to 9.8 with NaOH, and bringing it to a measured volume in a volumetric flask. A stock solution of equimolar EGTA/HEPES was similarly made and brought to pH 10.09. pH 10.09 was chosen because EGTA-CA = EGTA + Ca++ has a pK of 10.97[111]. 200 mls of EGTA/HEPES was titrated with the Ca++ solution using a 25 ml buret. The endpoint of 1 EGTA:1 Ca++ was determined graphically by plotting milliliters of Ca++ or EGTA/HEPES added vs pH.

III. Indo-1 Properties and Loading

A. Introduction

It is now possible to measure intracellular free calcium levels in single cells with the development of the fluorescent indicators, indo-1 and fura-2 [113-115,156]. Quin-2, the previously used indicator, has a low extinction coefficient and quantum yield so that its use has been limited primarily to bulk cell measurements in spectrofluorimeters[110,116,154,155,157]. This is particularly problematic when measuring the response of target cells to potentially lytic agents i.e. intact cytotoxic T cells or their isolated cytolytic granules. Nonspecific dye leakage and dye leakage due to cell death can interfere with fluorescent signals from intracellular dye causing incorrect results. We have, therefore, used the new fluorescent dye, indo-1, since its high extinction coefficient and quantum yield permit it to be used in a flow cytometer and at low intracellular concentrations.

Table 1

Indo-1 Properties[113]

	Free Anion	Ca++ complex
Absorption Maximum	349 nm	331 nm
Emission Maximum	480 nm	405 nm
Quantum Efficiency	0.38	0.56
Extinction Coefficient	3,400/M*cm	

Indo-1 is impermeable to cells because the molecule is negatively charged at physiologic pHs. The acetoxymethyl ester (indo-1 AM) is not charged and therefore is permeable to cells[31,113]. Hence cells are loaded with the ester which is cleaved to the indo-1 form by intracellular esterases trapping it inside the cell. The ester is shown in Figure 2. The dashed lines are the sites of deesterification. Indo-1 has a K_d for calcium of 250 nM[113]. Since most cells have a resting free intracellular calcium ion concentration of about 100 nM, this K_d makes the dye excellent for use with cells[102,113,114,117]. Because the K_d for Mg^{++} is 10 mM, the intracellular Mg^{++} (concentration = ~1 mM) is expected to have little effect on measurement of ICF Ca^{++}[113].

Indo-1 binds a single calcium atom in the same way as its predecessors, quin-2 and EGTA, using a four fingered claw ($-CH_2COO$) to chelate calcium[113,116]. Both the calcium-chelate and free forms of the dye are excited

FIGURE 2

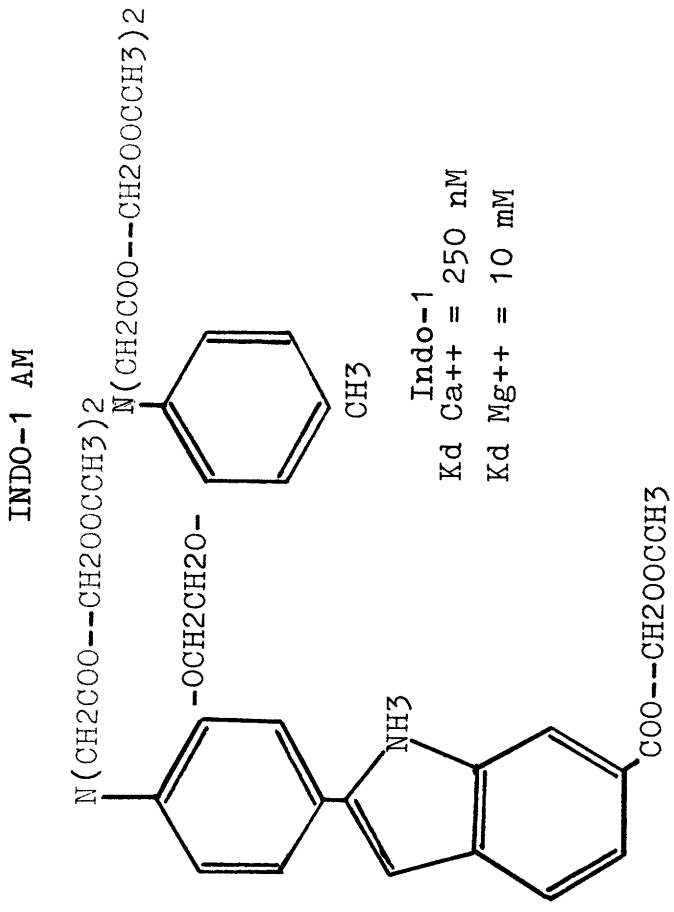
INDO-1 AM
N(CH2COO--CH2OOCCH3)2
N(CH2COO--CH2OOCCH3)2
-OCH2CH2O-
CH3
NH3
COO--CH2OOCCH3
Indo-1
Kd Ca++ = 250 nM
Kd Mg++ = 10 mM

FIGURE 2

Figure 2 shows the acetoxymethyl ester of indo-1. The five deesterification sites are indicated by the dotted lines (--).

maximally by ultraviolet light of nearly the same wavelength. The peak emission wavelength, however, shifts from 480 nm to 405 nm upon binding calcium. This shift in fluorescence allows a ratio of fluorescence intensities (405/480) to be determined independently of variations in the intracellular dye concentration, and cell size. The 405/480 ratio can be used as an indicator of changes in intracellar free calcium ion concentration or to calculate the actual intracellular free calcium concentration[113].

The equation relating the 405/480 ratio to the intracellular free calcium is derived as follows[113,60]

Absorption of Incident Light- Beer's Law[60]

1 $I = I_o * \exp(-2.3*E*C*L)$

I = intensity of light transmitted by solution of indo-1

I_o = intensity of incident light

E = extinction coefficient of indo-1

C = concentration of indo-1

L = path length of light through indo-1 solution

Fluorescence Equation[60]

2 $F = Q*f*d*(I_o-I)$

F = intensity of indo-1 fluorescence

Q = quantum efficiency of indo-1

f = fraction of indo-1 emission at the wavelength of interest

d = detector efficiency at the wavelength of interest

From equations 1 & 2

3 $F = Q*f*d*I_o*(1-\exp(-2.3*E*C*L))$

If $2.3*E*C*L \ll 1$ the case for most fluorescent measurements

then

4 $F = Q*f*d*I_o*2.3*E*C*L$

From equation 4 we note that

5 $F \sim C$

Using equation 5 [113]

6 $S_{f405} = \frac{\text{fluorescence of free dye at 405 nm}}{\text{free dye concentration}}$

7 $S_{f480} = \frac{\text{fluorescence of free dye at 480 nm}}{\text{free dye concentration}}$

8 $S_{b405} = \frac{\text{fluorescence of bound dye at 405 nm}}{\text{bound dye concentration}}$

9 $S_{b480} = \frac{\text{fluorescence of bound dye at 480 nm}}{\text{bound dye concentration}}$

where S_{f405}, S_{f480}, S_{b405}, S_{b480} are constants determined by the system.

10 $F_{405} = S_{f405}*C_f + S_{b405}*C_b$

C_f = concentration of free dye

C_b = concentration of bound dye

11 $F_{480} = S_{f480}*C_f + S_{b480}*C_b$

K_d Equation

12 $K_d = C_f*(Ca^{++})/C_b$

(Ca^{++}) = free calcium

From equation 10, 11, & 12

13 $$\frac{F_{405}}{F_{480}} = \frac{Sf405*C_f + Sb405*C_f*(Ca++)/K_d}{Sf480*C_f + Sb480*C_f*(Ca++)/Kd} = R$$

R = Ratio

Solving for (Ca++)

14 $$(Ca++) = \frac{K_d*(R-S_{f405}/S_{f480})*Sf480}{(S_{b405}/S_{b480}-R)*S_{b480}}$$

When the total calcium = 0, $C_b = 0$

15 $$Rmin = \frac{F_{405}}{F_{480}} = \frac{Sf405}{Sf480}$$

R_{min} = R at total calcium = 0

$$16 \quad S_{f480} = \frac{F_{480}}{C} \text{ at } (Ca^{++})=0$$

C = total dye concentration

At saturating (Ca^{++}) levels, $C_f = 0$

$$17 \quad R_{max} = \frac{F_{405}}{F_{480}} = \frac{S_{b405}}{S_{b480}}$$

R_{max} = R at saturating (Ca^{++}) levels

$$18 \quad S_{b480} = \frac{F_{480}}{C} \text{ at sat'd } (Ca^{++})$$

Substituting equations 15, 16, 17, and 18 into 14

$$19 \quad (Ca^{++}) = \frac{K_d*(R-R_{min})*F_{480},Ca^{++}=0}{(R_{max}-R)*F_{480},\text{sat'd } Ca^{++}}$$

$$20 \quad \text{let } S = \frac{F_{480},Ca^{++}=0}{F_{480},\text{sat'd } Ca^{++}}$$

The constants R_{min}, R_{max}, S are determined by the experimental set-up.

B. Verification of Indo-1 Fluorescence and Ca++ Binding Properties

Standard calcium solutions were prepared to verify the fluorescence properties of indo-1 and also for possible use as solutions for calculating calibration constants of the intracellular dye[112,118,119]. Since the K_d of the dye and the intracellular free Ca++ is in the nM range, it is necessary to be able to make solutions with the free Ca++ at this level. The technique developed by Moiesescu and Pusch using EGTA as a buffer was followed[112,118,119,151]. To use the buffers, it is necessary to know accurately the ratio of Ca++ to EGTA, thereby obtaining a good estimate of the free Ca++ concentration. Briefly, the technique involves the preparation of an EGTA:Ca++ solution in a 1:1 molar ratio; this solution is then mixed in varying proportions with EGTA alone to form the buffers. A known solution of Ca++, prepared from $CaCO_3$ baked in an oven at 500°F for 3 hours, was used to titrate a solution of equimolar EGTA and HEPES to the endpoint of 1:1 EGTA/Ca++. As Ca++ is added to the EGTA/HEPES, H+ is released from the EGTA causing the pH to drop as shown in Figure 3. At the equivalence point (1 EGTA: 1 Ca++), the pH abruptly ceases to drop as essentially no more H+ can be released by adding Ca++. The solution can be titrated through the equivalence point to locate it, and then back titrated with EGTA/HEPES. The

FIGURE 3

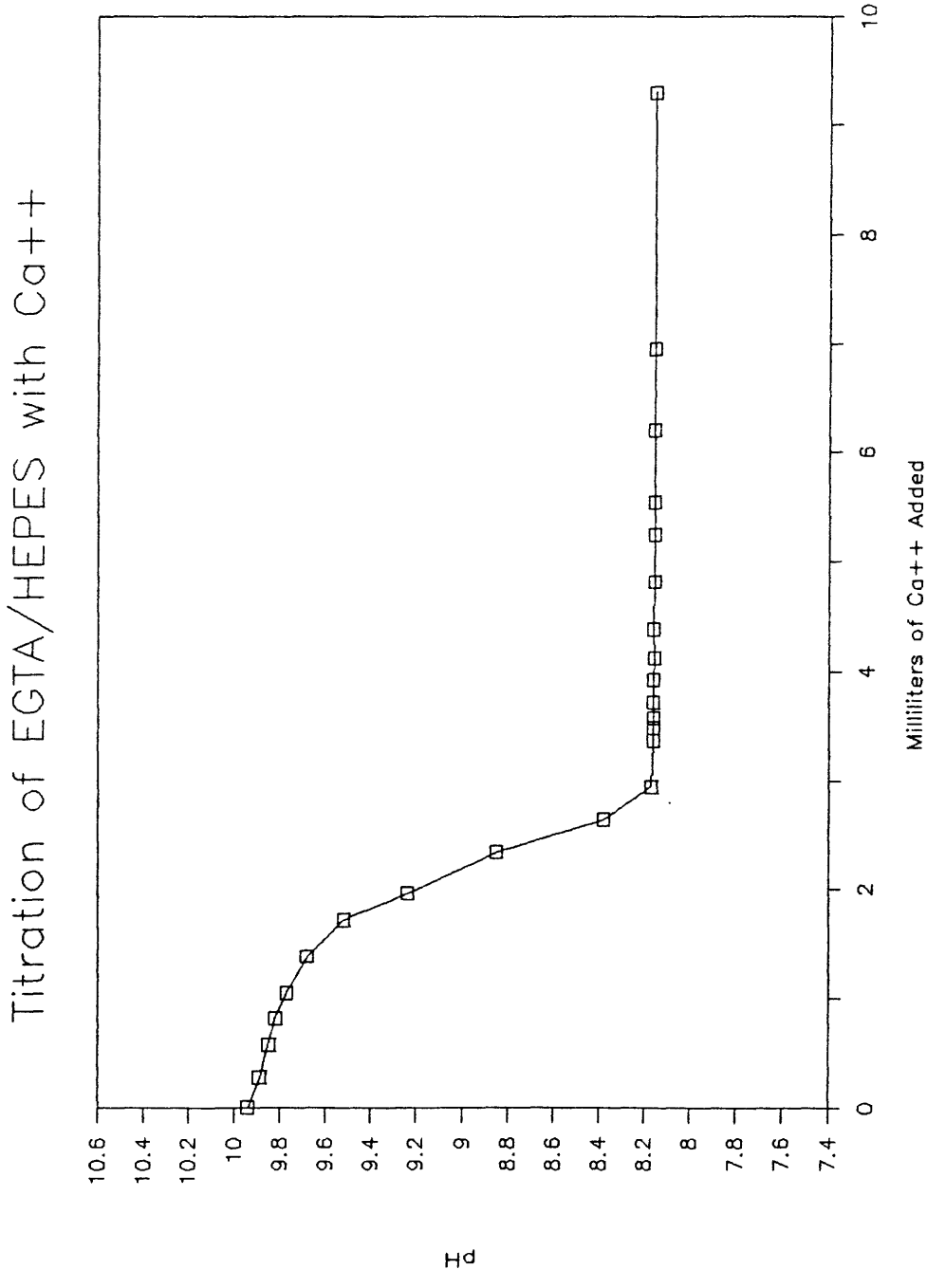
Titration of EGTA/HEPES with Ca++
pH
10.6
10.4
10.2
10
9.8
9.6
9.4
9.2
9
8.8
8.6
8.4
8.2
8
7.8
7.6
7.4
0
2
4
6
8
10
Milliliters of Ca++ Added

FIGURE 3

Figure 3 shows the titration of an equimolar EGTA/HEPES (10 mM) solution with a 260.59 mM Ca++ solution, pH 9.02. The equivalence point clearly occurs after 3 mls of the Ca++ solution have been added.

titration shown in Figure 3 illustrates the sharpness and existence of an end point and Figure 4 shows the actual titration and back-titrations used to prepare the standard 1:1 Ca++/EGTA solution. The average of the two endpoints was used to calculate the Ca++/EGTA concentration. The concentration of the EGTA/HEPES by gravimetric means was 1.6% greater than the estimate of the EGTA concentration obtained from the Ca++ titration. In order to verify independently the EGTA concentration and hence the Ca++:EGTA titration technique, a solution of EGTA was titrated with a standard 1N NaOH solution. This titration indicated that the gravimetric measurement was an overestimate of the true EGTA concentration by 2.1%. This compares well to the 1.6% figure obtained by the calcium titration. The small difference is probably due to experimental error and the possibility that the EGTA is contaminated with a small amount of non-tetraacetic acid, which titrates with base but does not chelate Ca++.

The standard Ca++ solutions were prepared from the stock Ca++/EGTA/HEPES solution and the stock EGTA/HEPES solution[118,119,151]. The final concentration of EGTA/HEPES (9.8 mM) was kept constant while the quantity of calcium was varied by varying the ratio of Ca++/EGTA/HEPES to EGTA/HEPES. Figure 5 shows the fluorescence emission of 2 uM indo-1 in various standard Ca++ solutions that were prepared by this technique. The

FIGURE 4

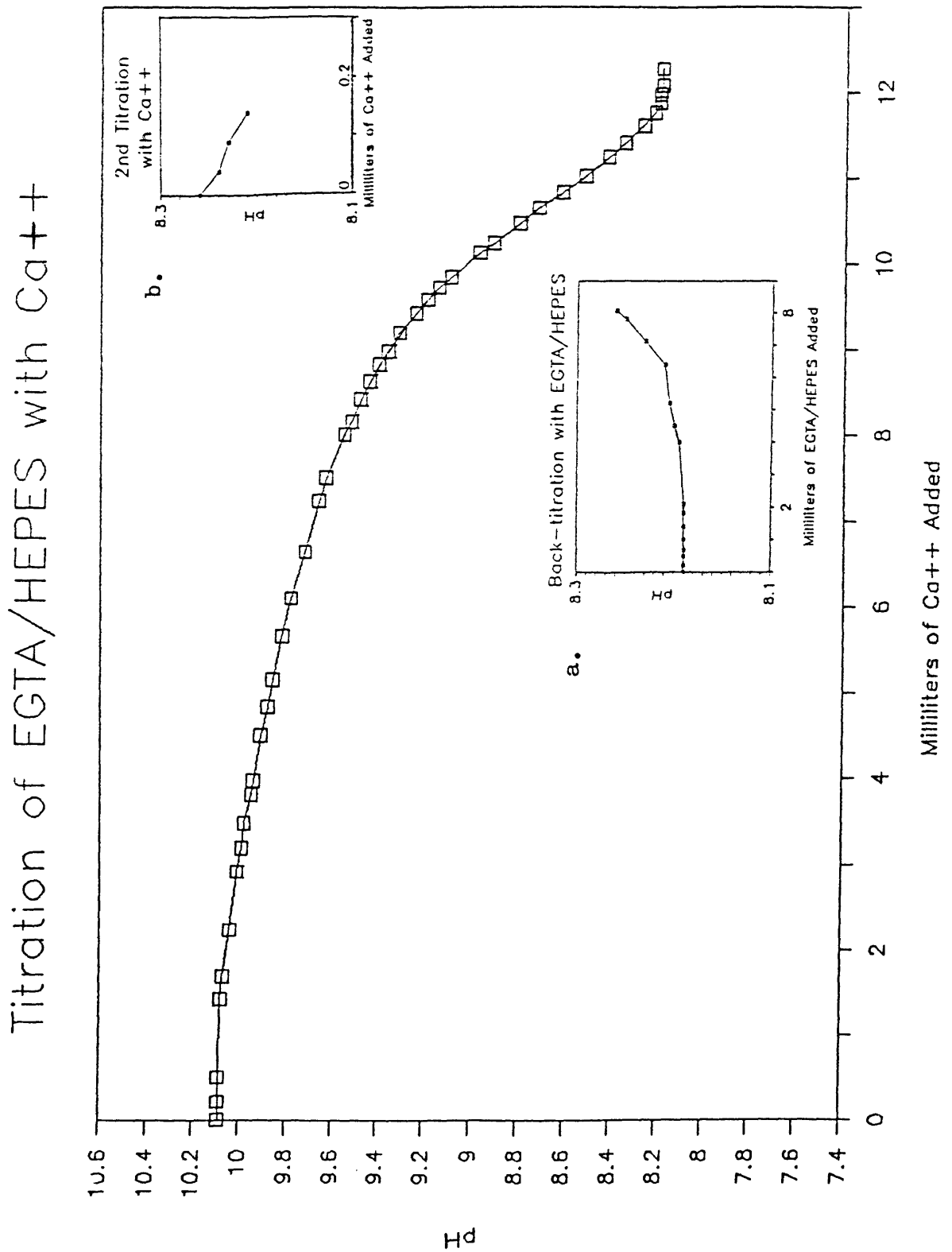
Titration of EGTA/HEPES with Ca++
pH
Milliliters of Ca++ Added
2nd Titration with Ca++
b.
Milliliters of Ca++ Added
Back-titration with EGTA/HEPES
a.
Milliliters of EGTA/HEPES Added

FIGURE 4

Figure 4 shows the titration of an equimolar EGTA/HEPES (20 mM) solution with a 253.13 mM Ca++ solution, pH 9.80. When the endpoint was reached the EGTA/HEPES/Ca++ solution was back-titrated through the equivalence point with 20 mM EGTA/HEPES, pH 10.10 (inset a). The final titration to the equivalence point with the 253.13 mM Ca++ solution is shown in inset b. The concentration of Ca++ and EGTA was calculated using the endpoints from the two titrations with Ca++.

FIGURE 5

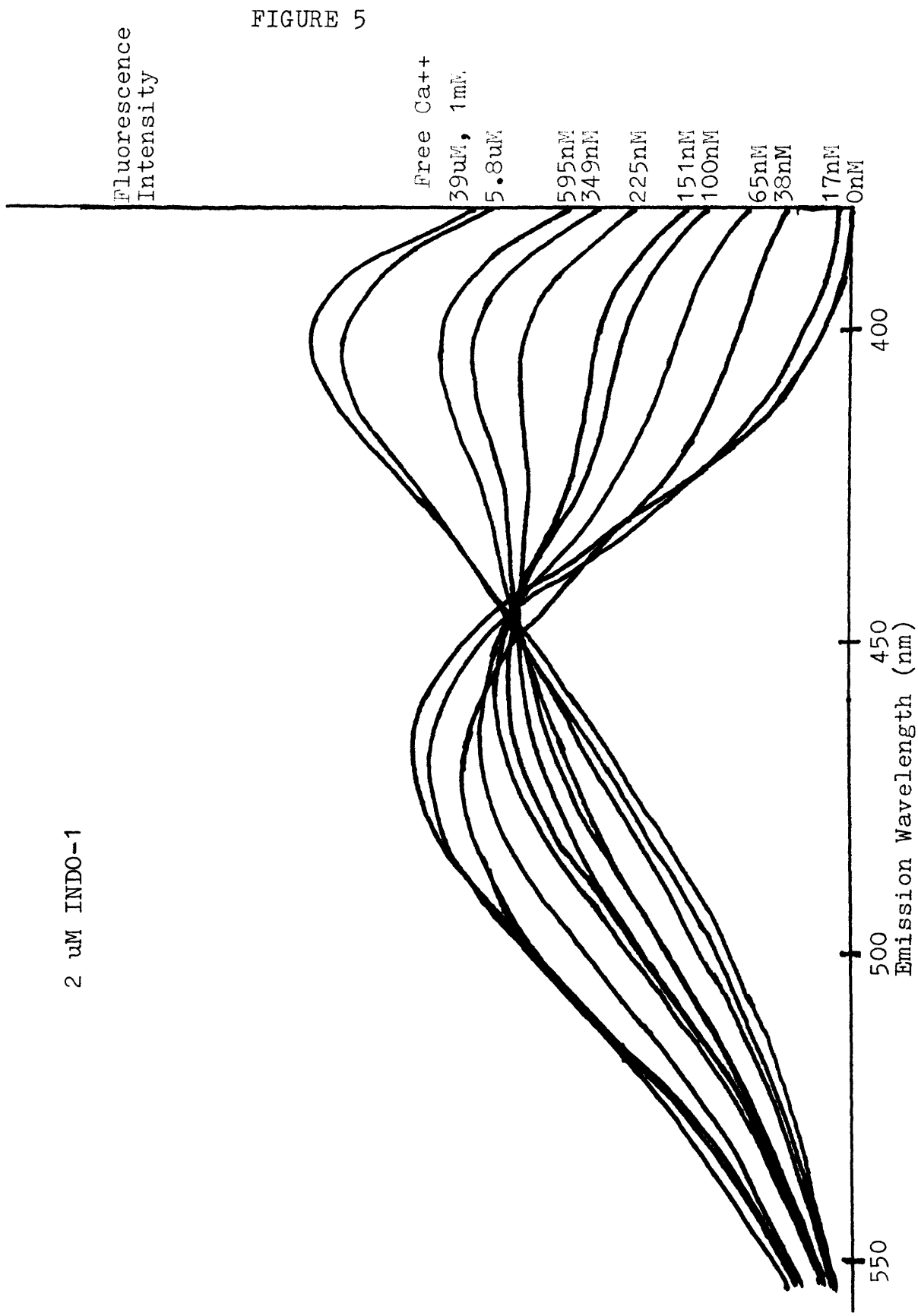
Fluorescence Intensity
Free Ca++
39uM, 1mM
5.8uM
595nM
349nM
225nM
151nM
100nM
65nM
38nM
17nM
0nM
2 uM INDO-1
400
450
500
550
Emission Wavelength (nm)

FIGURE 5

ECBS solutions with EGTA and Ca++ and 2 uM indo-1 were prepared to give the indicated free calcium concentrations. Fluorescent emission spectra were recorded using an excitation wavelength of 350 nm.

equation, K_d = (EGTA)*(Ca++)/(EGTA-Ca) = 151 nM (at pH 7.2, 20°C) was used to calculate the free (Ca++) in the standard solutions[113]. Figure 6 shows the Ca++ concentration of the standard solutions plotted against the Ca++/K_d calculated from the ratio of indo-1 fluorescent intensities. The Ca++/K_d is given since the K_d for indo-1 under the conditions used here has not been published.

C. Indo-1 AM Loading

Since cells were loaded with an esterified form of indo-1, it was important to verify that the cells metabolised the dye to the appropriate form[120]. Verification was accomplished by loading the cells with the indicated concentration of dye for the indicated times, washing them twice with PBS, lysing them by resuspending them at a concentration of 10^6 cells/ml in extracellular buffered salt solution (ECBS) with 0.02% triton and either 1 mM Ca++ or 5 mM EGTA and thereby releasing intracellular dye into the supernatant. Emission spectra were then taken to assess the dye's fluorescent characteristics in the presence and abscence of Ca++. Indo-1 AM fluoresces maximally at 445 nm and is unresponsive to changes in the extracellular calcium concentration.

FIGURE 6

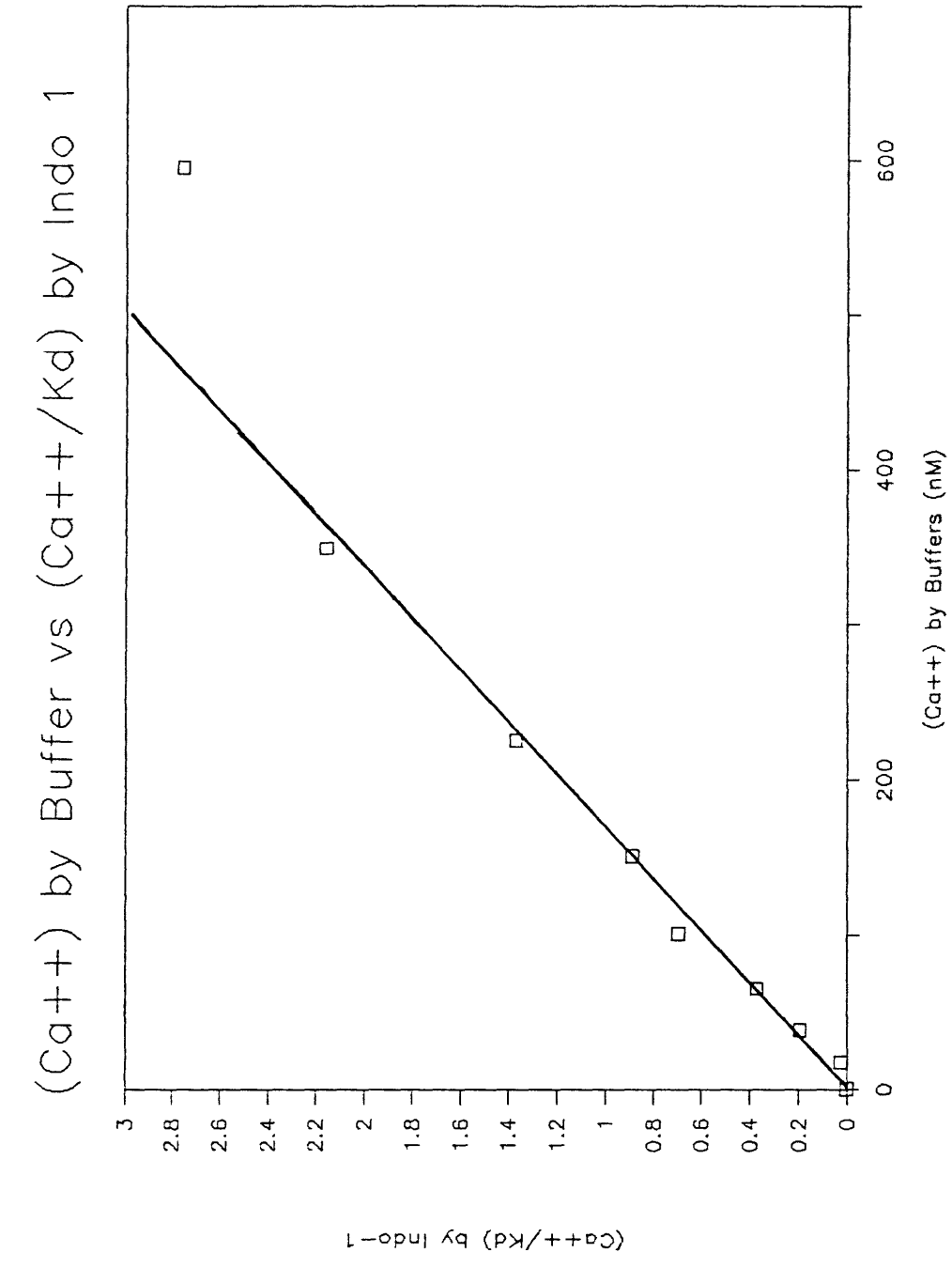
(Ca++) by Buffer vs (Ca++/Kd) by Indo 1
(Ca++/Kd) by Indo-1
(Ca++) by Buffers (nM)
0
0.2
0.4
0.6
0.8
1
1.2
1.4
1.6
1.8
2
2.2
2.4
2.6
2.8
3
0
200
400
600

FIGURE 6

The Ca++/K_d was calculated from the 405/480 ratio of the indo-1 fluorescence spectra of Figure 5 (K_d is for indo-1). Figure 6 plots this quantity versus the free Ca++ concentration calculated from the EGTA-Ca++ equilibrium. The linearity of the points shows the ability of indo-1 to measure the Ca++ ion concentration.

The indo-1 AM molecule is difficult to synthesize[113]. This was reflected by the fact that the earliest lots received were not fully metabolizable by 2C cells, a CTL clone (as judged by spectra of dye released from lysed cells). Therefore all batches were checked for metabolism by 2C cells before use in experiments. Lots purchased later in the study were free of this problem.

Lower concentrations of dye for longer periods of time seemed to be better metabolized than higher concentrations for shorter times. In general the lowest concentration of indo-1 AM that could be used with a given cell line was limited by cellular autofluorescence and nonspecific dye leakage. Tumor cells leaked the dye faster than T cells and were generally incubated first in 3-5 uM indo-1 AM for 1.5 hours and then for 0.5 to 1.5 hours in the absence of the dye. CTLs were incubated first with and then without 0.5-1.5 uM indo-1 AM for the same time periods. The general procedure for loading cells consisted of:

1. Initial loading with the dye in RPMI + 45 mM HEPES, 37°C, 5% CO_2 incubator.
2. Wash 1X
3. A final incubation without indo-1 AM in K medium, 37°C

The second incubation without indo-1 AM was to allow time for unmetabolized dye to be metabolized or to diffuse back

into the extracellular medium.

As shown in Figure 7, the T cell clone, 2C, appeared to fully metabolize the dye. Lysates of these cells in 1 mM Ca++ had a peak fluorescence at 405 nm and those in 5 mM EGTA a peak at 460 nm. There is no peak or shoulder at 445 nm indicating that the dye is well metabolized. The unmetabolized dye fluoresces maximally at 445 nm. But such a shoulder was seen in lysates of some tumor cells indicating that a substantial fraction of the dye was still esterified (Figure 8). While this shoulder may effect quantitative estimates of the ICF Ca++, it does not effect qualitative changes in the 405/480 ratio. When intact Yac-1 cells were incubated with 3 uM ionomycin in the presence of 5 mM EGTA or 1 mM Ca++, resulting in low and high intracellular calcium concentrations, the 405/480 ratio was 0.28 and 2.6, respectively by flow cytometry. These numbers are almost identical to the maximum and minimum ratio obtained with 2C cells under similar conditions. These results demonstrated the feasibility of using the 405/480 ratio to measure the intracellular free calcium concentrations.

D. Calculation of Intracellular Dye Concentration

High intracellular dye concentrations can buffer (Ca++) changes[28,114,121]. A buffering effect in Jurkat

FIGURE 7

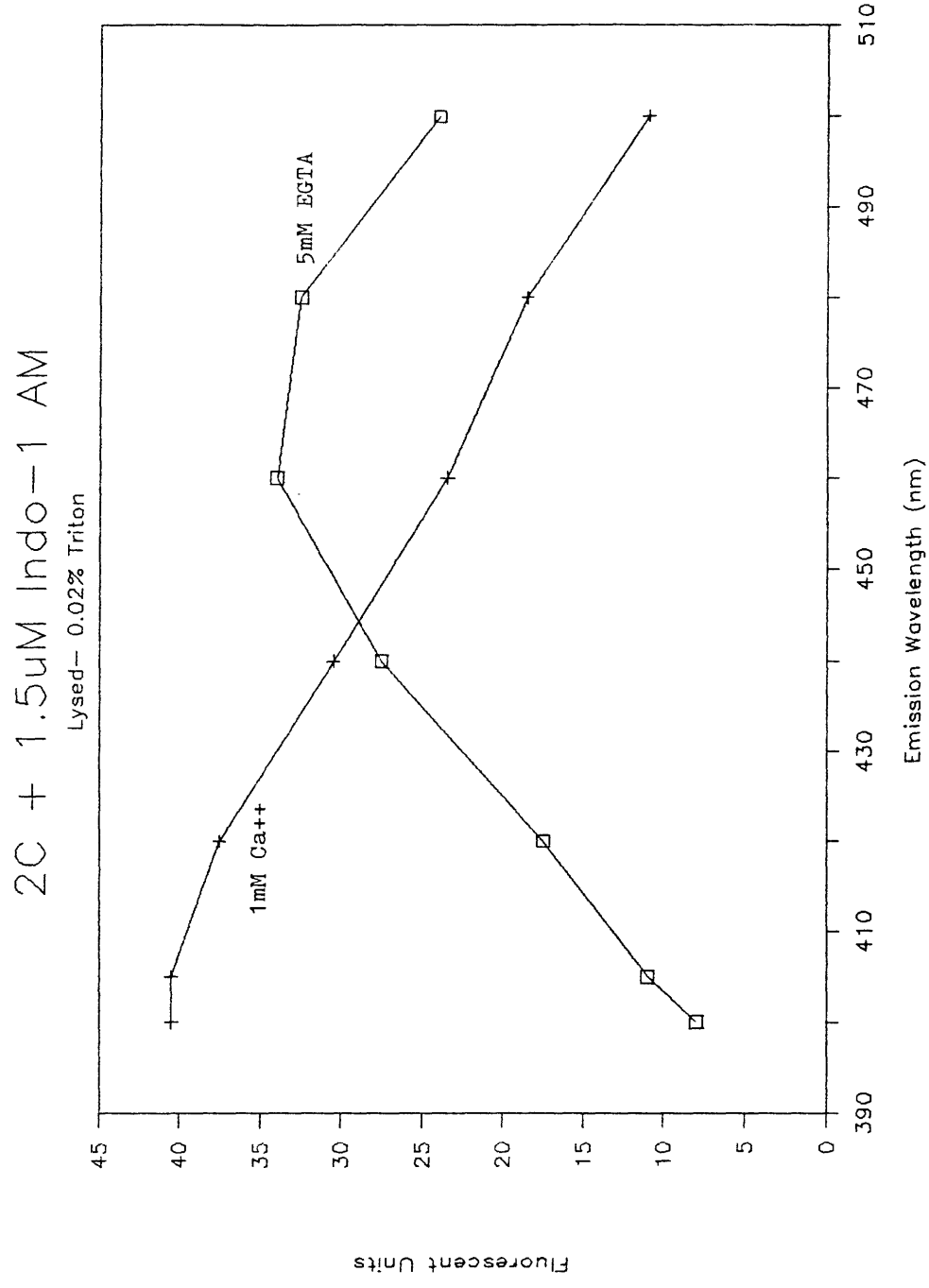
2C + 1.5uM Indo-1 AM
Lysed- 0.02% Triton
1mM Ca++
5mM EGTA
Fluorescent Units
Emission Wavelength (nm)
0
5
10
15
20
25
30
35
40
45
390
410
430
450
470
490
510

FIGURE 7

2C were loaded with 1.5 uM indo-1 AM and then lysed at a concentration of 10^6 cells/ml in ECBS with 0.02% triton and either 1 mM Ca++ or 5 mM EGTA. Cell lysate solutions were excited at 350 nm and emission spectra were recorded between 400 and 500 nm. Emission spectra of cells not loaded with indo-1 and lysed under the same conditions were also taken (blank sample). Figure 7 displays the spectra of dye loaded and lysed cells after subtraction of the blank sample. Neither curve has a shoulder 445 nm indicating that little indo-1 AM is present.

FIGURE 8

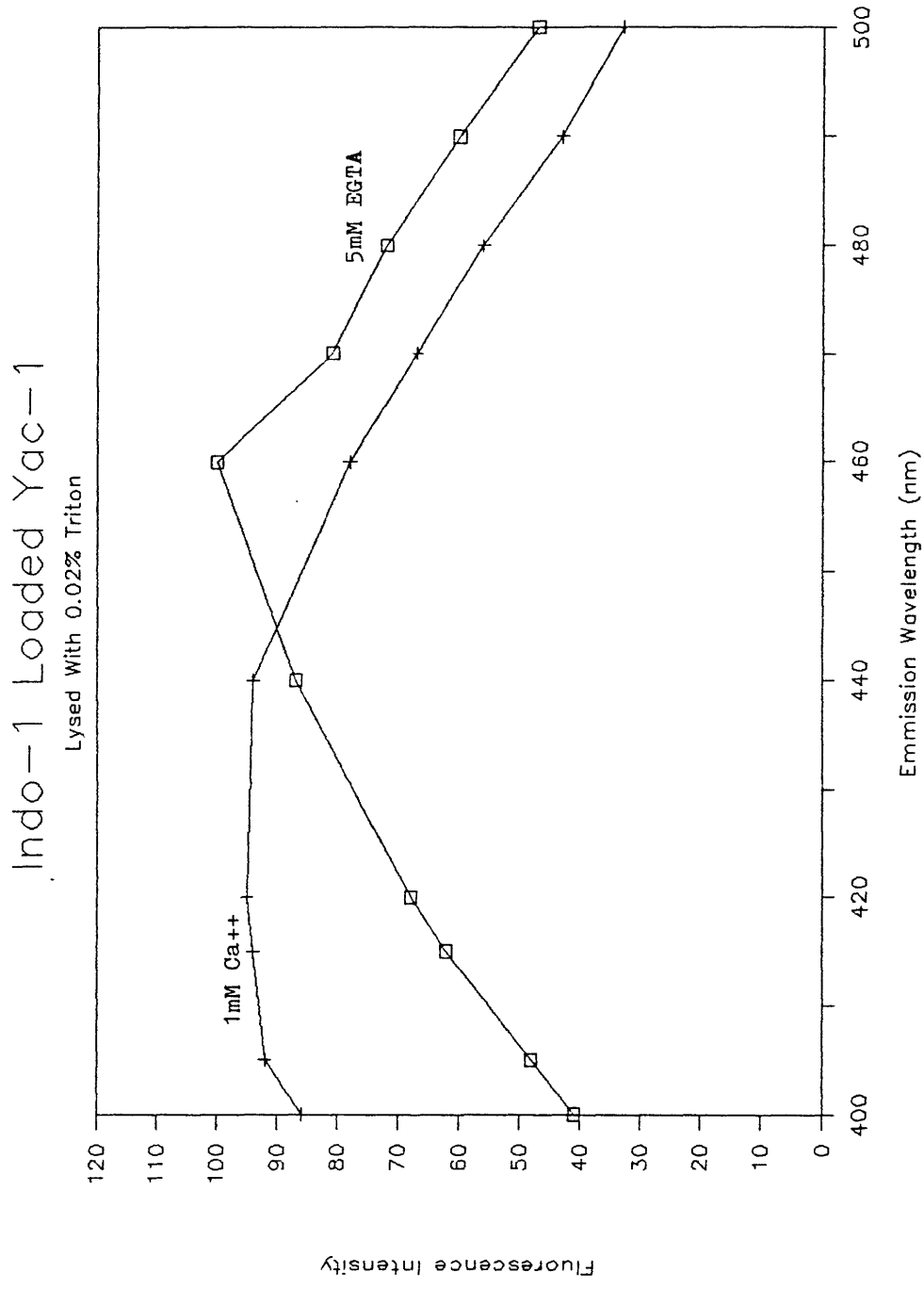
Indo-1 Loaded Yac-1
Lysed With 0.02% Triton
5mM EGTA
1mM Ca++
Fluorescence Intensity
Emmission Wavelength (nm)
120
110
100
90
80
70
60
50
40
30
20
10
0
400
420
440
460
480
500

FIGURE 8

Figure 8 was constructed in the same way as Figure 7 using Yac-1 cells loaded with 5 uM indo-1 AM. The curve with 1 mM Ca++ shows a shoulder at 440 nm indicating that indo-1 AM is present in the solution.

cells was substantial with quin-2 at 780 pMoles/10^6 cells but negligible with the dye at 60 pMoles/10^6 cells[28]. It is therefore important to estimate the intracellular dye concentration. This concentration was measured in 2C cells after loading them with 1, 2, and 5 uM indo-1 AM (using the standard loading procedure previously described). The cells were lysed with 0.02% triton in ECBS solution containing either 3 mM EGTA or 1 mM Ca++. The spectra of these cells was then compared to standards made from the potassium salt of indo-1. The fluorescence was measured at 480 nm for samples in EGTA and at 405 nm for samples in Ca++ was measured. The two values were averaged and compared to the same value for the standards. Figure 9 shows the standard curve and the fluorescent intensity of the lysed cells (corrected for cell concentration). The quantity of dye per 10^6 cells calculated from the standard curve is displayed in the following table

Table 2

Intracellular dye concentration

Indo-1 AM loading	pMoles/10^6 cells
1uM	40, 26
2uM	68
5uM	148

FIGURE 9

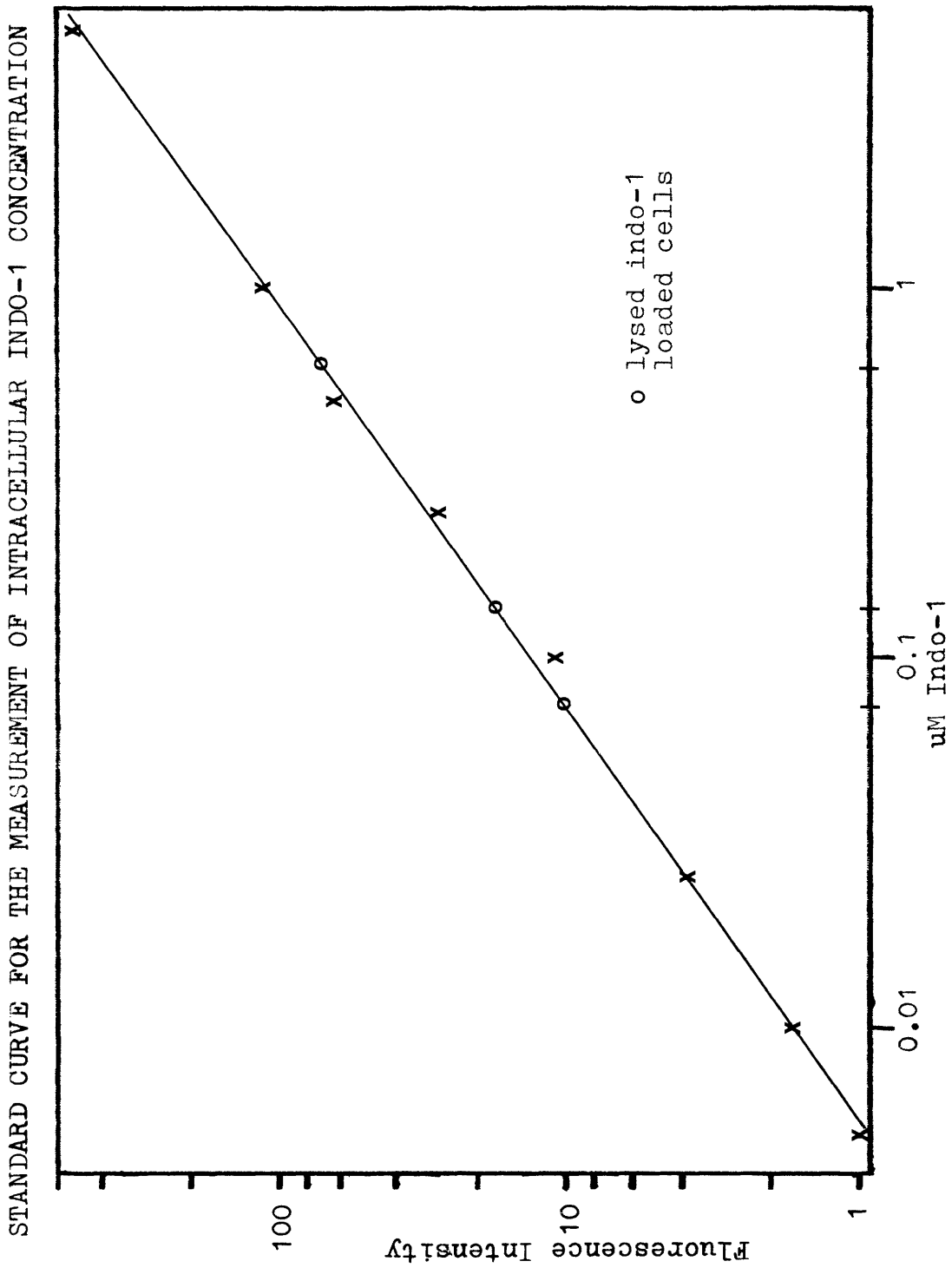
STANDARD CURVE FOR THE MEASUREMENT OF INTRACELLULAR INDO-1 CONCENTRATION
Fluorescence Intensity
100
10
1
0.01
0.1
1
uM Indo-1
o lysed indo-1
loaded cells

FIGURE 9

Figure 9 shows an indo-1 standard curve. The points represented by an X were obtained from indo-1 solutions of known concentration excited at 350 nm. The points represented by an O are the fluorescent intensities measured from cell lysates (10^6cells/ml) after background subtraction. The x-axis of these points was used to calculate the intracellular indo-1 concentration.

Assuming a radius as indicated, the cells are calculated to have the following intracellular dye concentration.

Table 3

Intracellular dye concentration

Indo-1 AM loading	radius = 5um	8um
1uM	70, 46 uM	17, 11 uM
2uM	120 uM	29 uM
5uM	260 uM	63 uM

If the T cell clones and Jurkat cells have similar intracellular volumes, the intracellular dye in the 2C cells should have had no significant buffering effect[28]. It is not unreasonable to assume that the Jurkat cells and T cell clones have similar volumes since the T cells are blasts and microscopically appear as large as most tumor cell lines. Based on these results lymphocytes were loaded for all experiments with dye at 0.5-1.5 uM and other cell lines were loaded with indo-1 AM at concentrations that gave them approximately the same fluorescence intensity as 2C cells loaded at 1 uM. Tumor cells were loaded at 3-5 uM; the need for a higher loading concentration with tumor cells may have been due to slower uptake and metabolism of the dye and a higher leakage rate. These intracellular dye concentrations give very minimal buffering according to Imboden et al and as

evident (see Figure 25 below) by the rapid rise and recovery of the intracellular calcium level in tumors in respose to lytic granules (<30 seconds for P815 cells)[23].

E. Effect of Calcium Chelating Dyes on Cellular Function and Death

It is important to know whether intracellular indo-1 (and quin-2) affected the cellular events that were being measured. Figures 10, 11, and 12 show that intracellular quin-2 and indo-1 had no effect on:

1. The ability of P815-indo-1 cells to be killed by 2C cells.
2. The ability of RDM4-quin-2 cells to be lysed by cytotoxic granules.
3. The ability of 2C-indo-1 cells and 2.1.1 -indo-1 cells (both CTLs) to kill P815 cells.

In addition indo-1 had no effect on lysis of RDM4 cells by cytotoxic granules, and quin-2 had no effect on the lysis of RDM4, P815, and Yac-1 cells by granules or ionomycin. In particular, we looked for the effect described by Carney et al with complement[121]. They showed that high levels of intracellular quin-2 enhanced the susceptibility of cells to complement lysis by abolishing a sharp rise in intracellular calcium. The spike in calcium was thought to be a signal initiating membrane repair. That these

FIGURE 10

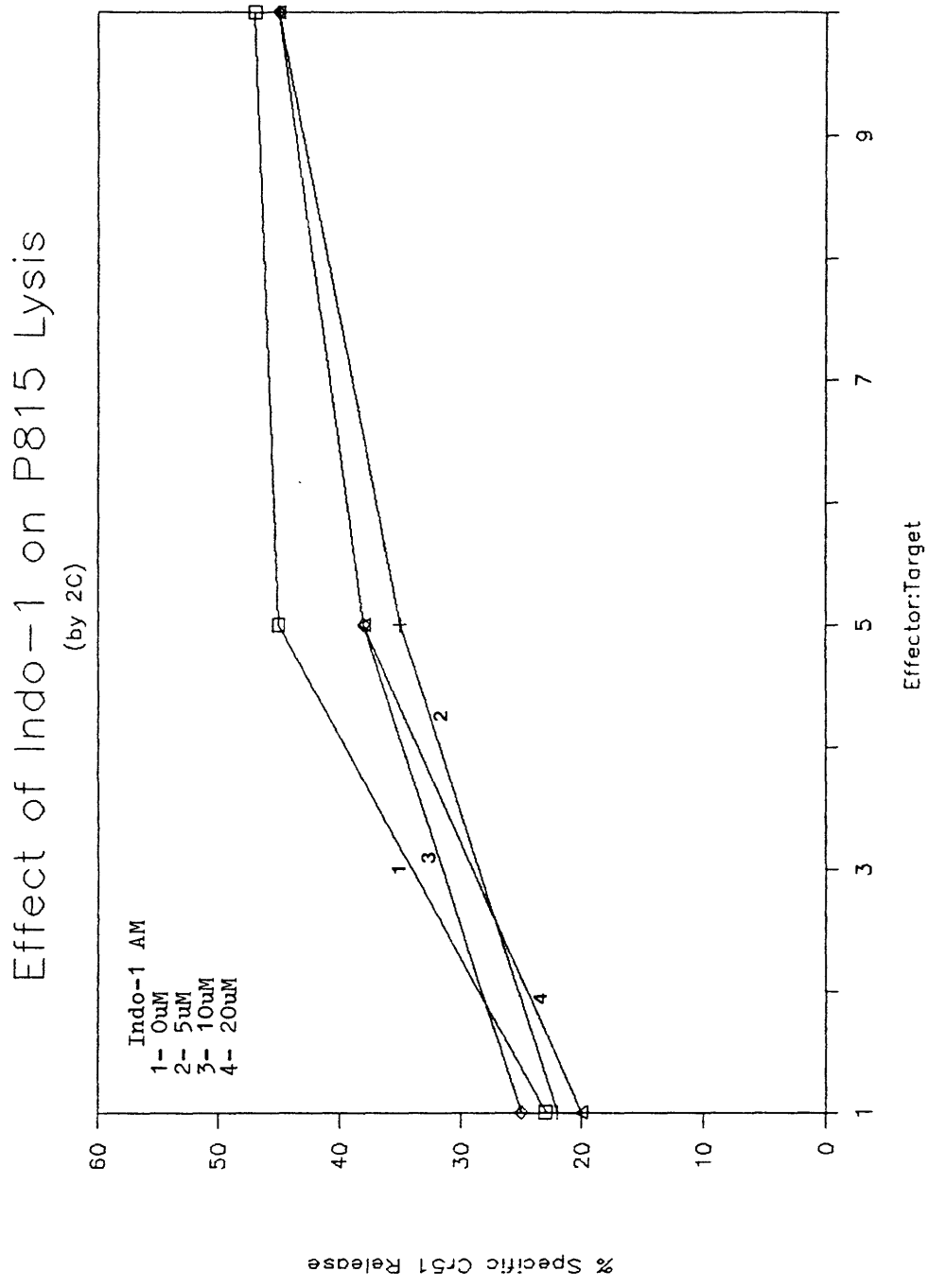
Effect of Indo-1 on P815 Lysis
(by 2C)
Indo-1 AM
1- 0uM
2- 5uM
3- 10uM
4- 20uM
% Specific Cr51 Release
Effector:Target
0
10
20
30
40
50
60
1
3
5
7
9

FIGURE 10

P815-Cr^{51} cells were loaded with indo-1 AM at the concentrations indicated in the upper corner of the graph. The ability of 2C to kill these dye-loaded cells was measured at E:T ratios of 1, 5, and 10.

FIGURE 11

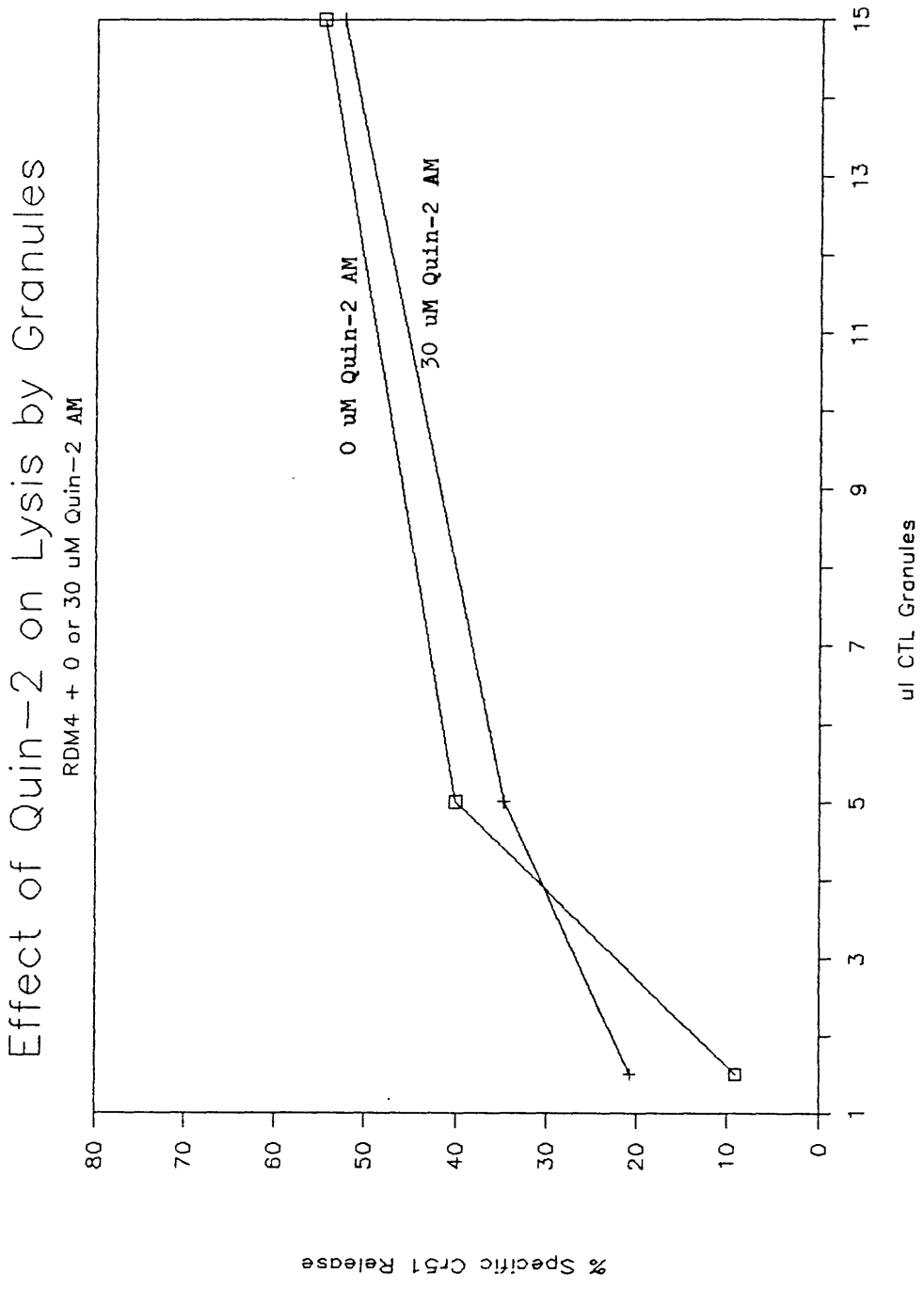
Effect of Quin-2 on Lysis by Granules
RDM4 + 0 or 30 uM Quin-2 AM
0 uM Quin-2 AM
30 uM Quin-2 AM
% Specific Cr51 Release
ul CTL Granules
80
70
60
50
40
30
20
10
0
1
3
5
7
9
11
13
15

FIGURE 11

RDM4-Cr^{51} cells were loaded with either 0 or 30 uM quin-2 AM. Figure 11 shows the susceptibility of the cells to cytolytic granules isolated from 3H2 cells.

FIGURE 12

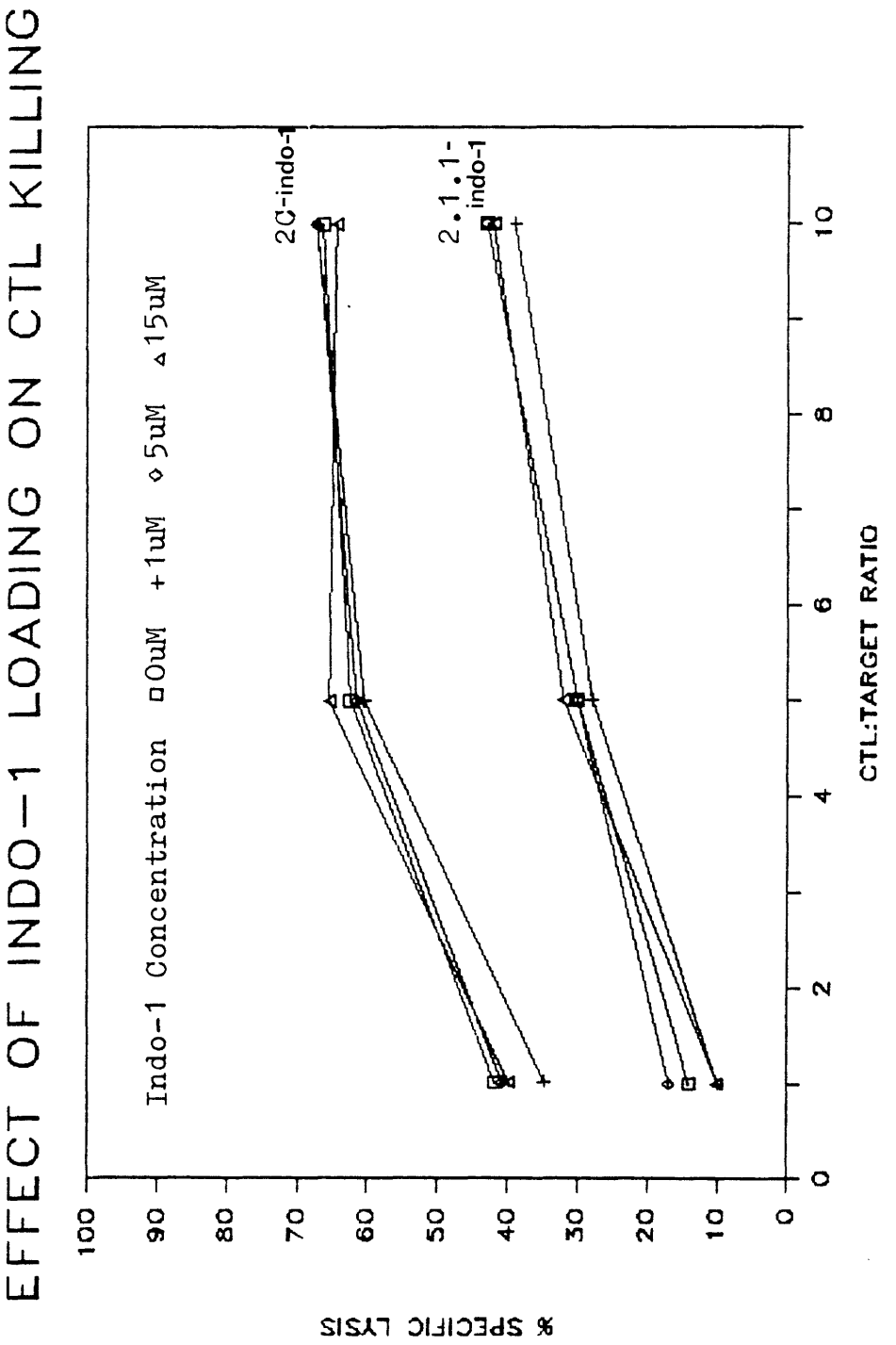
EFFECT OF INDO-1 LOADING ON CTL KILLING
Indo-1 Concentration □0uM +1uM ◇5uM △15uM
2C-indo-1
2.1.1-indo-1
% SPECIFIC LYSIS
CTL:TARGET RATIO
0
10
20
30
40
50
60
70
80
90
100
0
2
4
6
8
10

FIGURE 12

2C and 2.1.1 cells were loaded with indo-1 AM at the indicated concentrations. The ability of these dye-loaded cells to kill P815-Cr^{51} cells was measured at E:T ratios of 1, 5, and 10.

results are in disagreement with those reported here is not surprising since complement and CTLs appear to cause cell death in different ways. In addition the buffering capacity of these dyes is exhausted in a very short time (<2-3 minutes) even at very high intracellular concentrations of dye[28]. The calcium influx can be blunted briefly but not prevented, and death due to a calcium influx would likewise not be prevented. Indo-1 AM loading concentrations for experiments were usually 1-5 uM, much less than the peak concentration of 20 uM used in the above experiments.

IV. Flow Cytometry

A. Introduction

Flow cytometry allows measurements to be made on large numbers of individual cells[122,158]. As shown in Figure 13, cells flow in single file in a central fluid core surrounded by a sheath fluid; the latter fluid flows in a laminar pattern, maintaining the position of the cells in the center of the fluid stream. The cells are illuminated by light sources (usually arc lamps or lasers) that are focussed to a spot slightly larger than the cell. Light is then scattered and fluoresced from the cell. The signal is processed with filters, and dichroics and imaged onto detectors, photomultiplier tubes (PMTs) or photodiodes. The electronic information is amplified, and processed[124]. Feature extraction generally consists of "gating" and simple calculations but may be quite sophisticated[123]. Data is usually displayed as histograms of light intensity vs cell number or X-Y plots between other parameters.

Flow cytometry offers many advantages. It is capable of examining large numbers of cells in a very short time (typically 100-400 cells/second.) Cells are interrogated individually so that population distributions instead of population averages are recorded. Multiple measurements can be recorded for each cell simply by using dichroics,

FIGURE 13

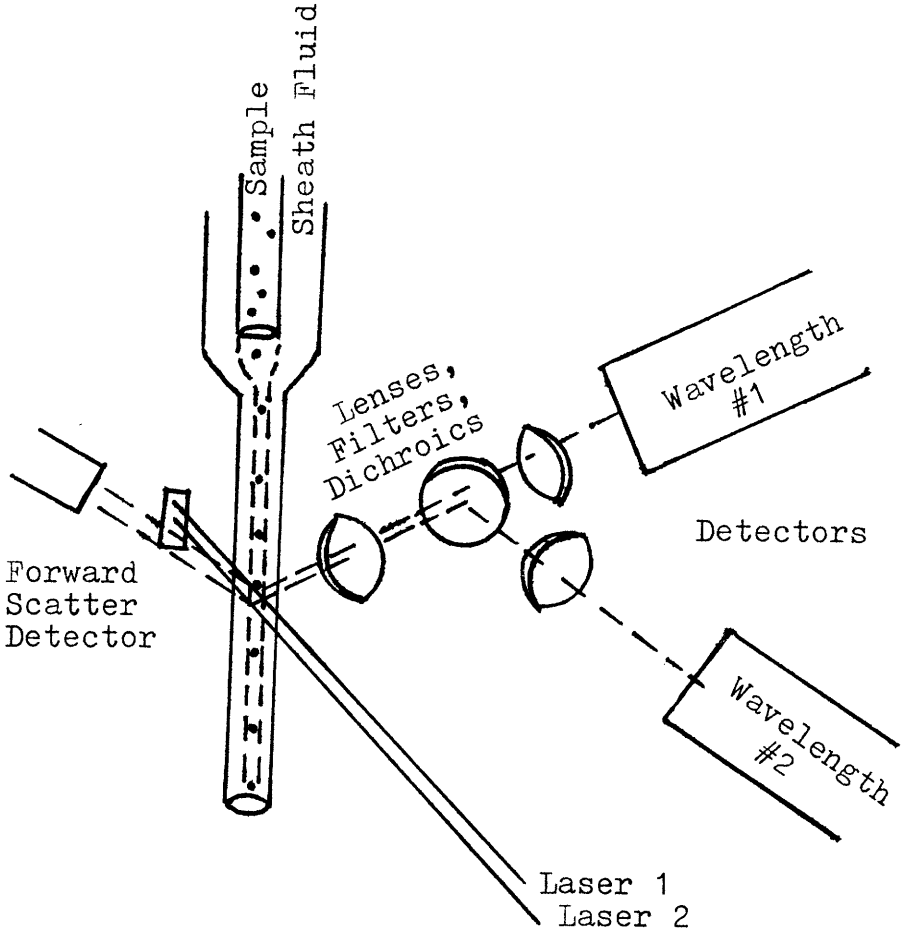
Sample
Sheath Fluid
Lenses,
Filters,
Dichroics
Wavelength
#1
Detectors
Forward
Scatter
Detector
Wavelength
#2
Laser 1
Laser 2

FIGURE 13

Figure 13 shows the orientation of the light sources (lasers) to the the light collection pathways in flow cytometry.

mirrors and more than one detector. Correlations between two or more different events can then be established. Errors due to leakage of dye into the extracellular media can be eliminated by electronic processing e.g. "background subtracters." For these reasons it is an excellent tool for identifying subpopulations of cells. These subpopulations can then be separated from other cells electronically or physically. Electronic separation is done by "gating," which allows one to select a subset of cells and examine their properties independently from the total population of cells. Physical isolation involves sorting which uses a piezoelectric transducer and electrically charged plates to break the flow stream into charged droplets and direct them to the appropriate container[125].

B. Flow Cytometry System and Set-Up

Flow cytometry was done with a Systems 50H Cytofluorograph from Ortho Diagnostic Systems linked to a 2150 computer. Indo-1 was excited with the 351-364 nm lines (70 mW) of a 5 watt, Coherent argon ion laser. Measurements of indo-1 alone used a blue reflecting dichroic (50% at 455 nm) to split the 405 and 480 nm fluorescent signals. The 405 nm signal was then collected using a 393-409 nm bandpass filter and the 480 nm signal with a 440-495 bandpass filter. Forward scatter was

collected using a blue reflecting dichroic (50% at 500 nm). The selection of these filters is discussed in the next section. The physical set-up of the flow cytometer is illustrated in Figure 14.

The UV forward scatter signal was used to gate debris from cells (Figure 15a). Cells meeting the forward scatter gate i.e. within window 1 of the forward scatter histogram, were displayed on a cytogram or plot of 405 nm fluorescence vs 480 nm fluorescence. Region 1 of the 405 vs 480 plot served as a gate for the ratio histogram (Figure 15b). This gate prevented unstained cells or cells with low quantities of indo-1 from being displayed on the ratio histogram. The ratio of the 405 fluorescence to the 480 fluorescence of all cells passing through the two gates was calculated digitally, multipled by 300, and displayed on the ratio histogram. The factor of 300 was used so the ratio would fit on the fixed scale (1-1000) of the histogram. Linear axes were used for all data.

Optical alignment of the flow cytometer was accomplished prior to every experiment with fluorescent beads. Initial alignment used 3 um diameter, UV-excited, green-fluorescent beads. With the 405 and 480 filters removed, the green fluorescence and UV right angle scatter signal of the beads could be used to optimize the signal received by the 405 and 480 PMT. In addition the forward scatter signal of the beads was used to align the optics

FIGURE 14

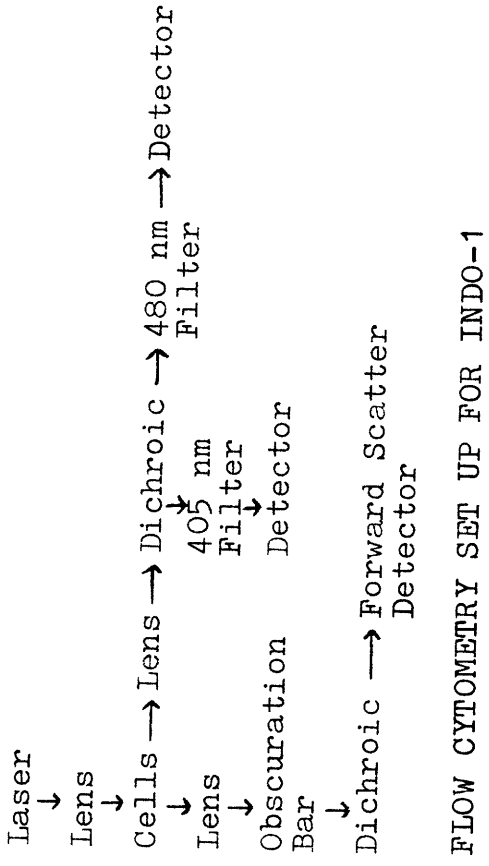

FLOW CYTOMETRY SET UP FOR INDO-1

FIGURE 14

Figure 14 shows the light paths, and filter and dichroic placement for indo-1 measurements on the flow cytometer.

FIGURE 15

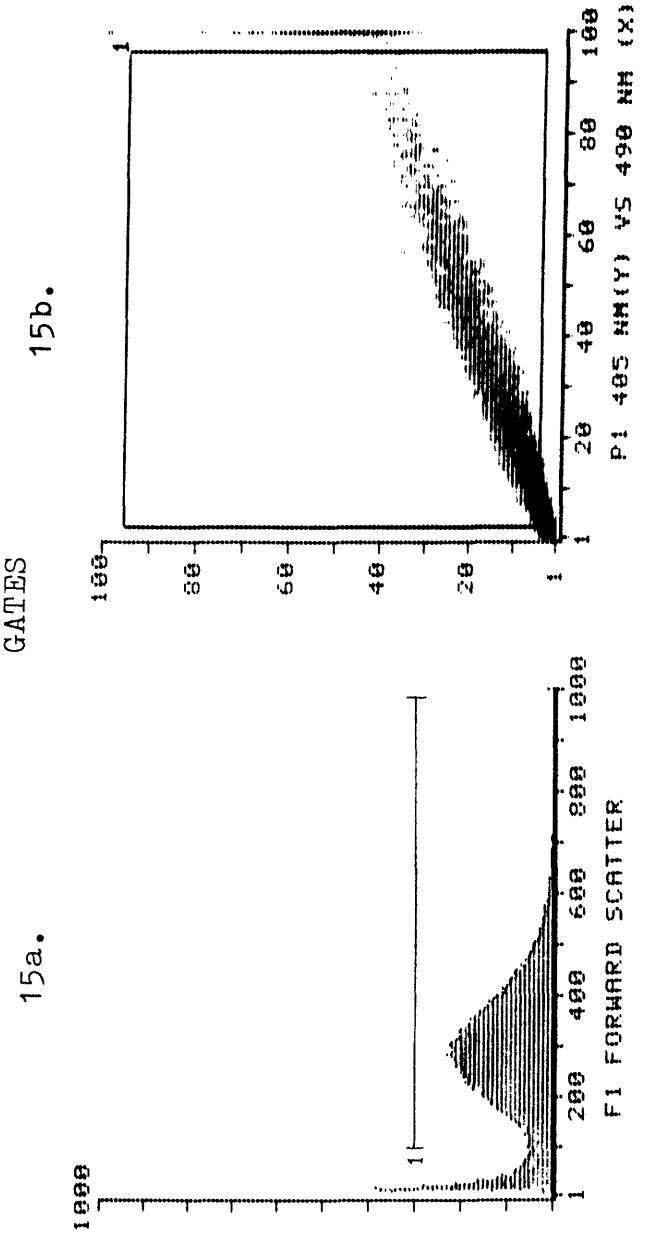

FIGURE 15

Figure 15a is a histogram of the forward scatter intensities of indo-1 loaded 2C cells. Region 1 indicated by the line on the graph is the gate. For this example, objects with a forward scatter intensity between 100 and 1000 were used for measurements of the 405 and 480 nm fluorescence intensities. Figure 15b is a graph of the 405 nm fluorescence intensity (y-axis) versus the 480 nm fluorescence intensity (x-axis). Each dot represents a cell so that darker areas indicate a higher density of cells. Region 1, the large box, is the indo-1 gate. A 405/480 ratio is calculated only for cells with a 405 and 480 fluorescent intensity inside the box. A circular region for this gate rather than a box was used for experiments. This is seen in later figures.

leading to the forward scatter PMT. These beads were used for initial alignment because they have a tighter distribution in size and fluorescent intensity than do cells or reticulocyte beads. The latter were originally designed as alignment standards for the detection of immature red blood cells containing ribosomes, i.e. reticulocytes. Because of their size (10 um diameter) and fluorescence between 360 and 500 nm when UV excited, the reticulocyte beads proved to be excellent tools for alignment of the flow cytometer prior to indo-1 measurements. Figure 16 shows the spectra of these beads when excited at 350 nm. Their intensities at 405 and 480 nm are similar to those of indo-1 stained cells; hence they allow the PMT gains to be set close to that used for cells. Figure 17 shows the 405 vs 480 nm cytogram and ratio histogram of reticulocyte beads at gain settings used for 2.1.1 cells that were loaded with indo-1 AM at 1 uM.

C. Indo-1 Filter Selection

Filters for flow cytometry were selected to split and bracket the 405 and 480 nm emission wavelengths. A dichroic with the following properties was chosen to direct the incoming light to the appropriate PMT, 470nm- 99% transmittance, 455nm- 50% transmittance and reflectance, 400nm- 99% reflectance. Several filters were

FIGURE 16

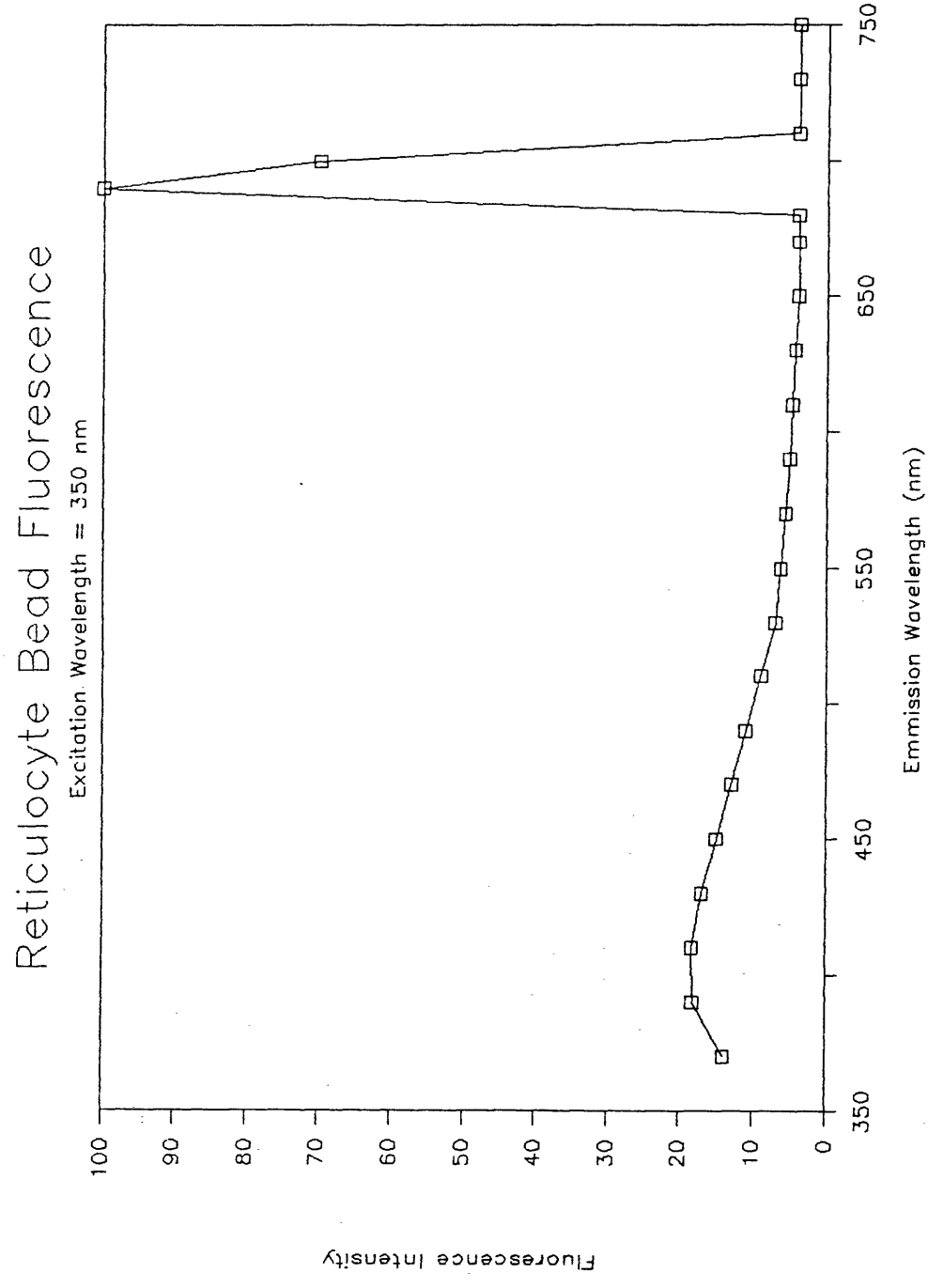
Reticulocyte Bead Fluorescence
Excitation Wavelength = 350 nm
Fluorescence Intensity
100
90
80
70
60
50
40
30
20
10
0
350
450
550
650
750
Emmission Wavelength (nm)

FIGURE 16

Reticulocyte beads were diluted into distilled water and excited at 350 nm in a spectrofluorimeter. Figure 16 shows the fluorescent emission spectra.

FIGURE 17

RETICULOCYTE BEADS

17a.

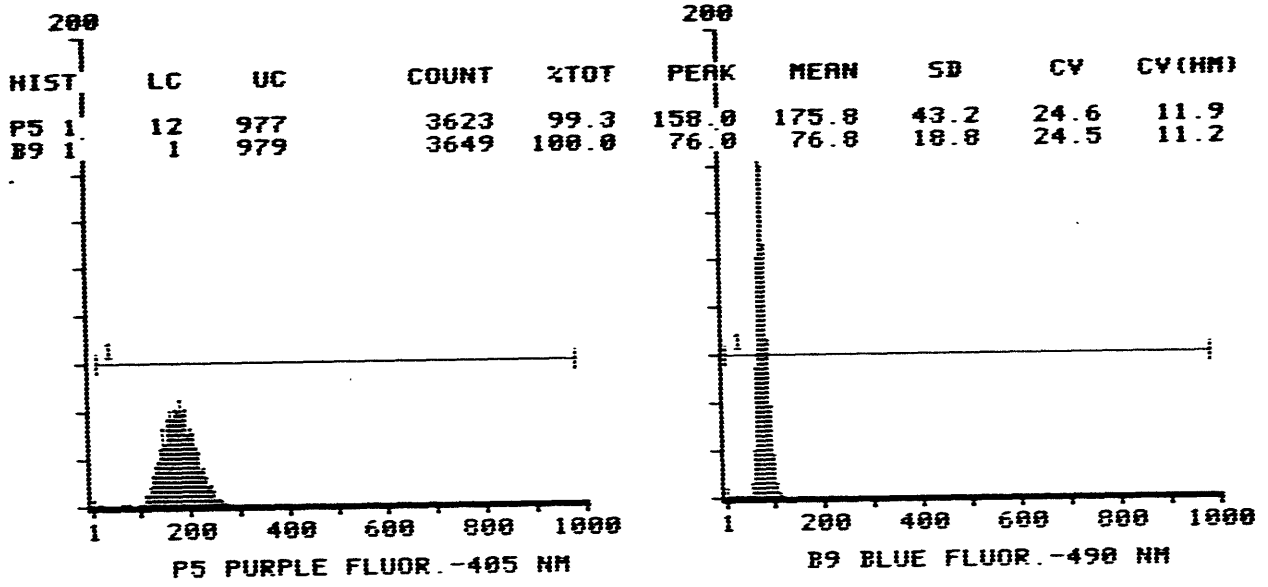

17b.

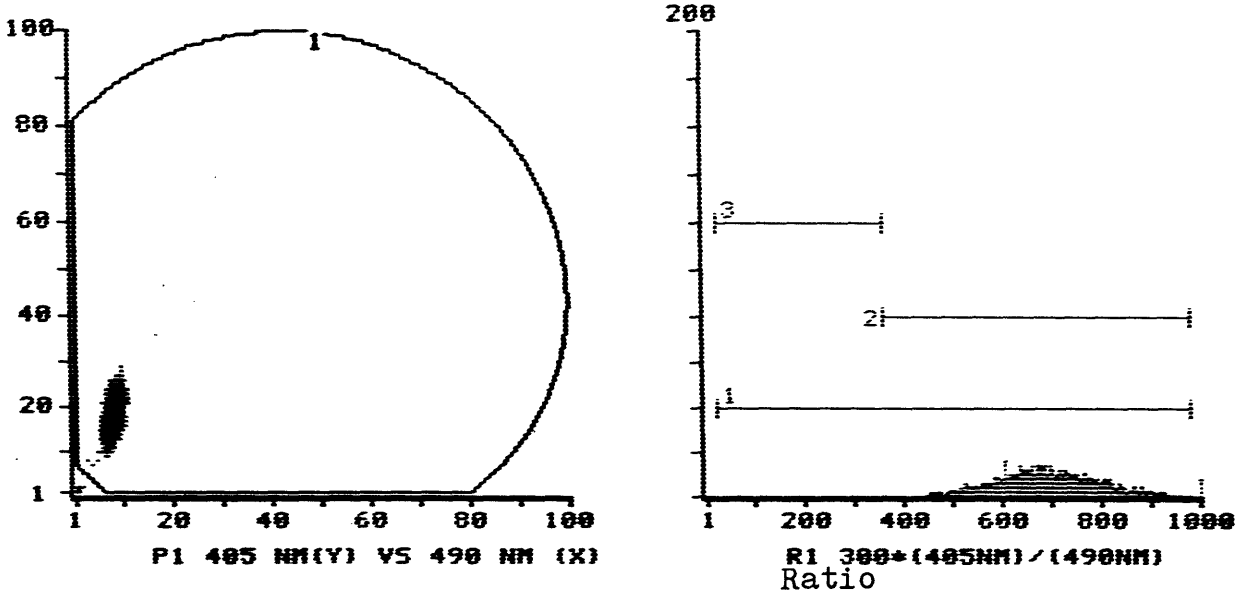

FIGURE 17

The upper half of Figure 17 shows histograms of the 405 and 480 (or 490) fluorescent intensities of the reticulocyte beads. The lower half shows a plot of the 405 vs 480 fluorescent intensity and a histogram of the 405/480 ratio. These measurements were made with the same flow cytometric set-up described for measurements of indo-1 in cells.

evaluated to be used directly in front of the PMTs to further filter the incoming light. These filters had the following transmittance characteristics:

Table 4

405 filters	480 filters
1. 393-409 nm	1. 440-495 nm
2. 360-500 nm	2. 480-494 nm
3. > 389 nm	

The filters were evaluated by flowing indo-1 dye in either Ca++ or EGTA through the flow cell and measuring the PMT voltages. R_{min} and R_{max} were calculated and filters giving the widest separation between R_{min} and R_{max} were selected for use. For the 405 channel, the 393-409 nm bandpass was clearly superior to the others. The two 480 filters were roughly equivalent and the 440-495 filter was used for all experiments.

D. Effect of Indo-1 AM Loading Concentration on Maximum and Minimum Ratio

Excessive or insufficient intracellular dye can effect the ratio measurements. Too little will cause excessive background noise from the light scatter and autofluorescence of cells. Light scatter will primarily effect the 405 nm signal since it is closest to the 350-360 nm excitation wavelength. UV excited autofluorescence is due to nicotinamide adenine dinucleotide (NADH) and

flavin fluorescence (riboflavin, coenzymes, proteins)[126-128]. The NADH emission peak occurs at 445 nm and in cells is 50-100 times stronger than the flavin peak which occurs at 520 nm. On the flow cytometer unstained cells had a low 405/480 ratio (~0.33) that was unresponsive to changes in ICF Ca++. Excessive dye loading may result in unmetabolized dye, with a peak fluorescence at 445 nm. Since a narrow 405 nm filter (393-409) but a wide 480 filter (~455-495) was used, unmetabolised dye would result in an artificial increase in the 480 nm signal over the 405 signal and a ratio which would be unresponsive to changes in ICF Ca++.

To assess the optimal concentration range for loading cells, 2C cells were incubated with indo-1 AM at varying concentrations and the ratio in the presence of 4 uM ionomycin and either 3mM EGTA or 1mM Ca++ was recorded. Since the samples varied greatly in intensity, a single PMT gain could not be used for all of them. Instead the gains were adjusted so that the brightest cells extended approximately to the end of the 405 and 480 nm intensity ranges. Table 5 shows the ratio and indo-1 AM concentrations.

Table 5

Indo-1 AM Concentration	Mean Ratio		CV = coefficient of variation of ratio histogram peak	
	5mM EGTA	1mM Ca++	5 mM EGTA	1mM Ca++
5.0uM	0.48	2.13	29.8	17.6
2.5uM	0.47	2.29	26.6	16.4
1.0uM	0.52	2.40	27.5	16.0
0.5uM	0.54	2.26	29.4	18.0

Given the subjectiveness of the gain settings, there is little variation in the ratios for the concentrations used. Also the CV, a measure of the tightness of the distribution, is approximately the same. So at least for 2C cells indo-1 can be loaded successfully over a large range of concentrations.

E. Flow Cytometry Controls for Cells

Prior to every experiment, cells were tested for indo-1 dye metabolism by resuspending $5X10^5$ cells in 1 ml of ECBS solution containing either 1 mM $CaCl_2$ or 5 mM EGTA and 2-7 uM ionomycin. Ionomycin is a Ca++ ionophore and is described in a later section. The cells were checked to make sure that those in 1 mM calcium had a high ratio and those in 5 mM EGTA had a low ratio. These cells and an unstained aliquot of cells were used to set the gate on

the 405 vs 480 plot and the PMT gains for the 405 and 480 fluorescence and forward scatter signal. These gains were set so that less 1% of the unstained cells entered the 405 vs 480 nm gate. In addition, the 405 and 480 fluorescent intensities were set so that the 405/480 ratio*300 for cells in EGTA and ionomycin was approximately 100 (R = 0.3) and for cells in 1 mM Ca++ and ionomycin was approximately 700 (R = 2.3). This procedure helped to insure that the ratio corresponded to roughly the same calcium level from experiment to experiment.

Figure 18 compares P815 cells that had been loaded or not loaded with 5 uM indo-1. Figure 18a shows cells that have received no indo-1 AM. Only 12 of 10,000 cells escape the 405 vs 480 gate to appear on the ratio graph. Figure 18b shows indo-1-loaded cells in ECBS solution with 1 mM Ca^{++} but no ionomycin. These cells had a normal intracellular Ca^{++} level and a mean ratio of 0.77. In Figure 18c indo-1-loaded cells were placed in buffered salt solution with 1mM Ca^{++} and 7 uM ionomycin and immediately examined in the flow cytometer. These cells had a very high intracellular Ca^{++} and a mean ratio of 2.5. Figure 18d shows the effect of placing the indo-1-loaded cells in buffered salt solution with 5 mM EGTA: the result was a low intracellular Ca^{++} and a mean ratio of 0.28. All of the tumor cells examined responded to ionomycin in the same way as the P815 cells. T cell

FIGURE 18 (a., b.)

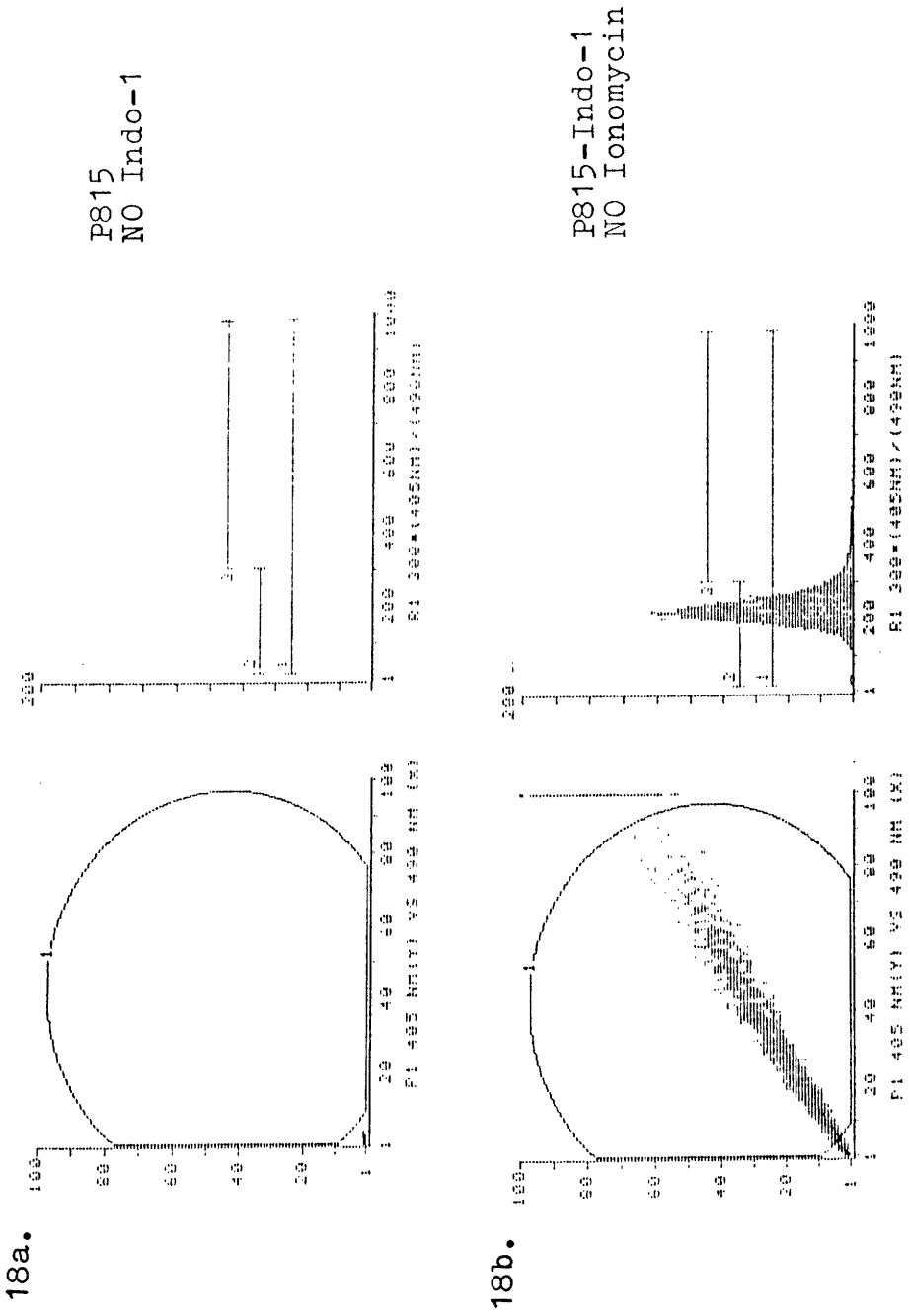

FIGURE 18 (c., d.)

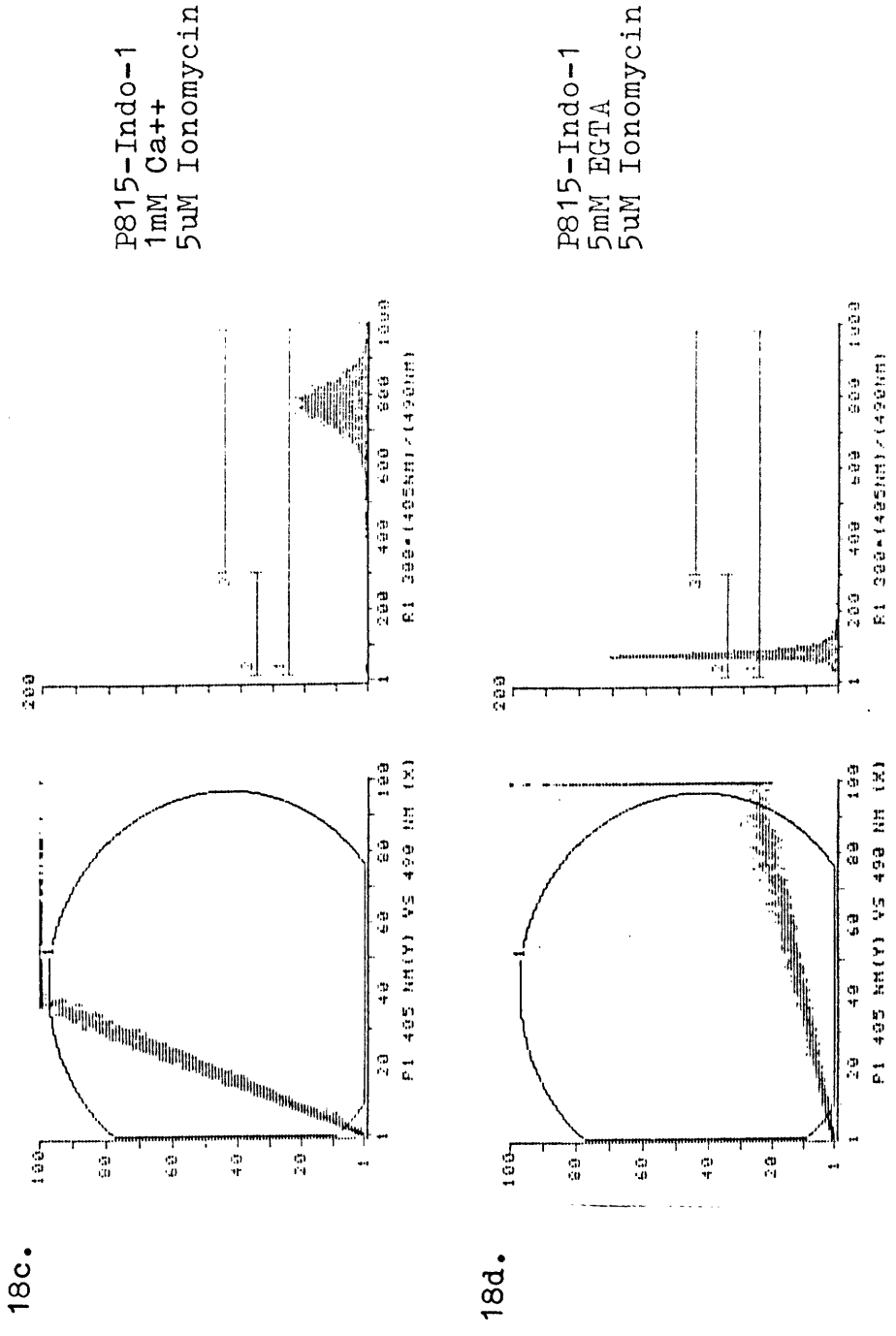
P815-Indo-1
1mM Ca++
5uM Ionomycin
P815-Indo-1
5mM EGTA
5uM Ionomycin
18c.
18d.

FIGURE 18

Figure 18a shows the 405 and 480 fluorescent signals from unstained P815 cells, while Figure 18b shows the fluorescence of indo-1 (3 uM) stained P815 cells. Figure 18c and 18d show the 405 and 480 fluorescence of indo-1 loaded P815 cells with ionomycin (5 uM) in the presence or absence of extracellular calcium. The left most graphs are cytograms of the 405 versus 480 fluorescence while the right-hand graphs are histograms of (405/480)*300. The factor of 300 is used so that the ratio will fit on the fixed scale of the graph.

clones, however, often gave a very heterogeneous response to ionomycin. This has been noted by others in peripheral blood lymphocytes[114]. To verify that the indo-1 was properly metabolized, 2C cells (a cloned T cell line) were lysed in media with and without Ca^{++} and emission spectra were determined on a spectroflourimeter (excitation = 350 nm). The indo-1 fluorescence did not differ from that shown previously (Figure 7).

F. Indo-1 Can Be Used As A Vital Stain With Flow Cytometry

Vital stains are dyes that are taken up and metabolised by living not dead cells; the dyes leak out of the cell upon cell death[122]. Hence they are often used to distinguish living from dead cells. Fluorescein diacetate is one of the most commonly used fluorescent vital stains. In the uncharged, esterified form, this dye, like indo-1 AM, permeates into cells[31,110]. Upon entry into the cell, it is deesterified and converted into a charged molecule that is trapped intracellularly. The use of a vital dye to record measurements insures that recordings are made only on living cells.

Flow cytometry takes advantage of these properties of vital dyes. As stated, a gate on the 405 vs 480 nm fluorescent intensity plot can be used to remove cells which have no or very little indo-1 dye. Thus a ratio measurement is performed only on intact cells that have

not developed a substantial leak of indo-1. Dye leakage into the extracellular medium does not introduce errors since the flow cytometer circuitry contains a "background subtracter" and is designed to be used with fluorescent dyes free in the media, e.g. as with acridine orange or membrane potential dyes. In contrast, dye leakage can not be ignored and results in erroneous data in a spectrofluorimeter.

We confirmed that indo-1 acts as a vital dye, since cytolytic agents caused cells to disappear from the sample population staining positive for indo-1, but not from the forward scatter population. Indo-1-loaded cells that were lysed in 0.02%-0.001% triton did not appear on the ratio histogram although the signals due to intact nuclei still pass through the forward scatter gate. Also addition of lytic doses of CTL granules or ionomycin caused the number of cells appearing on the ratio histogram per minute to decrease rapidly while running at a constant flow rate (Figure 19). This was not due to sedimentation or nonspecific dye leakage since cells not receiving ionomycin or granules, or cells resistant to the granules did not undergo this decrease. As shown the number of cells entering the forward scatter gate remained constant so that the loss could not be attributed to this gate (Figure 20). Indo-1 dye leakage as measured in a spectrofluorometer (by analyzing the supernatant of

FIGURE 19

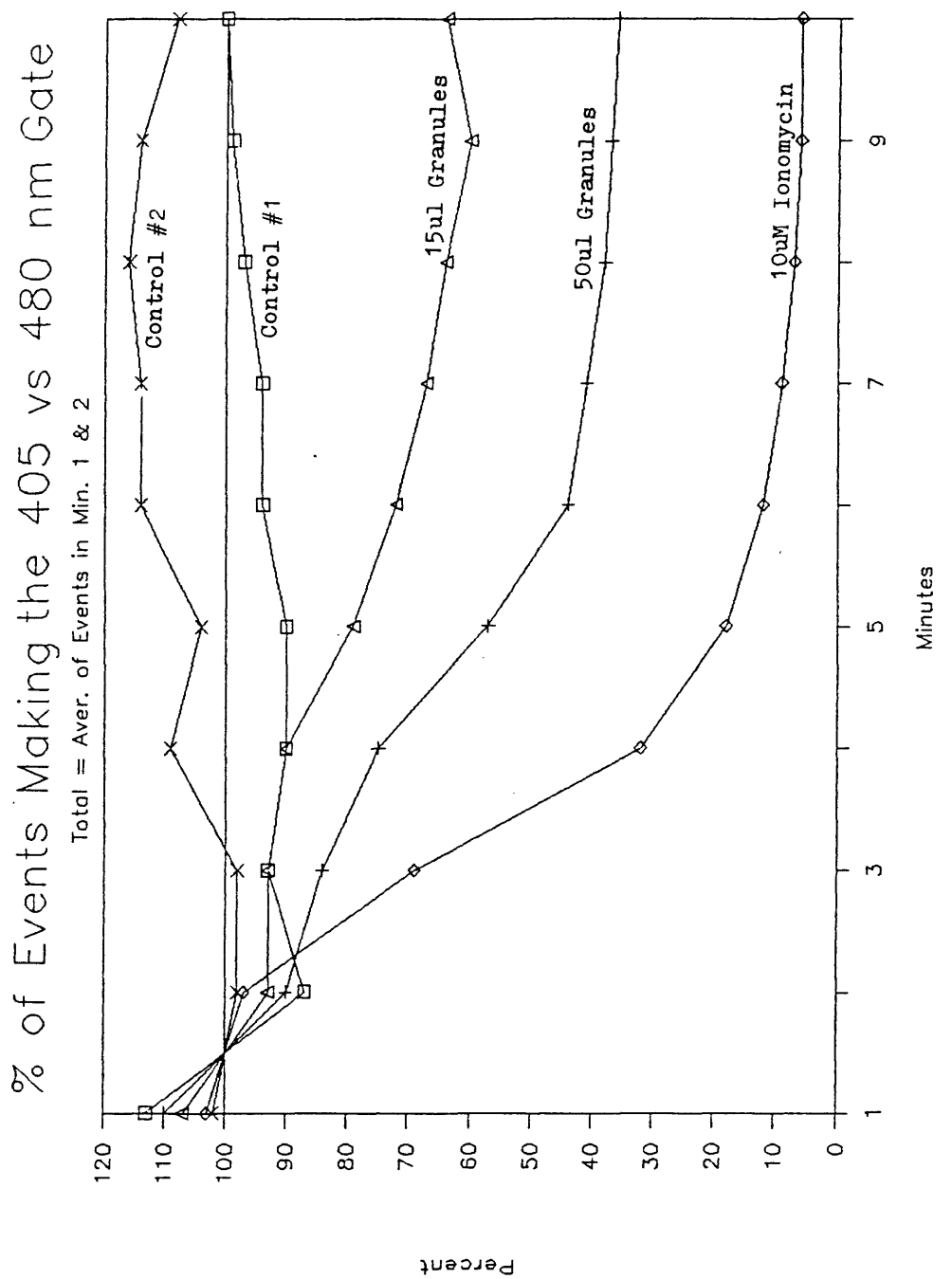
% of Events Making the 405 vs 480 nm Gate
Total = Aver. of Events in Min. 1 & 2
Control #2
Control #1
15ul Granules
50ul Granules
10uM Ionomycin
Percent
120
110
100
90
80
70
60
50
40
30
20
10
0
1
3
5
7
9
Minutes

FIGURE 19

Yac-1 cells were loaded with 5 uM indo-1 AM. 3H2 granules, ionomycin, or nothing was added to the cells and data collected continuosly for 10 minutes as described in the methods section. The number of cells entering the 405 versus 480 gate was measured for each minute and expressed as the % of the average number of cells in minutes 1 and 2. Control 1 (received nothing) and was the first sample run on the flow cytometer while control 2 was the last sample run. 10 uM ionomycin and 50 ul of this granule batch caused 70% or greater Yac 1 cell death as measured in a Cr^{51} release assay.

FIGURE 20

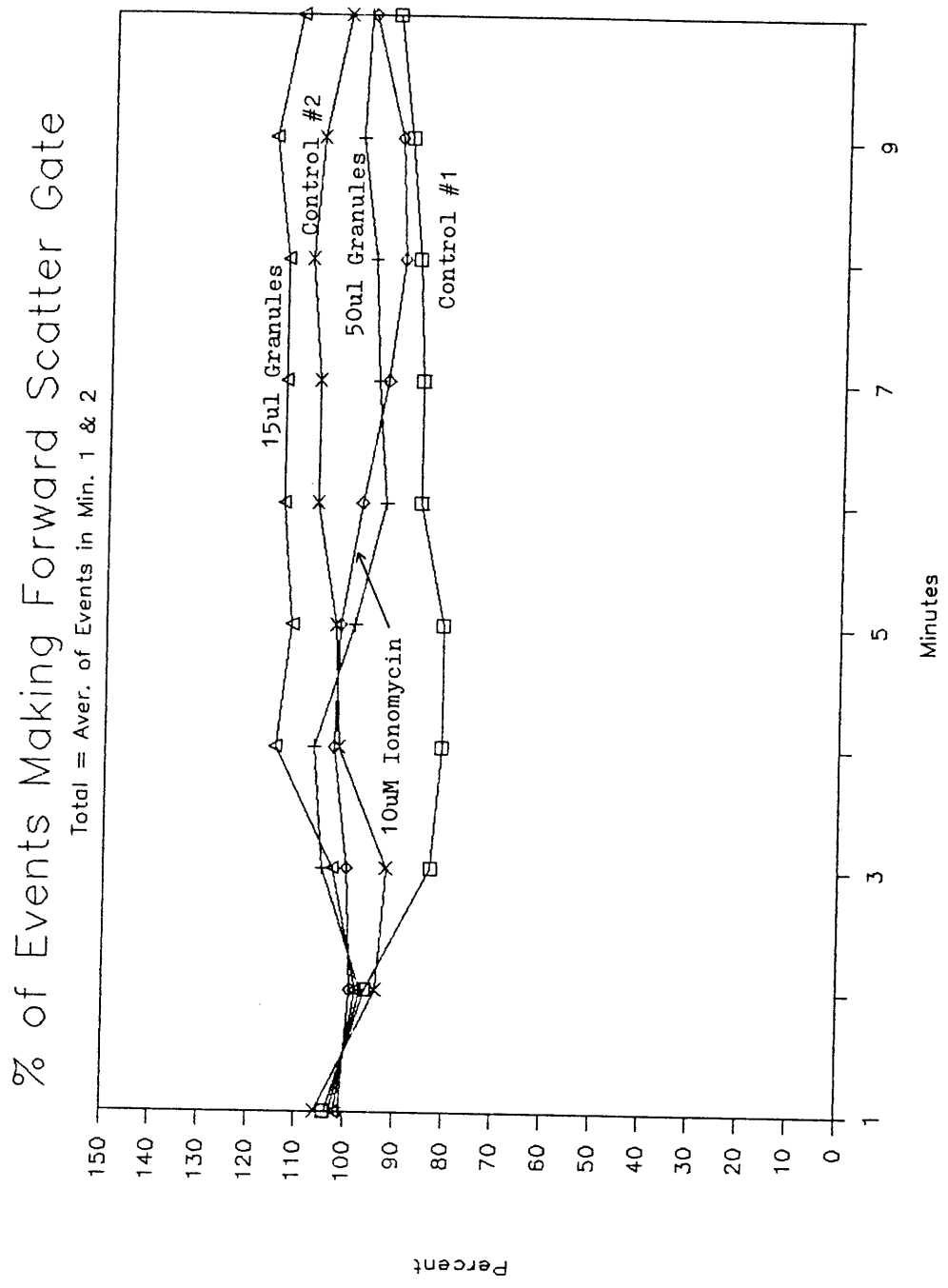
% of Events Making Forward Scatter Gate
Total = Aver. of Events in Min. 1 & 2
15ul Granules
Control #2
50ul Granules
Control #1
10uM Ionomycin
Percent
Minutes
150
140
130
120
110
100
90
80
70
60
50
40
30
20
10
0
1
3
5
7
9

FIGURE 20

Figure 20 shows the percent of events making the forward scatter gate for the data of Figure 19. It was constructed in the same way as Figure 19 but using the number of cells entering the forward scatter gate.

cells) appeared to parallel Cr^{51} release although, this was difficult to measure since the amount of nonspecific dye leakage from cells over the 1.5-2 hour assay time used could be as high as 40% (Figure 21).

FIGURE 21

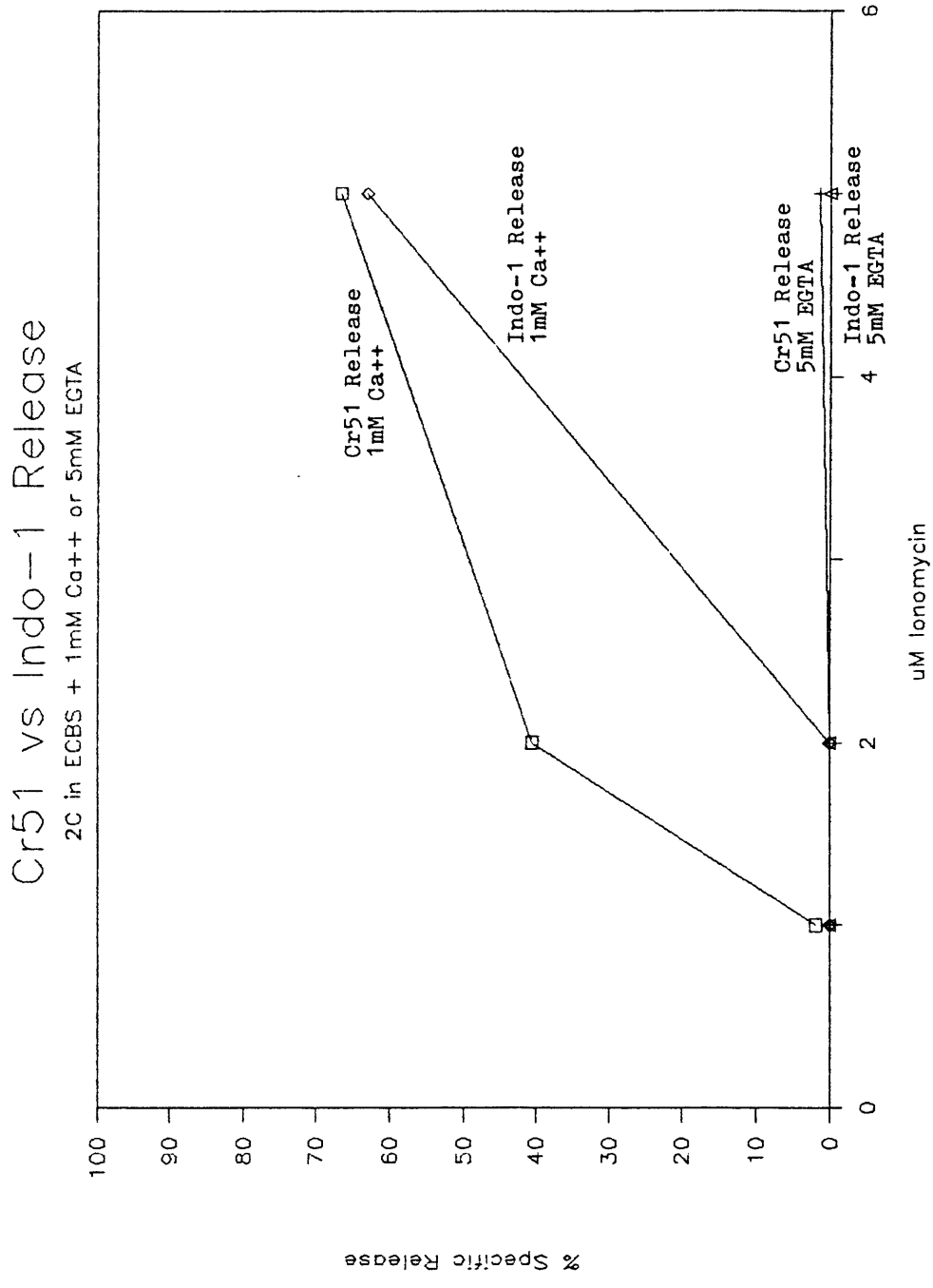
Cr51 vs Indo-1 Release
2C in ECBS + 1mM Ca++ or 5mM EGTA
% Specific Release
uM Ionomycin
Cr51 Release
1mM Ca++
Indo-1 Release
1mM Ca++
Cr51 Release
5mM EGTA
Indo-1 Release
5mM EGTA
0
10
20
30
40
50
60
70
80
90
100
0
2
4
6

FIGURE 21

Figure 21 compares the rate of Cr^{51} to indo-1 release from 2C cells. 2C cells were loaded with Cr^{51} or 1 uM indo-1 AM. The cells were exposed to 1, 2, or 5 uM ionomycin in ECBS with 1 mM Ca++ or 5 mM EGTA. Ionomycin is significantly more toxic in the presence of extracellular calcium (see section on ionophore toxicity). The Cr^{51} release was measured 1 hour after the addition of ionomycin and the percent specific release was calculated using the formula in the Cr^{51} release methods section. Nonspecific Cr^{51} release was < 5% while nonspecific indo-1 leakage was ~40% (during the 1.5-2 hours of the assay).

G. Flow Cytometry Standardization

The 405/480 ratio, R, is nonlinearly related to the free calcium ion concentration. To calculate [Ca++] from this ratio, the constants, R_{min}, R_{max}, and S in equation 19 must be determined from the instrumental set-up. In the case of a spectrofluorimeter these constants are usually calculated by lysing the cells in media with and without Ca++ [110]. However, in a flow cytometer, the constants cannot be calculated in this manner since the electronics are designed to detect and measure attributes of pulses (and not a constant voltage or current). In addition one would not want to run lysed cells through a flow cytometer since the proteins, etc. often form aggregates that could clog the machine.

Previous investigators have either measured these constants in a spectrofluorimeter and assumed that they carry over to the flow cytometer or simply not calculated the actual Ca++ concentration[114,117,130,162]. These assumptions may not produce a good estimate of the calcium level. It is clear that these constants are not necessarily the same in the flow cytometer and spectrofluorimeter. Flow cytometers, unlike spectrofluorimeters, use one or more narrow laser lines for excitation; they also use dichroics and filters, not gratings, to select emission wavelengths, and have separate photomultiplier tubes (i.e. different gains) for

the 405 and 480 measurements. Rabinovitch et al measured R and R_{max} for resting lymphocytes in a flow cytometer and spectrofluorimeter[130]. Since the numbers were similar in both instruments, it was assumed that R_{min} and S would be the same. While this is a closer approximation than just simply assuming all three are identical, it ignores the independence of the 3 constants, R_{min}, R_{max}, and S. For example, Table 6 shows three cases where R_{min} and R_{max} are identical but S varies significantly.

Table 6

$F_{405,free}$	$F_{405,sat'd}$	$F_{480,free}$	$F_{480,sat'd}$	Rmin	Rmax	S
2	3	4	1	0.5	3	4
1.5	4	3	1.3	0.5	3	3
1	3	2	1	0.5	3	2

$F_{480,free}$ and $F_{480,sat'd}$ may not be related by the same proportionality constant in flow cytometry and spectrofluorimetry since they are affected by excitation wavelengths, lense properties, and cut-off characteristics of filters. In addition these constants may be different for different cell lines because: 1. small amounts of unmetabolised dye may be present in some cells, 2. cellular autofluorescence may be different, and 3. the intracellular milieu may vary. Finally, it may not be possible, desirable, or optimal to adjust the flow

cytometer so that all constants are equivalent to that of a spectrofluorimeter.

For these reasons, I attempted to find the calibration constants directly from the flow cytometer. It would be best if the intracellular free calcium of intact cells could be completely equilibrated with the extracellular solution so that indo-1-loaded 2C cells could be used as standards. This was attempted using indo-1 loaded 2C cells placed in media of varying calcium concentrations and 1 uM ionomycin. Figure 22 is a set of spectra obtained from these cells in 0, 50, 100, 200, 450, 600, or 39,000 nM extracellular calcium. Between 0-600 nM the cells maintain a constant intracellular calcium irrespective of the extracellular calcium level. Only at 39 uM [Ca++] did the curve shift slightly. The dotted lines show lysed cells proving that the dye has been properly metabolised. Addition of 0.1% or 0.2% azide to cells with ionomycin did not lead to equlibration of intra and extracellular calcium, because it caused accelerated dye leakage and cell death. (The azide was added to inhibit ATP production thus disabling the cells ability to pump calcium out of the cell).

Since intact cells could not be used as standards, we tried to use the flow cytometer as a spectrofluorimeter e.g. to make measurements on free dye. It is best to use dye from lysed cells since the dye may not be 100%

FIGURE 22

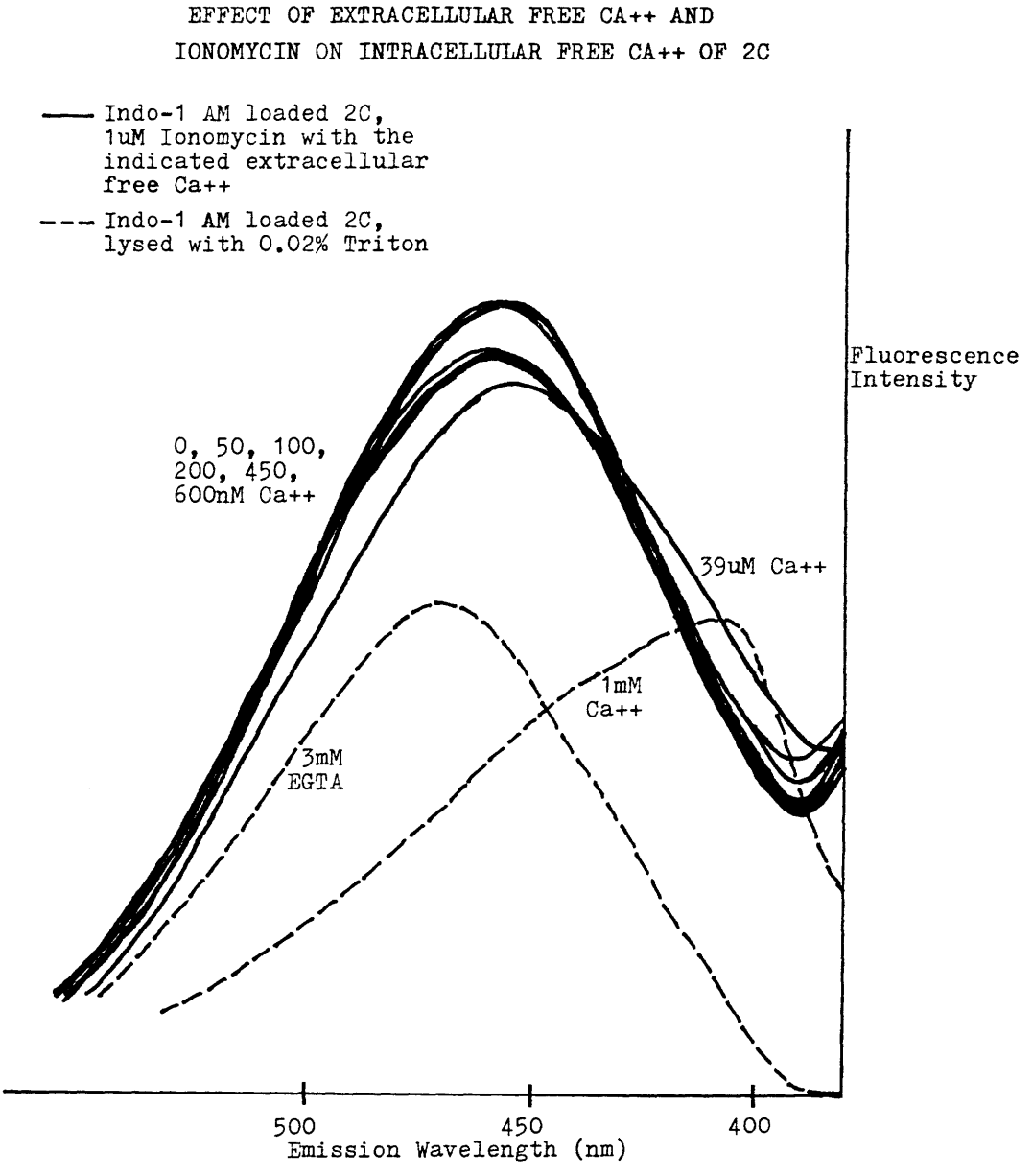
EFFECT OF EXTRACELLULAR FREE CA++ AND
IONOMYCIN ON INTRACELLULAR FREE CA++ OF 2C
Indo-1 AM loaded 2C, 1uM Ionomycin with the indicated extracellular free Ca++
Indo-1 AM loaded 2C, lysed with 0.02% Triton
Fluorescence Intensity
0, 50, 100, 200, 450, 600nM Ca++
39uM Ca++
1mM Ca++
3mM EGTA
500
450
400
Emission Wavelength (nm)

FIGURE 22

2C cells were loaded with 1 uM indo-1 AM. The solid lines show cells (10^6/ml) placed in ECBS solutions with 1 uM ionomycin and varying levels of extracellular free Ca++. These solutions were made using the EGTA-Ca++ buffers described in the methods section. The dotted lines show cells (at a lower concentration) that were lysed with 0.02% triton. Excitation was at 350 nm.

metabolised and the signal may be affected by cellular proteins. In the flow cytometer this is not possible due to problems related to clogging and the inability to get sufficiently high concentrations of dye from lysed cells. For these reasons measurements were made on the potassium salt of indo-1 in solutions designed to mimic the concentrations of intracellular ions (i.e. intracellular buffered salt solution). One cannot simply run dye and measure the final electronic output since flow cytometers are designed to make measurements on pulses and in addition have "background subtracter" circuitry. This circuitry measures the fluorescence of the extracellular medium and subtracts it from the cellular fluorescence. Therefore one must measure the DC voltage of the PMTs. Since the preamplifiers contain part of the "background subtracter," the voltage cannot be measured from them and they must be disconnected from the PMTs and replaced with a constant load. In this case, a one megaohm resistor was connected in parallel with a voltmeter and the PMT. Initial measurements, made in this fashion (by running dye solutions) produced a PMT voltage that slowly drifted upward. This was not due to PMT instability since shining a light of constant intensity into the PMT produced a constant PMT voltage. Therefore, it was suspected that dye was slowly diffusing out of the core stream and into the sheath fluid where it was being trapped. Clamping the

sheath fluid line so that the entire flow cell filled with dye produced a constant PMT voltage. In order to check the validity of this procedure and the linearity of the system in the voltage ranges used, serial dilutions of fluorescein were run through the flow cell and the PMT voltage recorded. The results are shown:

Table 7

fluorescein dilution	PMT voltage
ddH_2O	-0.5mV
1/400	-60mV
1/200	-116mV
1/100	-257mV
1/50	-530mV
1/10	-2470mV

These results were also verified using varying concentrations of the potassium salt of indo-1.

The next goal was to calibrate the flow cytometer using the indo-1 dye with the same gains and filters used for actual cells. Indo-1 AM loaded cells in ECBS with ionomycin and either 5mM EGTA or 1mM CA++ were used to set the gains for the 405 and 480 nm PMTs. It was not possible to simply reconnect the PMTs to the 1 megaohm load, run indo-1 dye, and measure the voltage. This was because the preamps and flow cytometry circuitry were different for the 405 and 480 signal and so introduced different amplication factors into the signal. While

hardware components and design may be the same for two circuits, the circuits never behave identically due to variations in the specifications of the actual electrical elements. This was verified by running standard fluorescent beads through the flow cytometer and measuring their mean fluorescent intensity. Switching either the preamp cards or other circuitry but not the PMT or PMT gain caused the mean fluorescent intensity to vary, often considerably. For this reason the following protocal was used for calculating the standardization constants:

1. Set the 405 gain (PMT2) and 480 gain (PMT1) using indo-1 loaded cells.
2. Run the reticulocyte beads and record the mean 405 fluorescence, mean 480 fluorescence, and 480 gain (PMT1).
3. Move PMT1 to record the 405 signal.
4. Run the reticulocyte beads and adjust the gain of PMT1 so that the mean 405 fluorescence is the same as in step 2 (when it was being received by PMT2). Record this 405 (PMT1) gain.
5. Connect PMT1 to the voltmeter and 1 megaohm load.
6. Run solutions of indo-1 dye recording all voltages off PMT1. When recording the 405 fluorescence use the 405 (PMT1) gain and when recording 480 fluorescence use the 480 (PMT1) gain.

This technique could theoretically be repeated for each

experiment but it is far easier to use the reticulocyte beads as standards. The calibration constants would then be known for a given reticulocyte bead 405 and 480 fluorescences.

This calibration technique was used for two experiments each with a different CTL cell line, 2C or 2.1.1. For these CTL clones, there were always two nonoverlapping groups of cells: a very large group with a low calcium level (referred to as a resting population) and a small group with a higher calcium level. The total population refers to the average calcium of all cells. The results were as follows:

Table 8

Experiment 1- 2C cells loaded with 1 uM indo-1 AM.

R_{min} = 0.075 $\pm$ 0.001

R_{max} = 2.39 $\pm$ 0.05

S = 3.52 + 0.07

2C cells- Resting population (Ca++) = 257 $\pm$ 20 nM

Total population (Ca++) = 380 $\pm$ 11 nM

+ 1 uM ionomycin (Ca++) = 1160 nM

Experiment 2- 2.1.1 cells loaded with 1 uM indo-1 AM

R_{min} = 0.082 $\pm$ 0.003

R_{max} = 2.59 $\pm$ 0.05

S = 3.51 + 0.32

2.1.1 cells- Resting population (Ca++) = 302 ± 7 nM

Total population (Ca++) = 700 ± 21 nM

+ 1 uM ionomycin (Ca++) = 1183 nM

The samples in 1 uM iononmycin consisted of cells in ECBS with 1 mM Ca++ and 1 uM ionomycin; the value reported is the highest average calcium level attained by those cells. Figure 23 shows the calibration curve between the ICF Ca++ and ratio for these two experiments. Since the gains on the 405 and 480 PMTs were set so that the control cells in ionomycin and 1 mM Ca++ or 5 mM EGTA had nearly the same ratio from experiment to experiment, this graph provides approximate values for ICF Ca++ concentrations in the remainder of this thesis.

These ICF Ca++ values are higher than the approximately 100 nM value that is generally reported in the literature for T cell clones[25,28,114,131,153]. For this reason the mean calcium ion concentration of 2C was measured in a spectrofluorimeter using indo-1 and quin-2. 2C loaded with 5 uM indo-1 had a ICF ca++ of 76 ± 7 nM. 2C loaded with 20 uM quin-2 gave a resting Ca++ level of 106 ± 10 nM and a peak Ca++ level of 1027 nM with 1 uM ionomycin. The equation relating quin-2 fluorescence to Ca++ is:

FIGURE 23

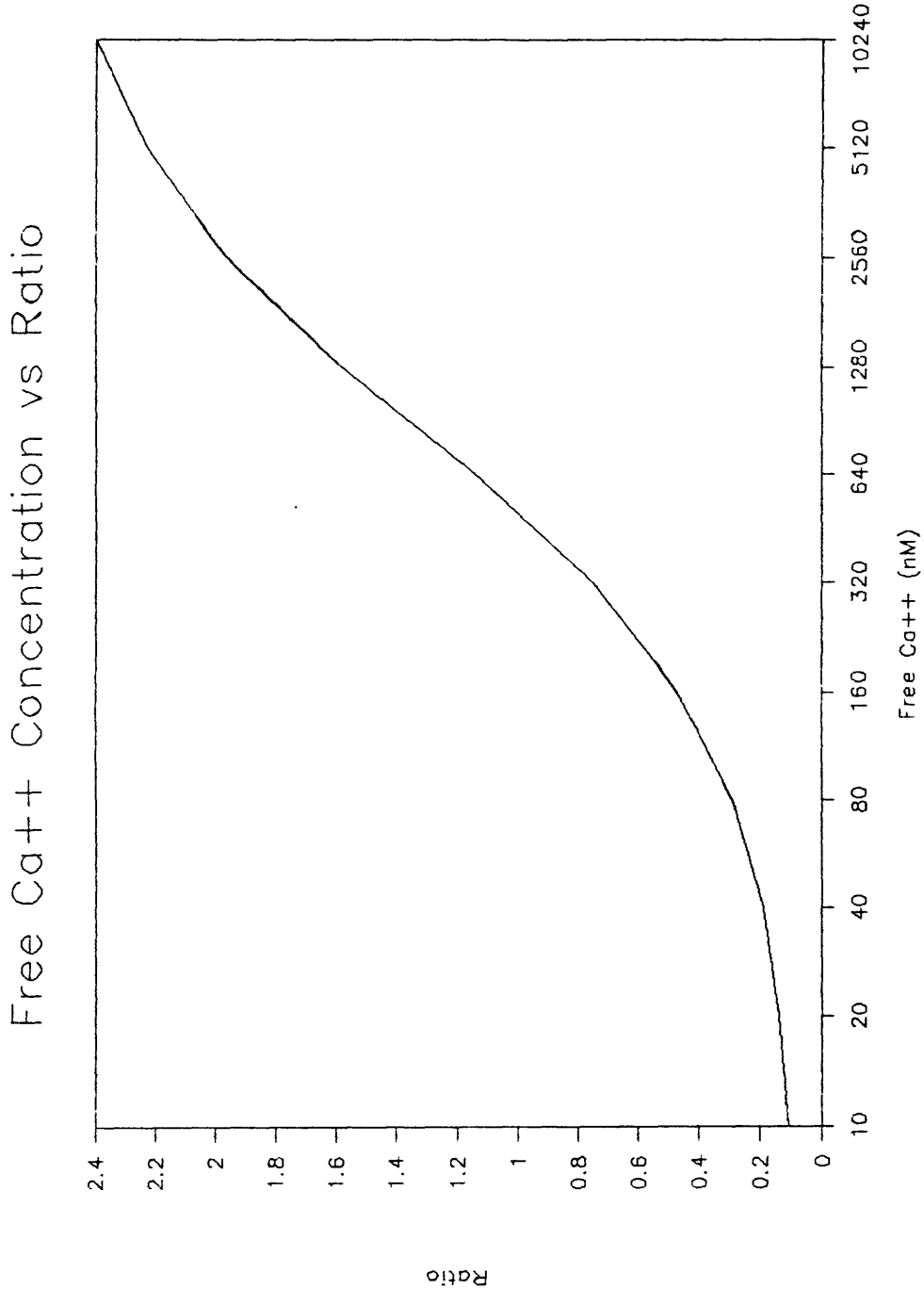
Free Ca++ Concentration vs Ratio
Ratio
2.4
2.2
2
1.8
1.6
1.4
1.2
1
0.8
0.6
0.4
0.2
0
10
20
40
80
160
320
640
1280
2560
5120
10240
Free Ca++ (nM)

FIGURE 23

Figure 23 shows the calibration curve between the 405/480 ratio and the ICF Ca++ concentration for the experiments with 2C and 2.1.1 cells (see text).

$$(Ca++) = \frac{K_d * (F - F_{min})}{(F_{max} - F)}$$

K_d = 115 nM [116]

F = test solution fluorescence

F_{min} = quin-2 fluorescence with total calcium = 0

F_{max} = quin-2 fluorescence with saturating calcium

This equation was derived in a way similar to the indo-1 equation (see section on Indo-1 Properties)[116]. The constants F_{min} and F_{max} for quin-2 and R_{min}, R_{max}, and S for indo-1 were determined by lysing dye-loaded cells with 0.02% triton in the presence or absence of calcium.

For calculations made in a spectrofluorimeter, it is possible to subtract the background noise and autofluorescence using unstained cells. This is not possible in a flow cytometer. Autofluorescence and background noise will cause the greatest error in the calculated Ca++ concentration whenever one of the signals is at a minimum. At the low Ca++ levels found in resting lymphocytes, the 405 signal is close to its minimum, which may explain why the resting calcium levels reported here are higher than those based on spectrofluorimetric measurments reported in the literature. However in experiments to determine the optimal dye loading

concentrations, higher concentrations of dye did not change the ratio (previous section). This suggests that the errors in the flow cytometric measurements of calcium are not due to autofluorescence. Since the calibration procedure is complicated and attempts to use the flow cytometer in an inappropriate way, it is the most likely source of error. Flow cytometric measurements of indo-1 are useful as an approximate rather than precise measure of ICF Ca++. This technique, however, is a very accurate and sensitive indicator of changes in the ICF Ca++ concentration.

V. Effect of CTL Granules on the Intracellular Calcium of Target Cells

A. Introduction

Membrane-bound cytoplasmic granules have been found in various kinds of cytolytic lymphocytes (CTL, NK cells, and "large granular lymphocytes"), and the presence of these granules correlates well, although not perfectly, with lytic activity[3,39,41,44,70,71]. Granules isolated from murine CTL, NK, LGL, and LAK cells are capable of lysing red blood cells and tumor cells in the presence of calcium[3,37-40,43,46]. Like cytolytic lymphocytes, the granules can form circular lesions (diameter = 160 A) in the membranes of target cells[3,38,41]. The granules contain (at least) two serine esterases, perforin (also called cytolysin), and lysosomal enzymes. Purified perforin, which resembles complement factor nine (C9), forms circular membrane lesions in lipid bilayers and is capable of lysing tumor cells in the presence of calcium[39,41,42,44-46,70,71]. Granules and perforin depolarize the membrane of nucleated cells and cause ion and marker release (COF, EGTA, Tris) from liposomes or lipid bilayers[38,41,42].

According to a widely recognized model, when a CTL adheres to and recognizes a target cell's antigens, granules in the CTL's cytoplasm migrate towards the target

cell and are released into the extracellular space between the adherent cells[3,42,51,133]. Since the isolated granules are cytolytic, it is reasonable to expect that they will mimic all essential features of the CTL's cytolytic mechanisms. Use of isolated granules has the additional advantages that they bypass the recognition and activation phase of CTLs and they can be frozen, greatly simplifying the experimental system. We used granules isolated from the murine CTL clones, G4, 3H2, and 3C11 to investigate the idea that increased ICF Ca++ waa the primary mode of target cell death.

B. Effect of Granules on Tumor Cells

We measured the intracellular changes in calcium in a variety of tumor cells after they were exposed to lytic granules from cytolytic T cells. P815 cells were loaded with 3 uM indo-1 AM and then given a sublytic dose of 3H2 granules (< 5% Cr^{51} release.) As shown in Figure 24, the P815s responded with a rapid influx of calcium in less than the 30 seconds that elapsed between adding the granules to a cell suspension and appearance of the cells in front of the laser beam. The ICF calcium rises to where it saturates the intracellular indo-1 (as determined with ionomycin) in less than one minute, and then begins to decrease immediately, falling to the levels in resting cells within three minutes. No subpopulations of P815

FIGURE 24 (pt. 1)

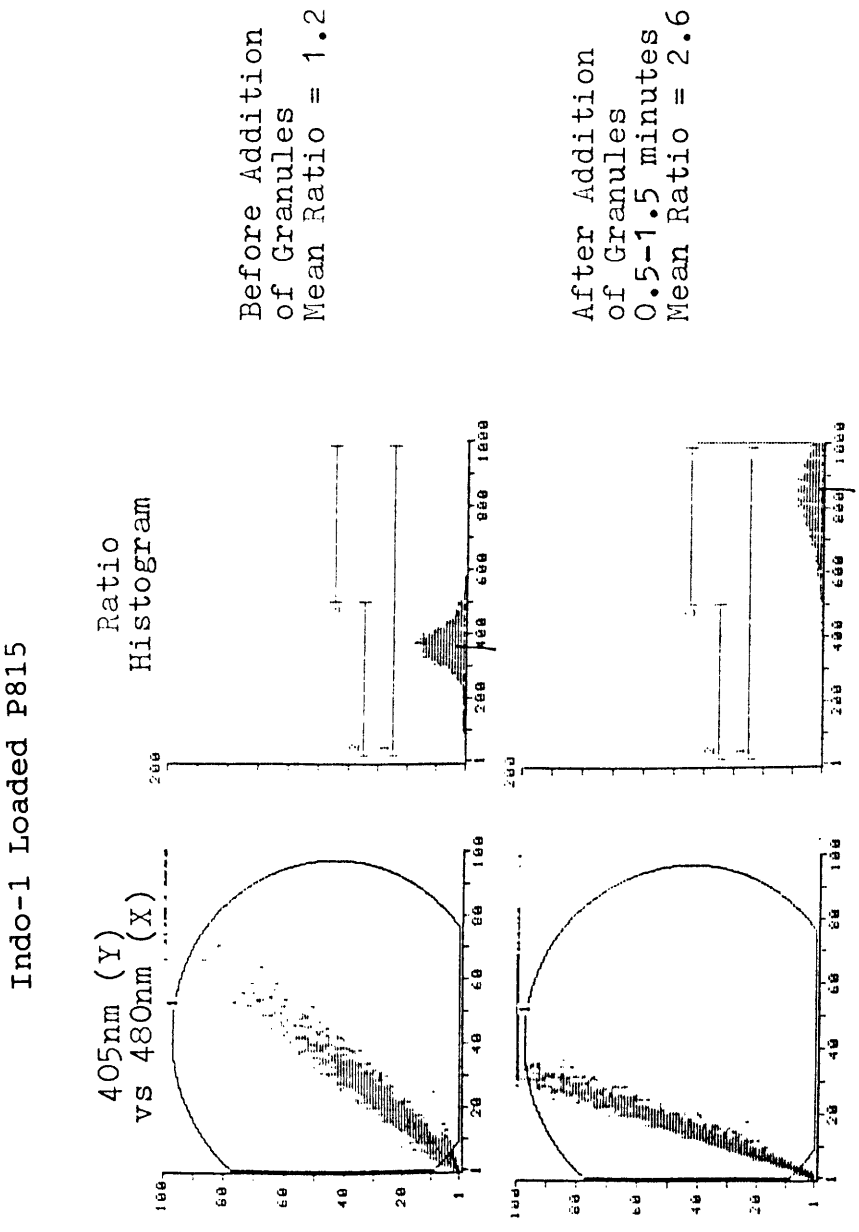

FIGURE 24 (pt. 2)

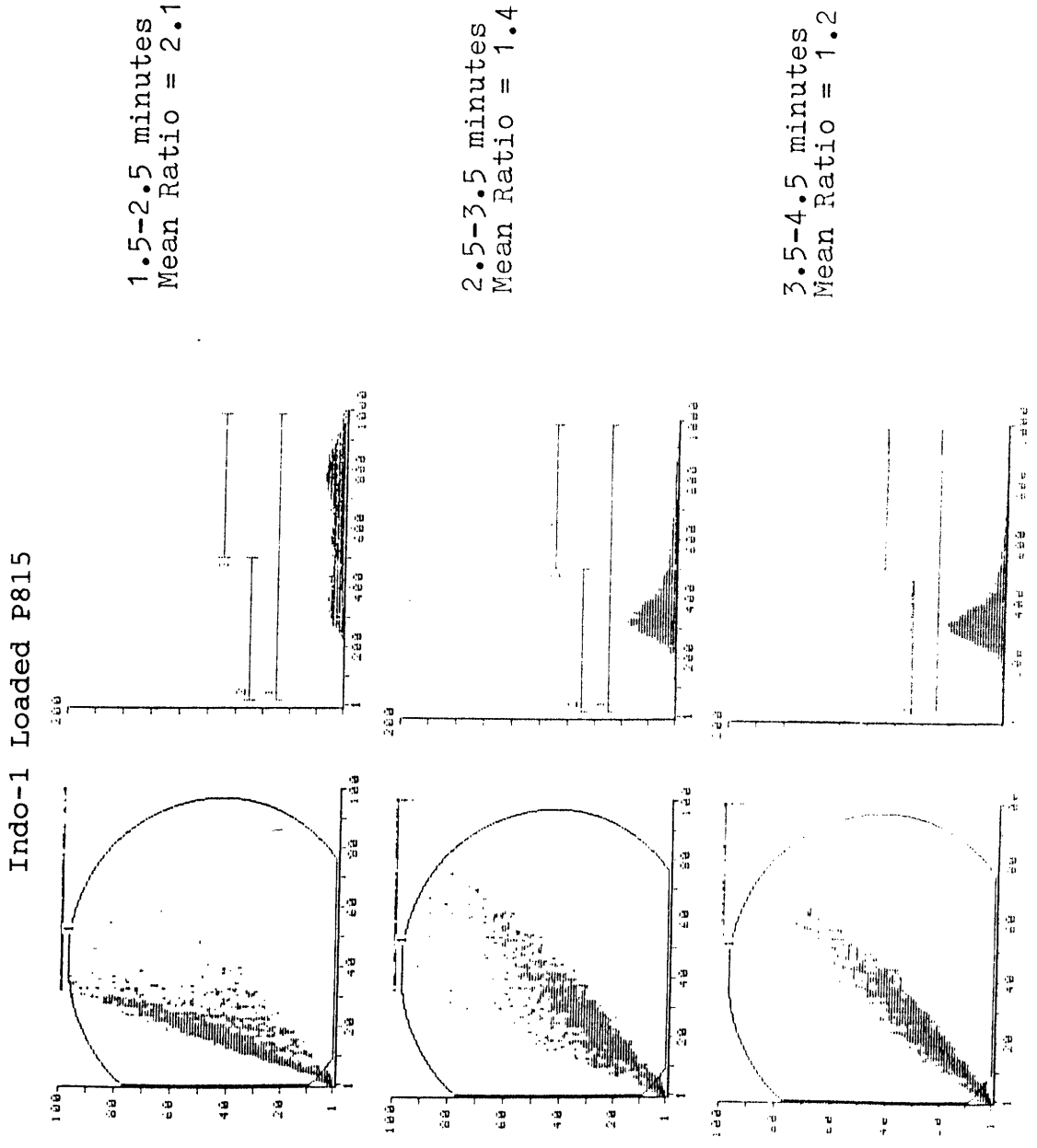

FIGURE 24

P815 cells were loaded with 3 uM indo-1 AM and resuspended in ECBS with 1 mM Ca++. Figure 24 shows the ratio measurements before and after addition of a "sublytic" quantity of 3H2 granules. The "sublytic" concentration of granules was determined by: a. measuring the Cr^{51} release of P815 cells after addition of serial dilutions of granules and, b. graphically determining the maximum dose of granules that caused no P815 cell lysis. This "sublytic" concentration for P815 cells was determined for every batch of granules and is the granule concentration used for Figures 24-35.

tumor cells were observed to be unresponsive to the granules i.e. by not having an increased intracellular free calcium. Other tumor cell lines tested (EL4, S49, RDM4, Yac 1) behaved similarly with an immediate rise in calcium and recovery within 10 minutes (Figures 25-28). The magnitude of the granule-induced increase in calcium appeared to depend on the granule dose (Figure 29). When P815, RDM4, and Yac 1 cells were exposed to a lytic dose of granules (> 50% Cr^{51} release), some cells were still able to recover, returning to a normal calcium level within 5-10 minutes, although as discussed earlier the number of cells no longer able to meet the 405 vs 480 gate, due to leaking dye, increases rapidly.

FIGURE 25

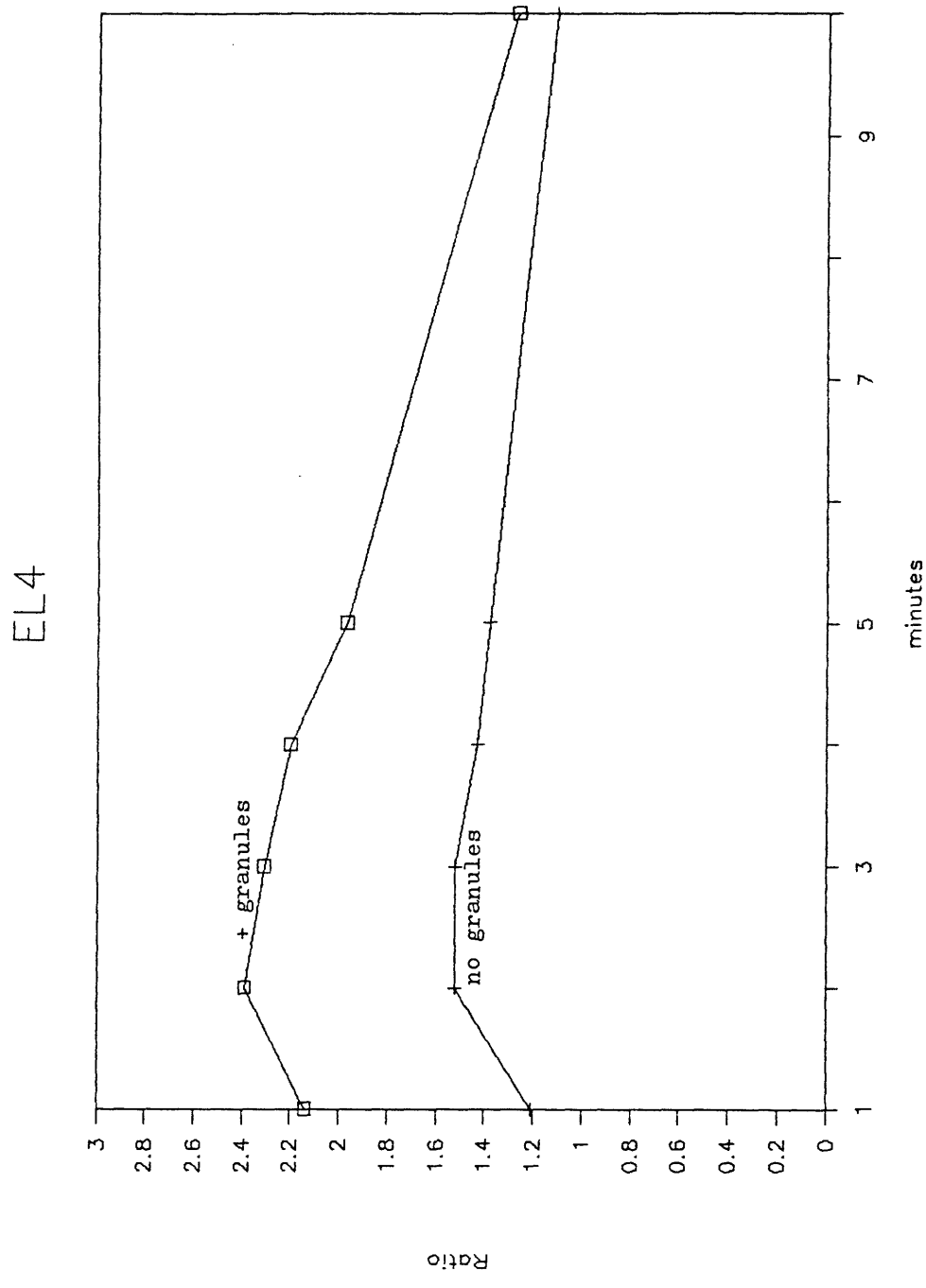
EL4
Ratio
minutes
+ granules
no granules
3
2.8
2.6
2.4
2.2
2
1.8
1.6
1.4
1.2
1
0.8
0.6
0.4
0.2
0
1
3
5
7
9

FIGURE 26

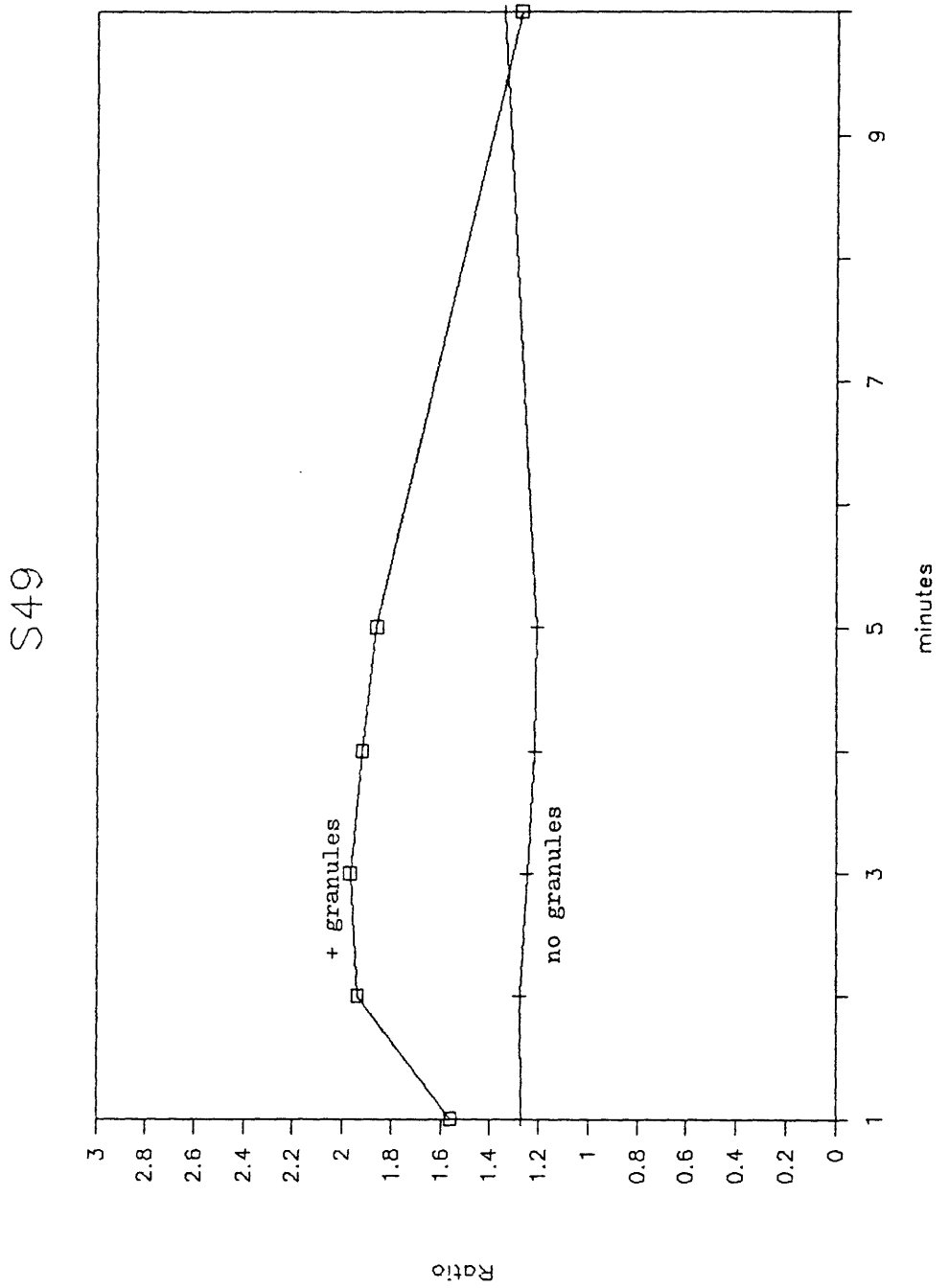
S49
Ratio
minutes
+ granules
no granules
0
0.2
0.4
0.6
0.8
1
1.2
1.4
1.6
1.8
2
2.2
2.4
2.6
2.8
3
1
3
5
7
9

FIGURE 27

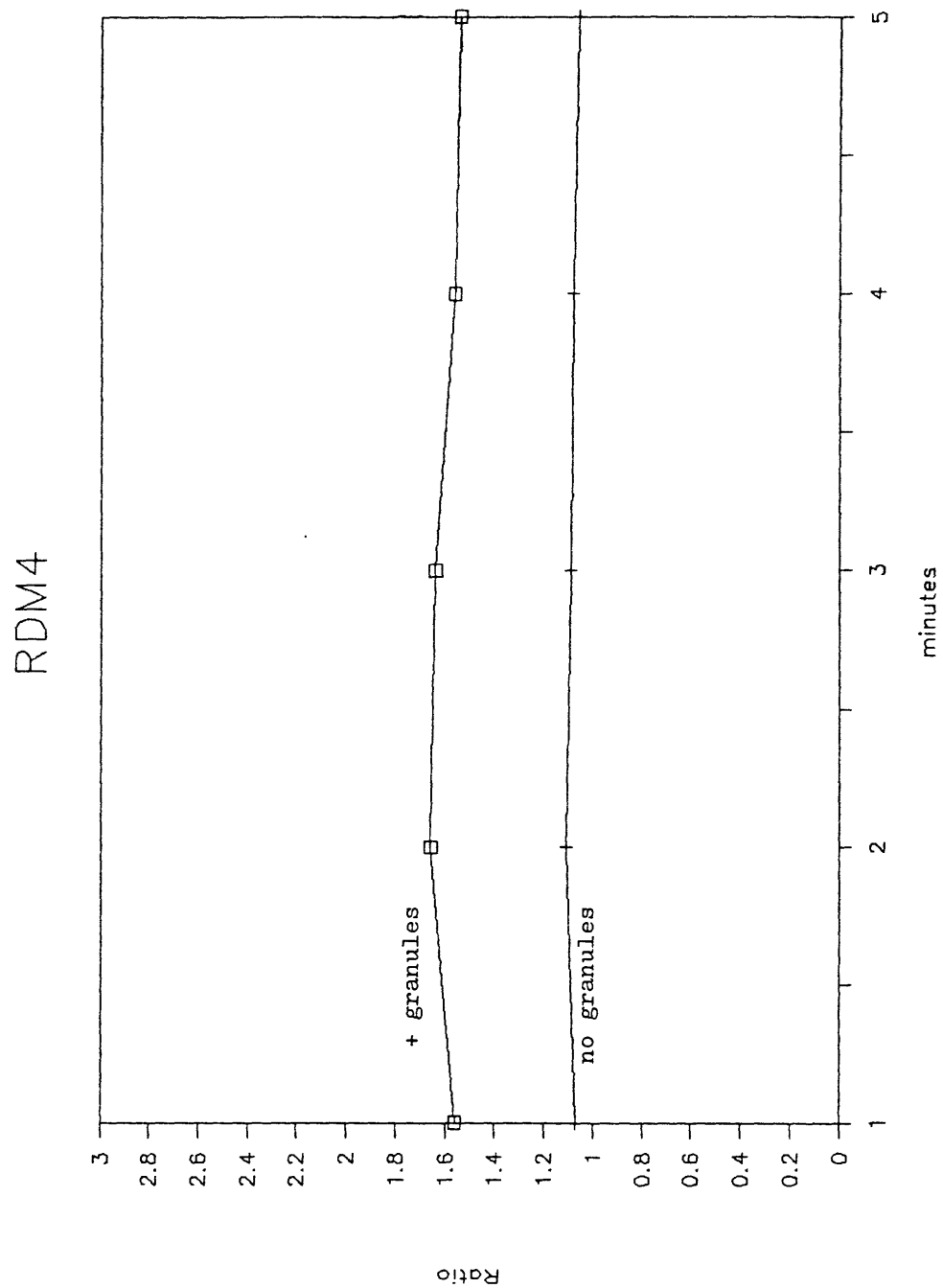
RDM4
Ratio
minutes
+ granules
no granules
3
2.8
2.6
2.4
2.2
2
1.8
1.6
1.4
1.2
1
0.8
0.6
0.4
0.2
0
1
2
3
4
5

FIGURE 28

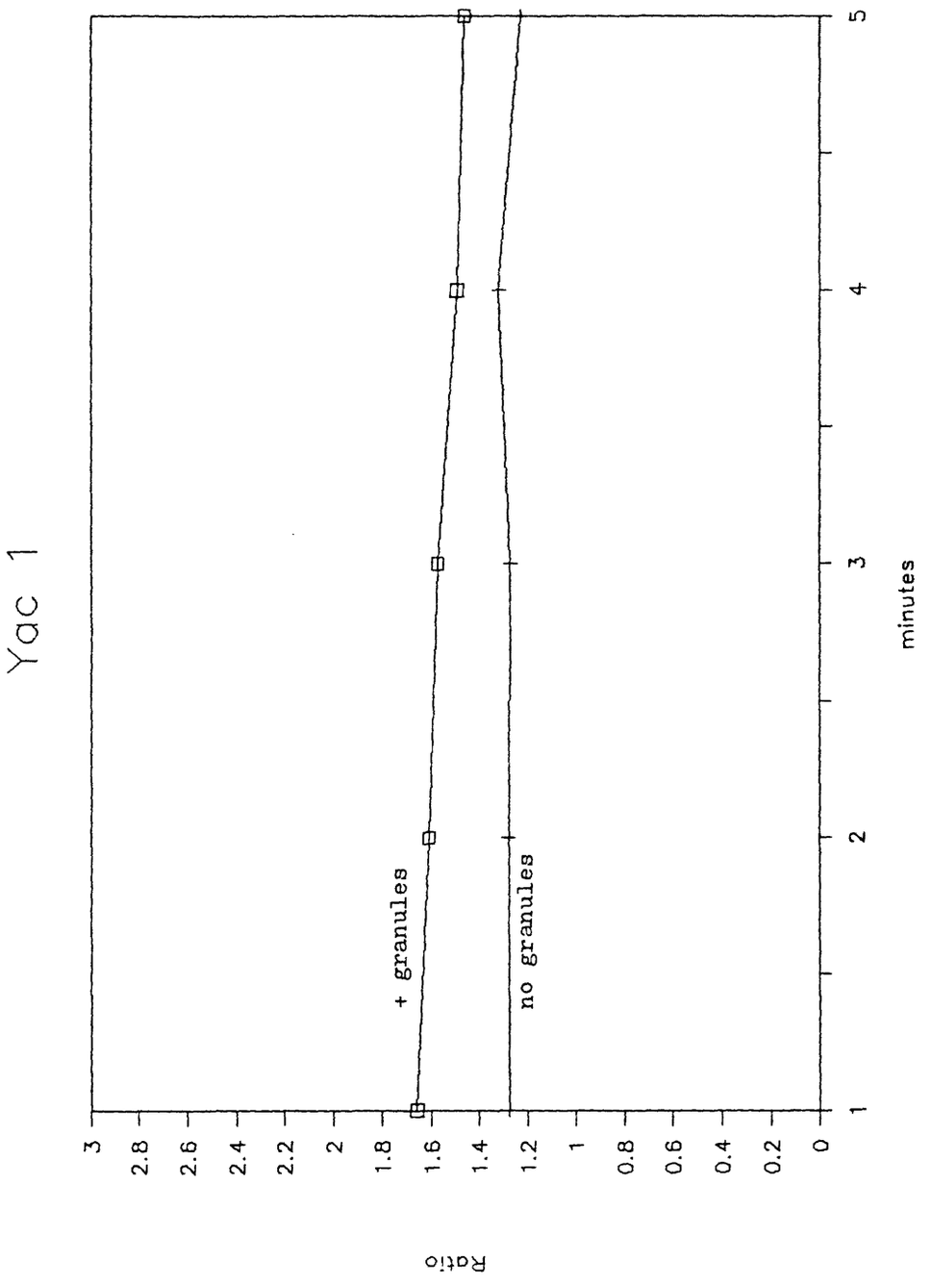
Yac 1
Ratio
minutes
+ granules
no granules
0
0.2
0.4
0.6
0.8
1
1.2
1.4
1.6
1.8
2
2.2
2.4
2.6
2.8
3
1
2
3
4
5

FIGURES 25-28

Figures 25-28 show EL4, S49, RDM4, and Yac 1 cells loaded with 3-5 uM indo-1 AM and resuspended in ECBS with 1 mM Ca++. The 405/480 ratio is plotted over time for samples with and without a dose of cytolytic granules identical to that received by the P815 cells in Figure 24. El4 cells received granules isolated from 3H2 cells while S49, RDM4, and Yac-1 cells received 3C11 granules.

FIGURE 29

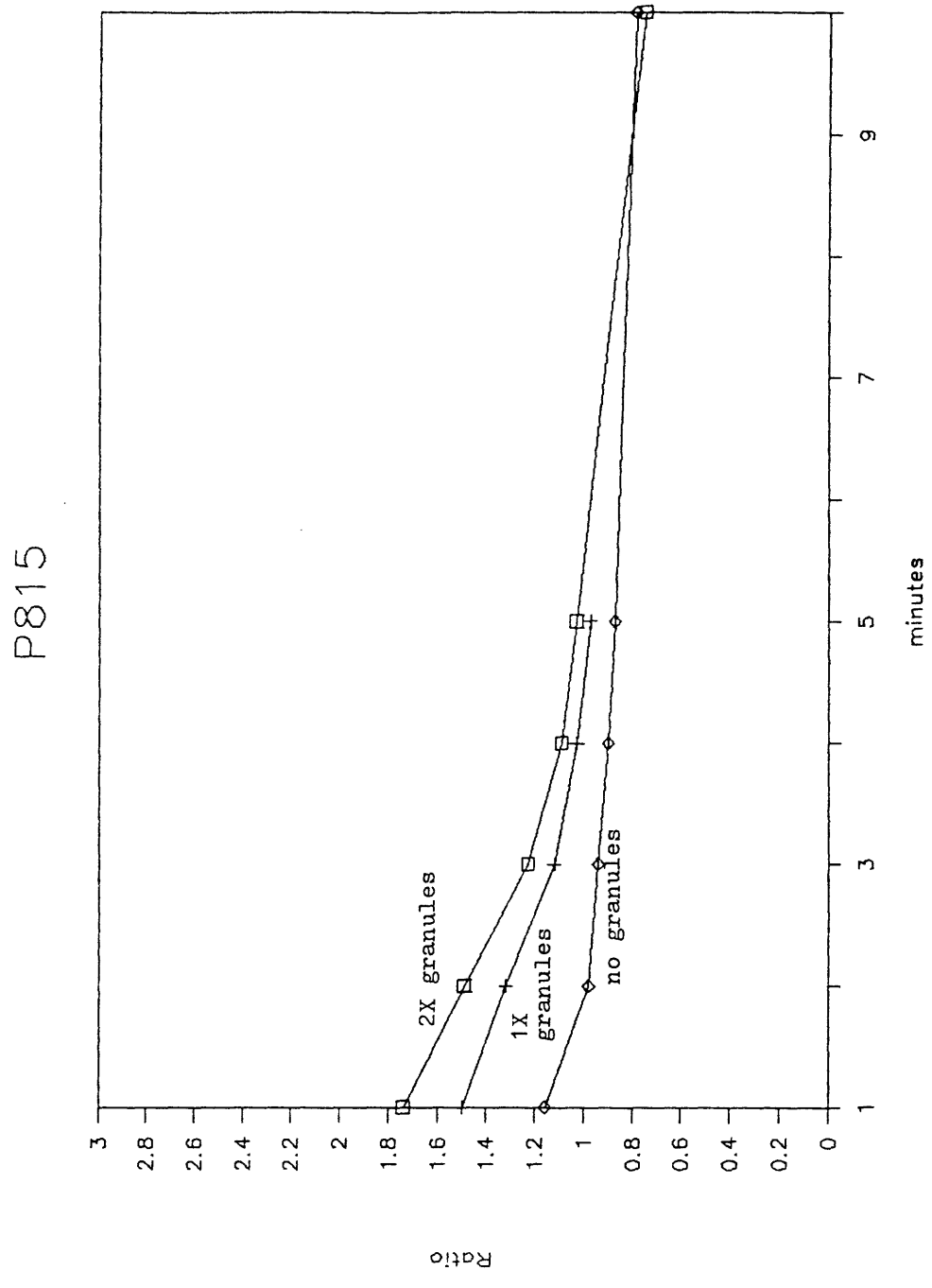
P815
Ratio
minutes
2X granules
1X granules
no granules
3
2.8
2.6
2.4
2.2
2
1.8
1.6
1.4
1.2
1
0.8
0.6
0.4
0.2
0
1
3
5
7
9

FIGURE 29

P815 cells were loaded with 5 uM indo-1 AM and resuspended in ECBS with 1 mM Ca++. The 405/480 ratio is graphed over time for samples with and without 3H2 granules. The 2X sample was sublytic to P815 (see legend, Figure 24).

C. Effect of Granules on Cloned T Cell Lines

It has recently been recognized that CTL clones are more resistant than tumor cells to the cytolytic effects of CTLs or their isolated granules[67,68]. We measured the ICF Ca++ level in these resistant cells after addition of cytolytic granules.

CTL clones (2C and G4), a T helper-killer clone (5.5) and a noncytolytic T helper clone (D10) showed no calcium rise in response to doses of granules that caused a substantial increase in tumor cells (Figures 30-33). The 2C cells had no calcium influx even at doses that lysed P815 cells. Upon exposure to granules, a small subpopulation of TDH1, a noncytolytic T helper clone developed an elevated calcium (Figure 34) but most of the TDH1 cells showed no calcium influx. This behavior is in contrast to the tumor cells tested where all cells responded in the same way. The subpopulation of TDH1 cells with an elevated calcium disappeared by 10 minutes and it is not clear whether this is due to recovery of a normal ICF calcium or loss of dye from the affected cell population.

It has been shown that when all cells except $CD8^+$ CTLs ($L3T4^+$, $Lyt\text{-}2^+$), are depleted of ATP (by incubation in azide and cyanide without glucose) they became much more susceptible to granule-mediated lysis[67]. To determine whether ICF Ca++ levels mirror this effect,

FIGURE 30

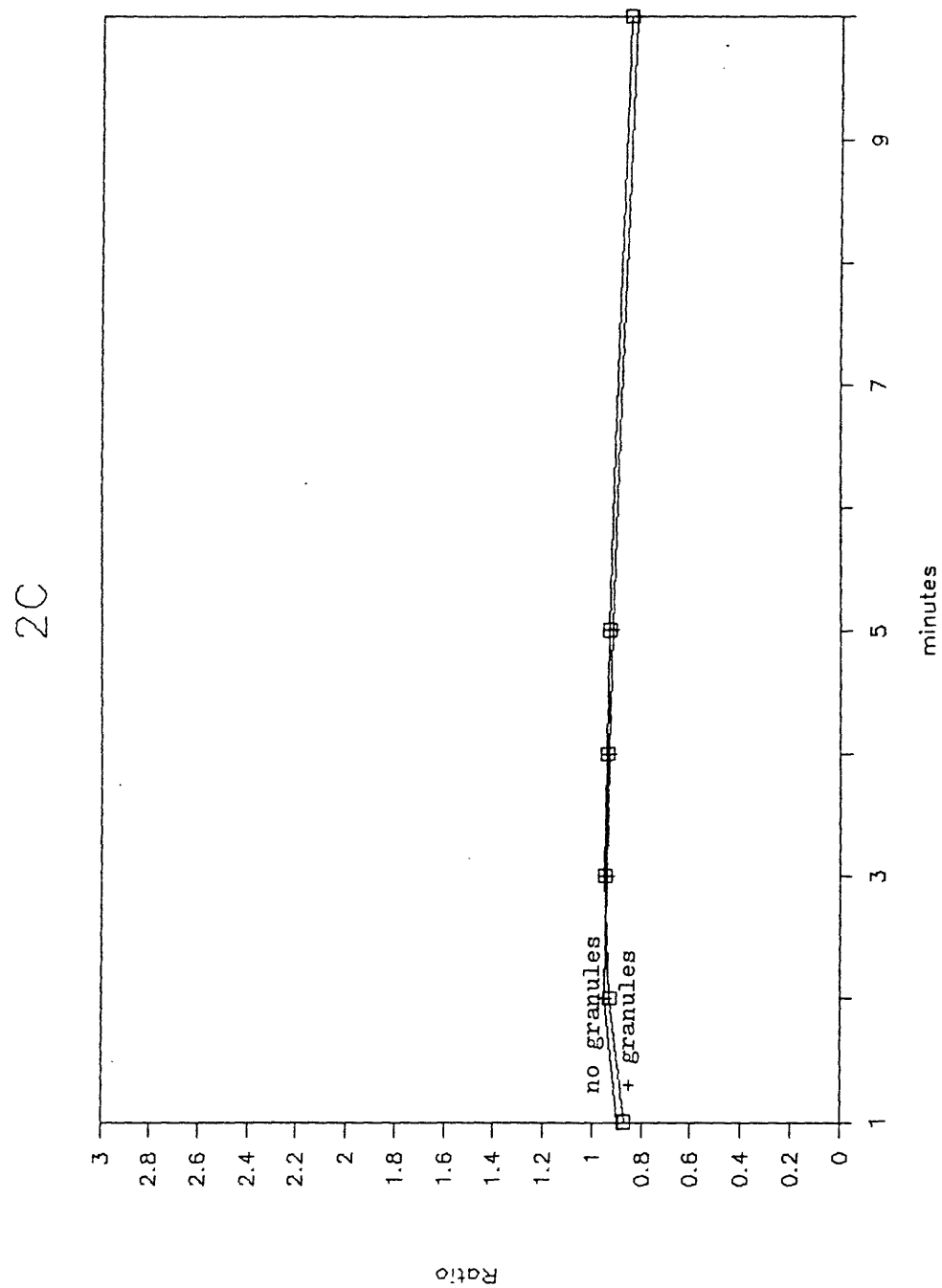
2C
Ratio
minutes
no granules
+ granules
0
0.2
0.4
0.6
0.8
1
1.2
1.4
1.6
1.8
2
2.2
2.4
2.6
2.8
3
1
3
5
7
9

FIGURE 31

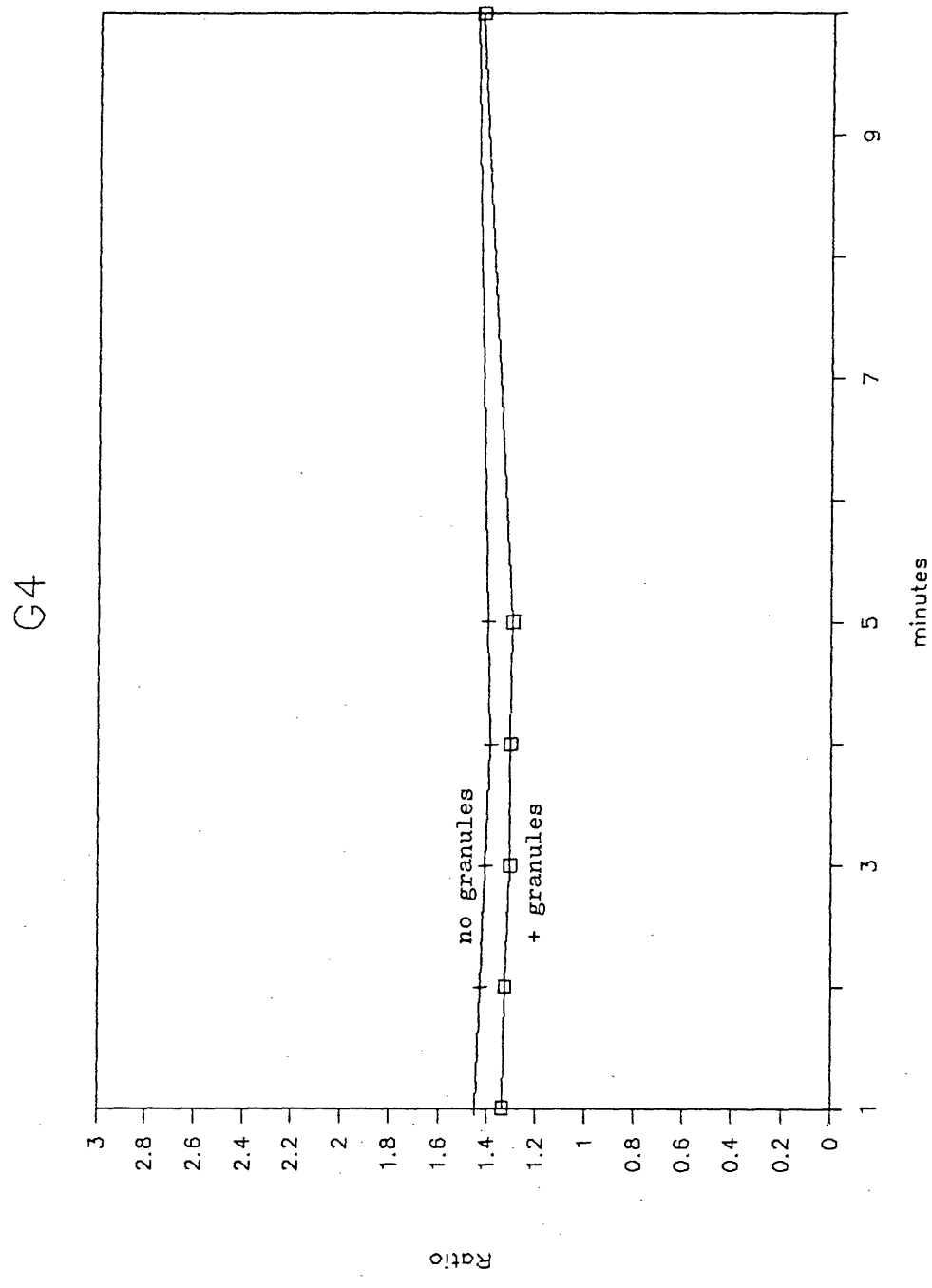
G4
Ratio
3
2.8
2.6
2.4
2.2
2
1.8
1.6
1.4
1.2
1
0.8
0.6
0.4
0.2
0
1
3
5
7
9
minutes
no granules
+ granules

FIGURE 32

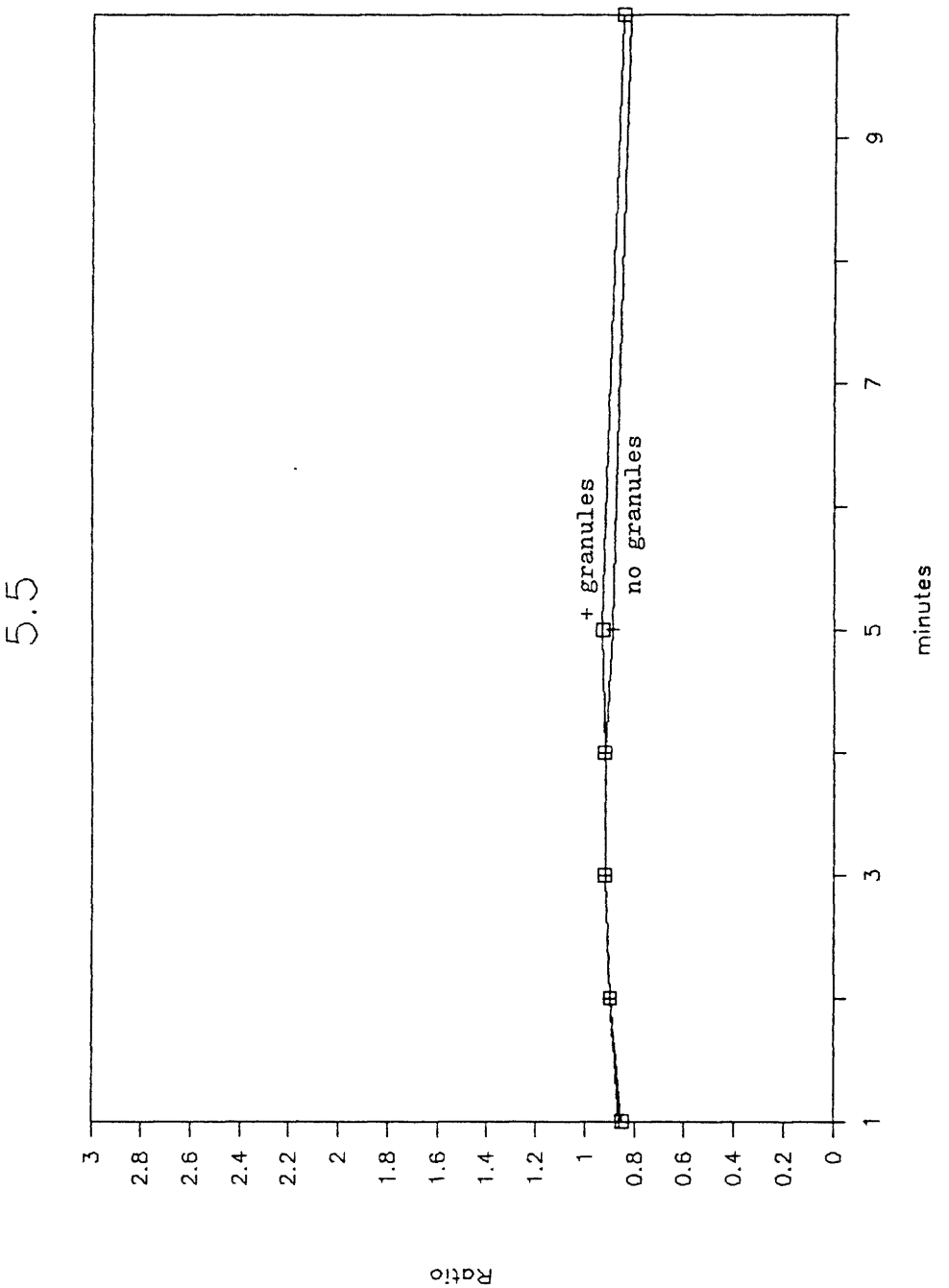
5.5
Ratio
3
2.8
2.6
2.4
2.2
2
1.8
1.6
1.4
1.2
1
0.8
0.6
0.4
0.2
0
1
3
5
7
9
minutes
+ granules
no granules

FIGURE 33

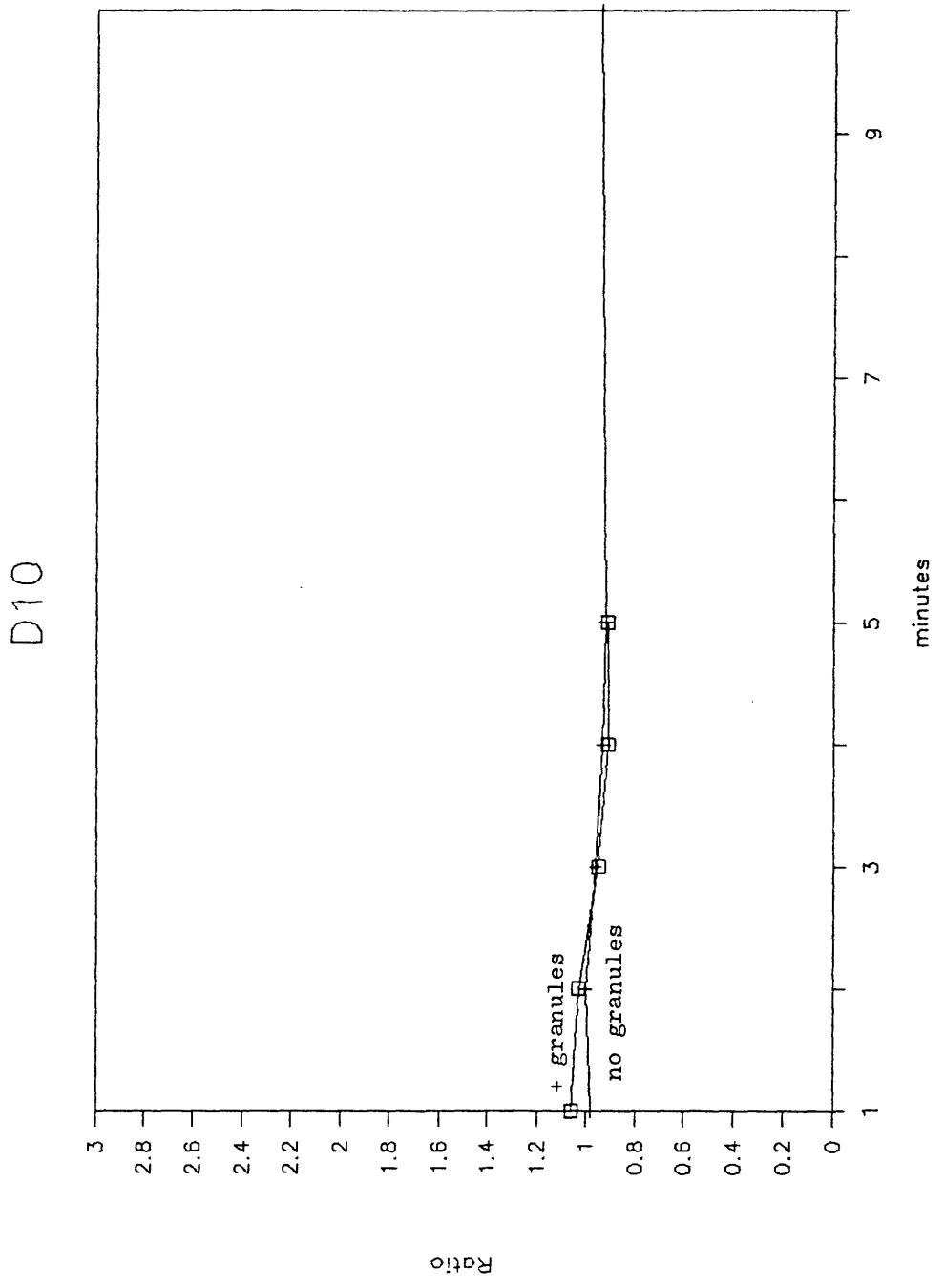
D10
Ratio
minutes
+ granules
no granules
3
2.8
2.6
2.4
2.2
2
1.8
1.6
1.4
1.2
1
0.8
0.6
0.4
0.2
0
1
3
5
7
9

FIGURE 34

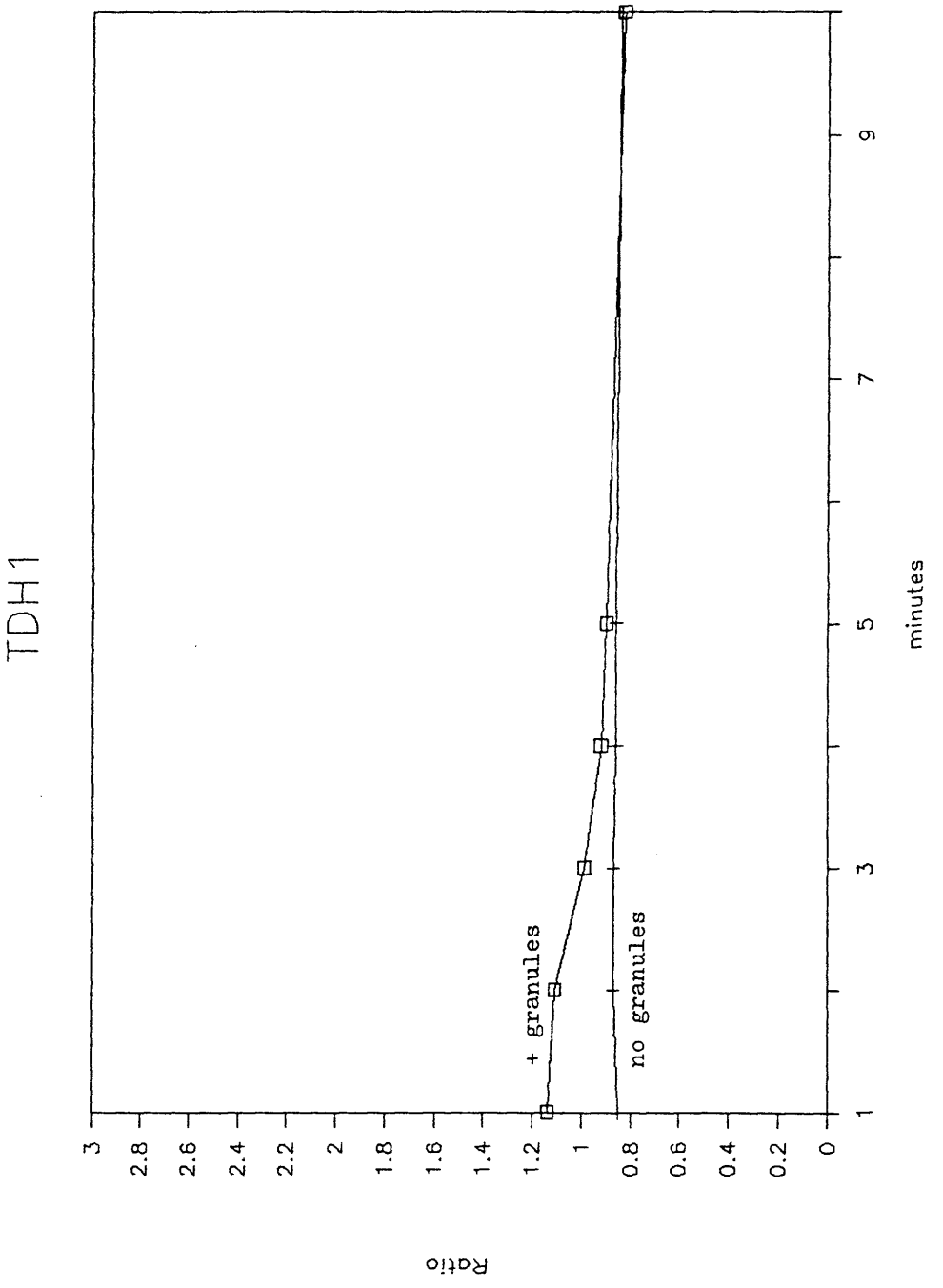
TDH1
Ratio
minutes
+ granules
no granules
3
2.8
2.6
2.4
2.2
2
1.8
1.6
1.4
1.2
1
0.8
0.6
0.4
0.2
0
1
3
5
7
9

FIGURES 30-34

Figures 30-34 show 2C, G4, 5.5, D10, and TDH1 cells loaded with 1.0-1.5 uM indo-1 AM and resuspended in ECBS with 1mM Ca++. The 405/480 ratio is plotted over time for samples with and without a dose of cytolytic granules identical to that received by the P815 cells in Figure 24. 2C cells received 3H2 granules while G4, 5.5, D10 and TDH1 received 3C11 granules.

indo-1-loaded 2C cells were preincubated with 1 mM CN, 3 mM azide in a glucose free media for 1.5 hours (to block ATP production) and then exposed to granules: no increase in ICF Ca++ was observed (Figure 35). When D10, noncytolytic CD4+ cells ($L3T4^+$, $Lyt\text{-}2^-$), were preincubated in the same way with CN and azide, they showed a subpopulation of cells with an elevated calcium. This subpopulation was present through out the 1-10 minute time course.

Thus all the observations show that the ICF calcium rise correlates with susceptibility to granule-mediated lysis. Tumor cells, which are highly susceptible uniformly responded with an ICF Ca++ increase. The T cell clones, which are less susceptible, required larger concentrations of granules to be lysed and do not respond in a homogeneous fashion like the tumor cells. The CD8+ CTLs seem to be uniquely resistant to the granules and also attack by intact CTLs[67,68] and they did not have a significant Ca++ increase in response to the granules even when the cells had been depleted of ATP by preincubation with azide and cyanide. While these findings do not prove that calcium plays a critical role in target cell death, they do provide evidence that this may be the case.

Reynold Verret, MIT postdoctoral fellow, provided the Cr^{51} release data for sections V.B. and V.C.

FIGURE 35

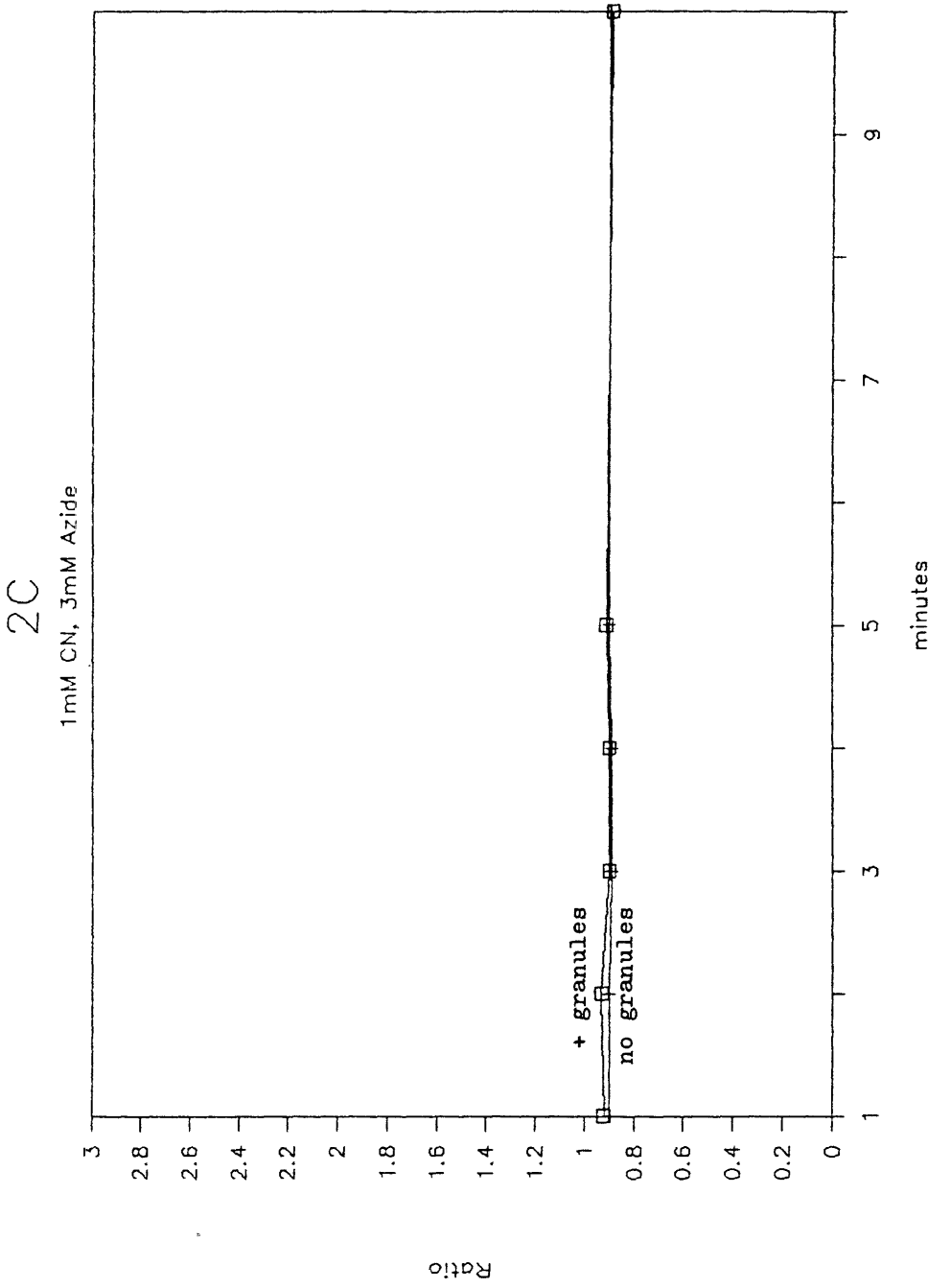
2C
1mM CN, 3mM Azide
+ granules
no granules
Ratio
minutes
3
2.8
2.6
2.4
2.2
2
1.8
1.6
1.4
1.2
1
0.8
0.6
0.4
0.2
0
1
3
5
7
9

FIGURE 35

2C cells were loaded with 1 uM indo-1 AM and resuspended in ECBS with 1 mM Ca++ and without glucose. The cells were incubated at 37°C for 1.5 hours with 1 mM CN and 3 mM azide. Figure 35 shows the change in the ratio over time after addition of 3H2 granules at the same concentraton as in Figure 24.

VI. The Effect of CTLs on the ICF Ca++ of Target Cells

A. Introduction

While granules isolated from CTLs lyse most cells and cause an immediate and substantial rise in the ICF Ca++ of target cells, it is not clear that the granules are the sole mediators of target cell death[3,62,65]. Thus, lytic granules have not been isolated from murine peritoneal exudate lymphocytes or from human T8+ CTLs[62]. Therefore, we examined changes in the intracellular free calcium of target cells that were exposed to intact CTLs.

It is possible to divide the stages of target cell killing by CTLs into three steps: conjugate formation, programming for lysis, and target cell lysis[3-5]. The first two steps have different cation and temperature requirements and thus can be separated. Conjugation occurs at room temperature and requires the presence of Mg++. Programming for lysis requires a 37°C temperature and extracellular Ca++. If calcium is absent or the cells are kept at room temperature, conjugation will occur but not cell lysis. Berke and Perez et al took advantage of these requirements to examine the kinetics of cell conjugation[17,18]. In these two studies, CTLs and target cells were labelled with different fluorescent markers and conjugates identified using a flow cytometer[17,18]. Cells were identified as conjugated or unconjugated and the

changes in the CTL-target cell conjugate numbers were followed quantitatively over time. In addition they verified that the percent of conjugates observed by flow cytometry is similar to that observed by microscopy[17,18]. We have modified their technique to observe changes in the ICF Ca++ of targets while they are conjugated.

B. Effect of Extracellular Medium on Killing by CTLs

It is important to know the effect of media on the ability of CTLs to kill. To decrease background noise it is desirable to use a medium that fluoresces minimally when excited in the UV. Both the vitamins and proteins in K medium can fluoresce[124]. For this reason Cr^{51} release (killing) assays were compared in several media: ECBS, ECBS + 1% FCS, ECBS + 5% FCS, and K medium (FCS is fetal calf serum). The ECBS contained 5 mM glucose and 1 mM Ca++. It is apparent from Figure 36 that even the addition of FCS to 5% cannot increase killing activity in ECBS to the level attained in K medium. K medium contains vitamins, amino acids, and salts (essentially the same as in ECBS), glucose and 10% FCS and any number of these components may be necessary for optimal killing. Accordingly K medium was used for all killing assays in the flow cytometer.

FIGURE 36

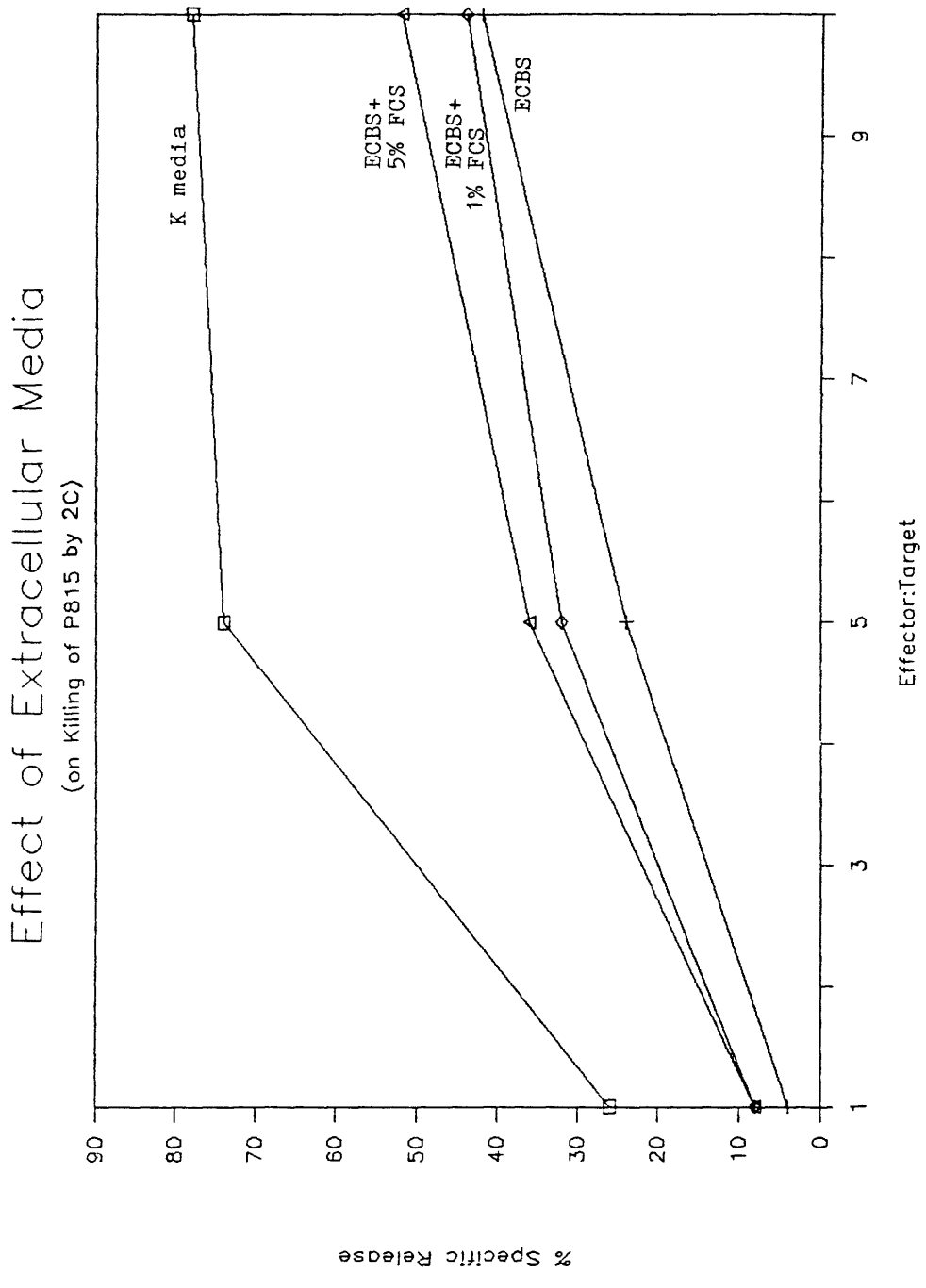
Effect of Extracellular Media
(on Killing of P815 by 2C)
% Specific Release
Effector:Target
K media
ECBS+
5% FCS
ECBS+
1% FCS
ECBS
0
10
20
30
40
50
60
70
80
90
1
3
5
7
9

FIGURE 36

The effect of the extracellular medium on the ability of 2C to kill P815-Cr^{51} was tested. Standard Cr^{51} release assays were done in the indicated medium using E:T ratios of 1, 5, and 10. The composition of K medium and ECBS is given in the methods section. FCS is fetal calf serum (heat-inactivated).

C. Single Labelling Experiment With P815 and 2C Cells

In a preliminary experiment, unlabelled 2C cells were mixed with indo-1-loaded P815 cells at (2C:P815) ratios of 0:1, 1:1, 5:1 in 1 ml K medium at 37°C; in all cases the number of P815 cells was $5X10^5$ cells. Figure 37 shows the proportion of P815 cells with an elevated calcium (R>1.0) over time. There are clearly more cells with an elevated Ca++ in the 5:1 than in the 1:1 or 0:1 mixtures. However, fluctuations in the percent of high-Ca++ cells in the control population and even in the 1:1 population was at times (0, 45 minutes) almost as large as the signal measured at 90 minutes. Moreover, a control mixture containing CTLs and inappropriate target cells was not included. Finally the data in Figure 37 gives no information about the kinetics of the Ca++ rise, i.e. pre- or post-conjugation. For these reasons more detailed experiments were conducted with fluorescently labelled 2C as well as indo-1-labelled target cells and, EL4 cells as inappropriate targets.

D. Evaluation of Fluorochromes for CTL Labelling

Several different fluors were evaluated as labels for 2C cells. It was necessary to choose a molecule whose fluorescence spectrum overlapped minimally with that of indo-1 and whose presence did not affect cytolytic

FIGURE 37

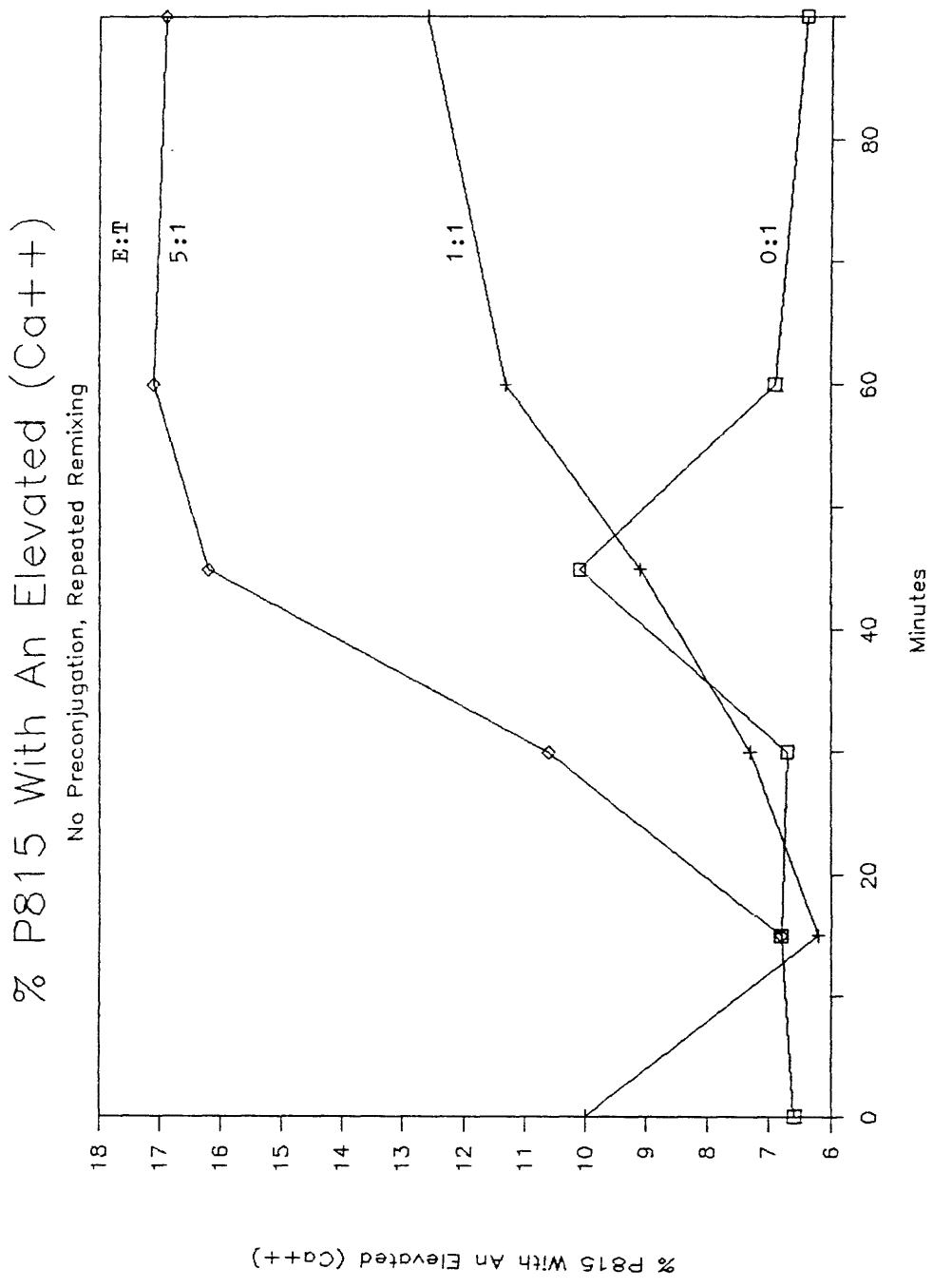
% P815 With An Elevated (Ca++)
No Preconjugation, Repeated Remixing
E:T
5:1
1:1
0:1
% P815 With An Elevated (Ca++)
Minutes
18
17
16
15
14
13
12
11
10
9
8
7
6
0
20
40
60
80

FIGURE 37

P815 cells were loaded with 5 uM indo-1 AM and resuspended in K medium. 2C cells were added to $5X10^5$/ml P815 cells at E:T ratios of 5, 1, and 0. Measurements of the 405/480 ratio were taken over 90 minutes (as described in the methods section). The percent of P815 cells with the 405/480 ratio > 1 was plotted on the y-axis.

activity. It was also necessary that an excitation source for the fluorochrome had to be available.

FITC (fluorescein isothiocyanate), APC (allophycocyanine), and PE (phycoerythrin) were evaluated.

Table 9

Dye	Excitation Maximum	Emission Maximum	Laser Lines
FITC[122]	490nm(also UV)	520nm	351-364nm
APC[108]	650nm	660nm	633 or 647 nm
PE[108]	495, 545nm	576nm	568nm
Indo-1[113]	349, 331nm	480, 405nm	351-364nm

Initially FITC was tried, since it is easy to attach to cells, can be excited with the UV beam already in use and has a good quantum efficiency and absorption coefficient[122]. However both FITC and indo-1 have fairly broad emission spectra and there was considerable overlap of each signal into the inappropriate PMT (i.e. indo-1 signal entering into the FITC channel and vice versa.)

Allophycocyanine (APC) is an algal protein with a long emission wavelength (660nm)[108]. Since this emission wavelength is widely separated from that of indo-1 and since a helium neon (HeNe) laser (633 nm) was available as an excitation source, APC was tried as a label for the

CTLs. To attach APC to the cells, the cells were biotinylated (see Methods) and then APC-avidin was added. At the highest concentrations of APC used, the APC fluorescence of the stained cells was not always well separated from the autofluorescence of the unstained control cells (on histograms of APC fluorescent intensity). At these staining levels the cell pellets were visibly blue so it is clear that large amounts of APC were on the cell surface. With this much dye on the surface of the cell it is possible that the 7mW HeNe laser was not capable of exciting all of the dye molecules. For this reason and since a krypton laser had become available, the 647 nm line of a krypton laser was used for APC excitation. This laser is capable of putting out over 100 mW at that line. APC stained and unstained cells were again only marginally separable primarily due to the difficulty of dividing the very close excitation and emission wavelengths. Multiple filters and dichroics were tried for both the HeNe (633) and krypton (647) excitation as well as coincident and delayed line-up of the laser beams with respect to the argon UV beam. Neither of these efforts significantly improved the results.

The level of APC staining used significantly reduced (by 50%) the ability of 2C to kill. Due to the marginal fluorescent signal and marked reduction in CTL killing

efficiency, it was decided not to pursue APC-CTL labelling further.

Phycoerythrin (PE), an algal protein with a high quantum number and absorption coefficient[108]. The krypton laser has a line at 568 nm (>100 mW) which is an excellent excitation source for PE. In addition, PE emits at 576 nm which should be sufficiently far from the indo-1 emission wavelengths.

PE was excited with the 568 nm line (50 mW) of a 5 W Coherent krypton laser. To measure simultaneously, indo-1 and PE emissions, the krypton beam was spatially separated from the argon beam so as to give a signal time difference of 35 usec. A UV bandpass filter was added to the UV forward scatter channel to remove scattered krypton laser light. A red-reflecting dichroic (50% at 540 nm) was used to separate the 480 nm indo-1 fluorescence from the PE fluorescence (576 nm). The PE signal was then passed through a longpass filter (>570 nm) before it was collected. Figure 38 outlines the physical flow cytometry arrangement. For the analysis of conjugates the ratio histogram was replaced by a plot of the ratio vs the PE fluorescence. This graph was gated by both the forward scatter histogram and the 405 vs 480 cytogram. All points displayed on the ratio vs PE graph contained cells loaded with indo-1, and all points with PE fluorescence were therefore defined as target cell-CTL conjugates.

FIGURE 38

FLOW CYTOMETRY SET UP FOR PE AND INDO-1

FIGURE 38

Figure 38 shows the light paths of the lasers, and the indo-1, PE, and UV forward scatter signals. The cells passed through the argon beam first and then the krypton beam (not shown).

Figure 39 shows unstained and PE-stained cells at the highest and lowest dilutions of PE used. There was a clear separation between the controls and PE-labelled cells. For experiments the lowest dilution (1/10) was used (see Methods). Aliquots of cells with and without PE labelling were used to set the positive and negative PE windows and PMT gain. Less than 0.1% of unlabelled cells and less than 1% of indo-1 stained cells (without PE) registered as positive for PE. These controls are presented in each experiments.

It was important to insure that the CTL killing efficiency was not diminished by the PE label. Figure 40 shows the effect of each of the steps of the labelling proceedure on the killing efficiency. It is clear that the biotinylation step was responsible for most of the decrement. As shown in Figure 41, decreasing the concentration of N-OH succinimidobiotin from 1.0% to 0.1% restored the killing ability of 2C. Since the biotin attaches to cell surface proteins via an amide linkage, the decrease in killing may have been due to excessive biotinylation of the T cell antigen receptor. Figure 42 shows the killing efficiency of 2C with the different steps of the modified PE labelling.

FIGURE 39

PHYCOERYTHRIN LABELLED 2C
(Cell # vs Fluorescent Intensity)

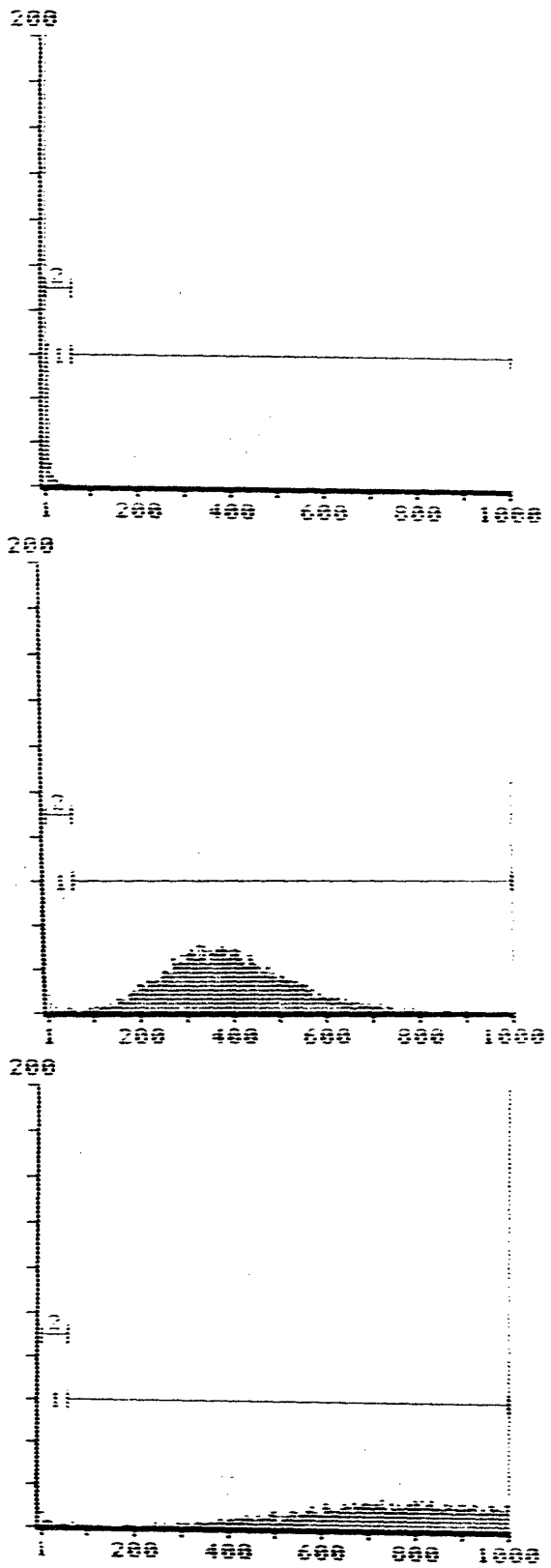

Unlabelled 2C
(mean = 2)

PE Labelled 2C
1/10 dilution of PE
(mean = 416)

PE Labelled 2C
7/10 dilution of PE
(mean = 795)

FIGURE 39

2C were stained as described in the methods section with a 1/10 and 7/10 dilution of PE-avidin. Figure 39 shows histograms of the PE fluorescent intensity for the different levels of staining. The mean channel of the fluorescent intensity is given in parenthesis.

FIGURE 40

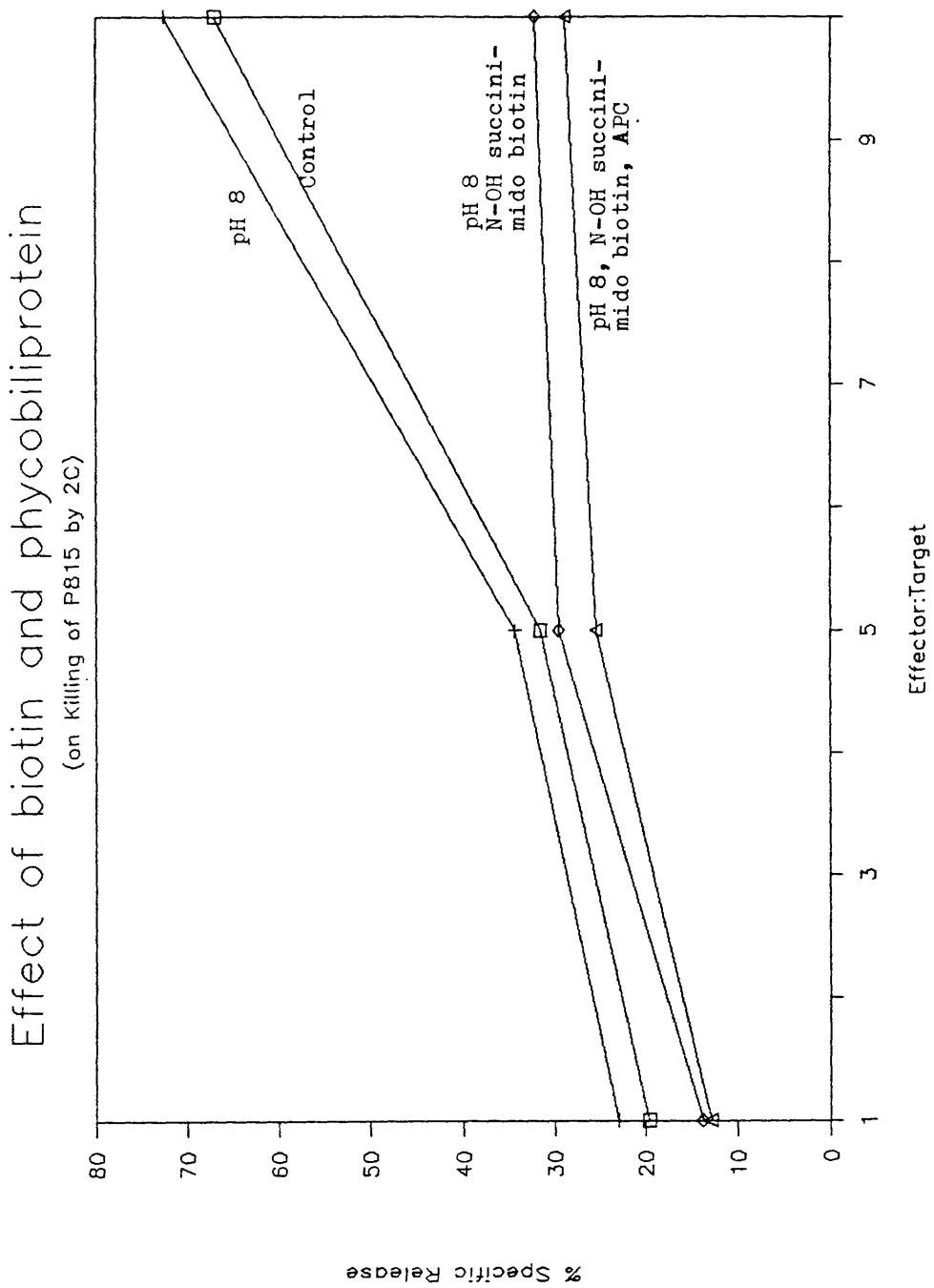
Effect of biotin and phycobiliprotein
(on Killing of P815 by 2C)
pH 8
Control
pH 8
N-OH succini-
mido biotin
pH 8, N-OH succini-
mido biotin, APC
% Specific Release
Effector:Target
0
10
20
30
40
50
60
70
80
1
3
5
7
9

FIGURE 40

Figure 40 shows the effect of labelling 2C with APC on the killing efficiency of 2C (target = P815). The labelling steps are identical to that of PE staining. Aliquots of 2C cells received successively more steps in the labelling procedure as indicated in the graph e.g. the pH 8 curve is from 2C cells placed in PBS, pH 8 but not receiving N-OH succinimido biotin or APC-avidin. Please see the methods section for a step-by-step list of the staining procedure. N-OH-succinimido biotin was used at 1% (volume/volume from a 1 mg/ml stock) for this experiment.

FIGURE 41

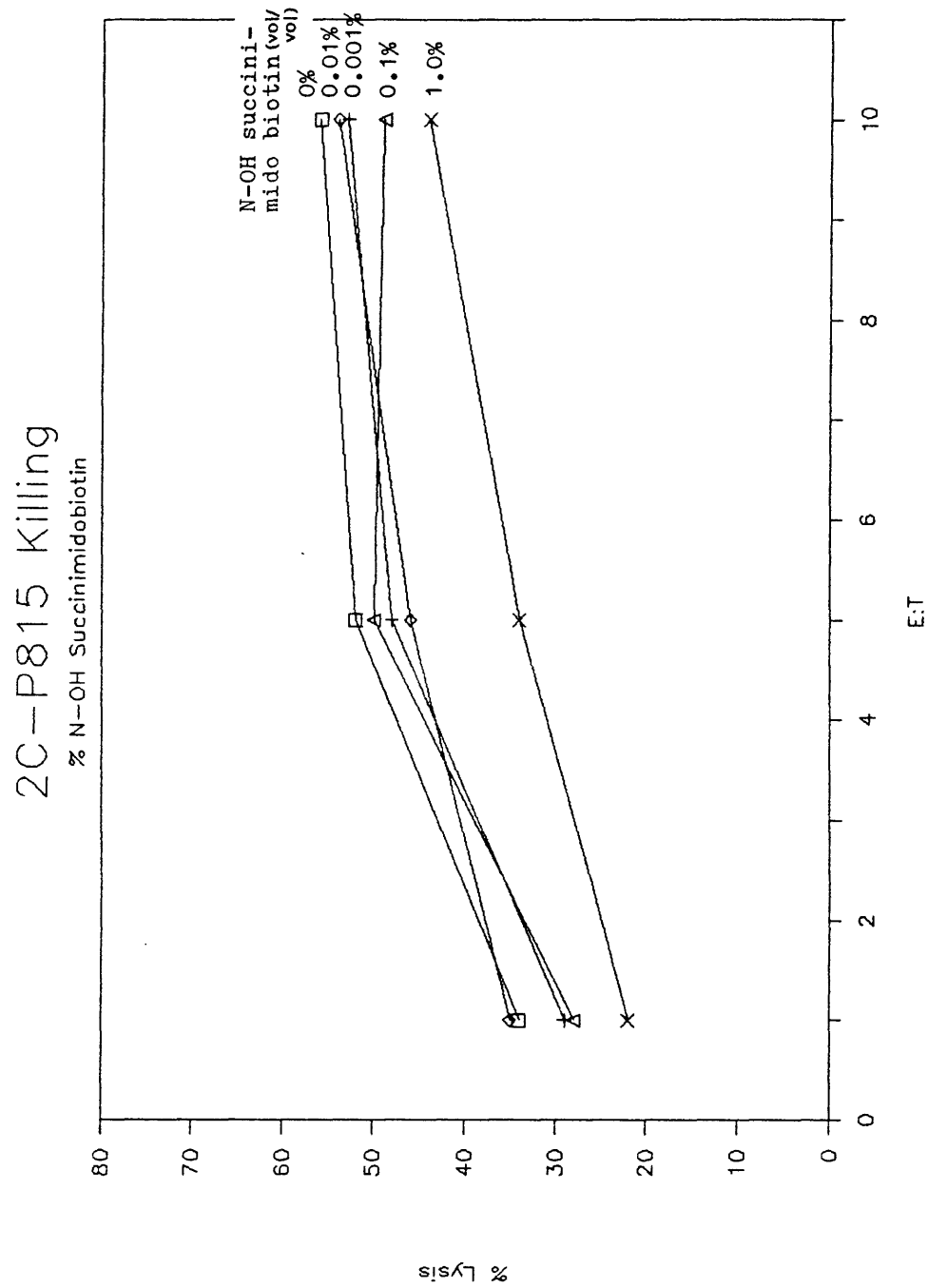
2C-P815 Killing
% N-OH Succinimidobiotin
N-OH succini-
mido biotin(vol/
vol)
0%
0.01%
0.001%
0.1%
1.0%
% Lysis
E:T
0
10
20
30
40
50
60
70
80
0
2
4
6
8
10

FIGURE 41

2C were labelled with varying concentrations of N-OH-succinimido biotin as indicated on the graph and tested for killing efficiency of P815 cells. The percent N-OH-succinimido biotin was measured as volume/volume dilution of a 1 mg/ml stock solution.

FIGURE 42

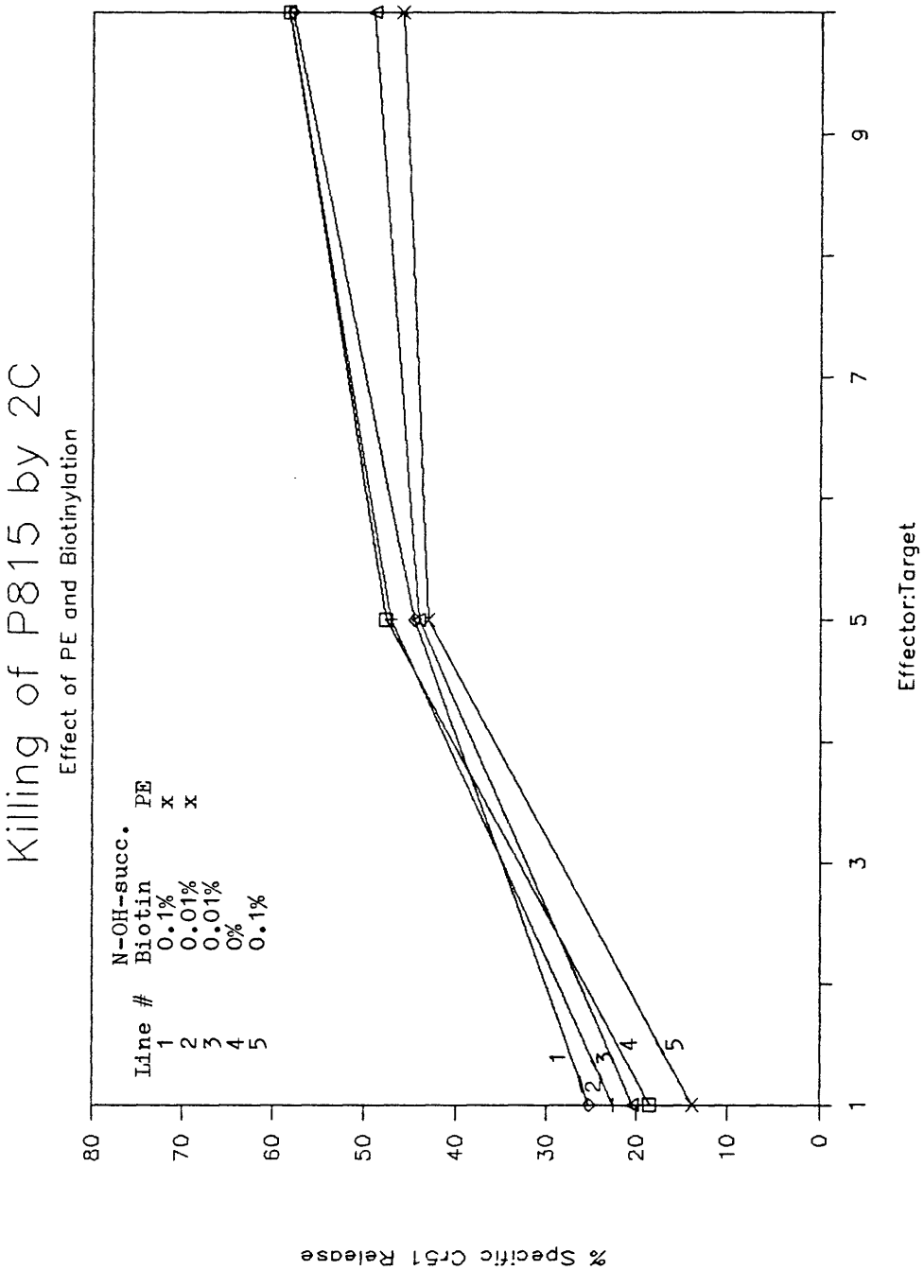
Killing of P815 by 2C
Effect of PE and Biotinylation
N-OH-succ. Biotin
PE
Line #
1 0.1% x
2 0.01% x
3 0.01%
4 0%
5 0.1%
% Specific Cr51 Release
Effector:Target
0
10
20
30
40
50
60
70
80
1
3
5
7
9

FIGURE 42

2C cells received varying steps in the PE labelling procedure as indicated in the upper corner of the graph and were tested for killing efficiency of P815 cells. For example, the 2C cells used to create line 1 received 0.1% N-OH-succinimido biotin followed by PE-avidin (1/10 dilution) while the cells used for line 3 recieved 0.01% N-OH-succinimido biotin but no PE-avidin.

E. Conjugate Formation

In order to assess the amount of time required for conjugates to form, targets (P815 cells) and CTLs (clone, 2.1.1) were mixed in a 1:1 ratio and the number of paired cells was counted (by microscope) at various time points. Some of the samples were centrifuged (300 g, 5 min) and then by vigorously resuspended. Before counting, all samples were vigorously resuspended to break-up nonspecific or unstable cell-pairs. Figure 43 shows the time course of conjugation at room temperature. At most, approximately 30% of the CTLs (or targets) were in conjugates at any given time. This agrees well with values reported in the literature and with later flow cytometer results[17,18]. While centrifugation clearly speeded up conjugation, it appeared that after 45 minutes the level of conjugation was almost the same in samples that had or had not been centrifuged at time zero. Since it required approximately 45 minutes to prepare the flow system, the preliminary centrifugation was omitted.

F. Double Label Conjugate Experiments

"Double-label congugate" experiments were conducted with PE-labelled 2C as well as indo-1-labelled target cells (P815) and indo-1-labelled EL4 cells as inappropriate targets. The haplotype of P815 cells is H-2^d and of EL4 cells is H-2^b. Thus 2C cells, which are

FIGURE 43

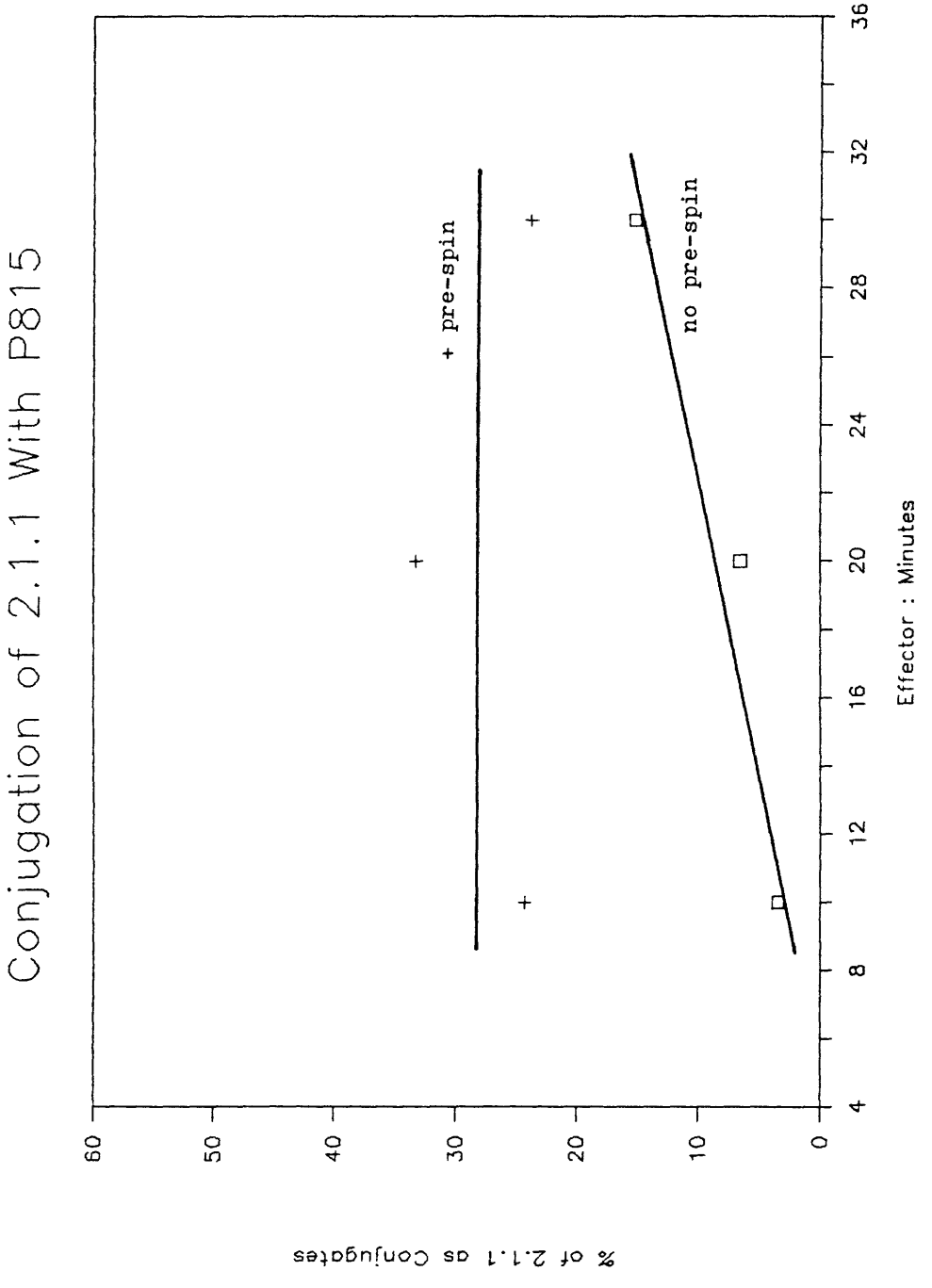
Conjugation of 2.1.1 With P815
% of 2.1.1 as Conjugates
60
50
40
30
20
10
0
4
8
12
16
20
24
28
32
36
Effector : Minutes
+ pre-spin
no pre-spin

FIGURE 43

P815 and 2.1.1 cells were mixed in a 1:1 ratio ($1X10^6$ P815/ml) and maintained at room temperature. A portion of the cells were given a prespin (300g, 5 minutes) while others were not. Separate aliquots of cells were used for each time point. The number of paired cells was counted with a microscope at the indicated times. The cells were vigorously resuspended before counting. P815-2.1.1 cell pairs were not distinguished from P815-P815 or 2.1.1-2.1.1 pairs. The percent of 2.1.1 cells conjugated was calculated assuming that half of the paired cells were 2.1.1 cells.

specific for H-2^d (actually for L^d), kill P815 but not EL4 cells. Two experiments were carried out. In the first, PE labelled 2C cells (2C-PE) were preconjugated (at room temperature) with indo-1-loaded P815 cells (P815-indo-1) and EL4-indo-1 in a ratio of 2.5 CTLs to 1 target cell. Also additional control samples of P815-indo-1 and EL4-indo-1 cells, each incubated alone, were prepared. A different sample was used for each time point to avoid the unknown effects of shaking or stirring the cell mixtures. Time zero was the time at which the samples were warmed to 37°C. All four time courses (i.e. for the two CTL/target cell mixtures and the two target cell controls) were run concurrently.

The second experiment was carried out in the same way except that P815 cells were replaced by indo-1-loaded EL4 cells that had attached to them a monoclonal antibody to the antigen-specific receptor of 2C cells. The antibody is called 1B2 and the cells termed EL4-indo-1-1B2. It has been shown that linkage of the 1B2 antibody to virtually any target cell regardless of its surface antigen or H-2 haplotype allows the 2C cells to kill target cells that they would not normally recognize and kill[8]. Figure 44 confirms that 2C cells lyse EL4-1B2 but not EL4 cells. To prepare the EL4-indo-1-1B2 cells, the cells were labelled first with 1B2 and then loaded with indo-1 AM. Since EL4-indo-1 cells were used as controls,

FIGURE 44

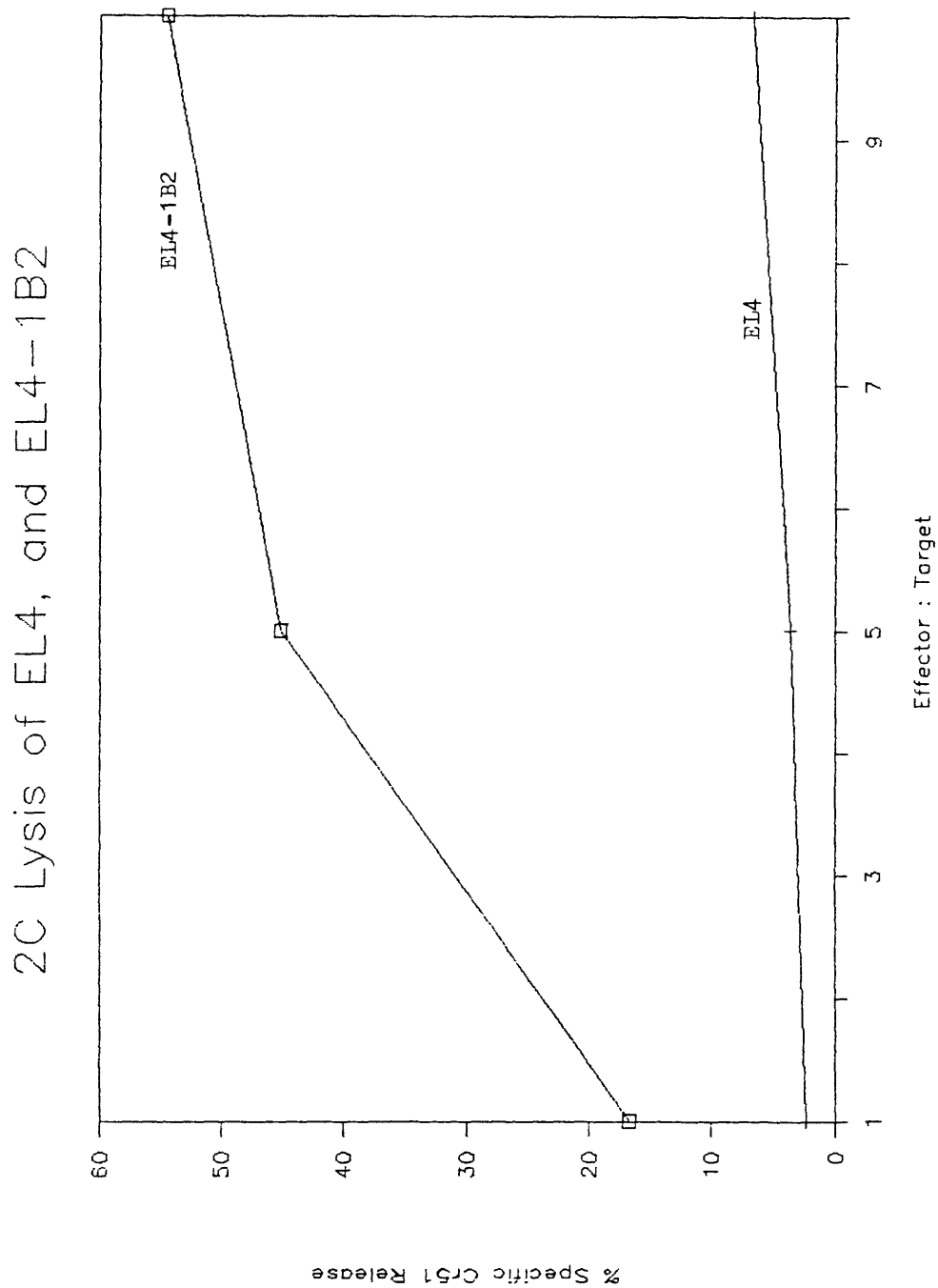
2C Lysis of EL4, and EL4-1B2
EL4-1B2
EL4
% Specific Cr51 Release
Effector : Target
0
10
20
30
40
50
60
1
3
5
7
9

FIGURE 44

EL4 cells were loaded with Cr^{51} alone or Cr^{51} followed by 1B2 labelling. Figure 44 shows the ability of 2C cells to lyse EL4 and EL4-1B2 cells.

the advantage of EL4-indo-1-1B2 over P815-indo-1 cells as specific targets eliminated the possibility that the P815 cells responded in a peculiar way to contact with other cell types, or that they were unusually susceptible to anoxia induced by cell crowding at the bottom of the tube.

Results from the experiment with EL4-indo-1-1B2 are presented in Figures 45-48 and Tables 10-14. Control data are shown in Table 10. There was very little interference of the PE with the indo-1 signal and vice versa.

Table 10- Controls

Cell Samples	Objects Staining Positive for Phycoerythrin	Counts on Ratio Cytogram	Counts on Ratio Cytogram that Are Positive for PE
2C	0.07%	0.06%	0.03%
2C-PE	98.4%	0.02%	0.01%
EL4	0.01%	0.01%	0.00%
EL4-indo-1	0.87%	81.8%	0.67%

Figure 45 shows the form of the data display. The two left-hand graphs are plots of the fluorescence intensity at 405nm(Y) vs 480nm(X). The large circular region labelled 1 is the indo-1 gate. The two right-hand graphs are plots of the PE fluorescent intensity(Y) vs the ratio*30(X). The 405/480 ratio was multiplied by a factor of 30 so it would fit on the fixed scale of the x-axis. The boxes on this graph are as follows: 1. unconjugated cells, normal ICF Ca++, 2. conjugated cells,

FIGURE 45

15 Minutes

2C + EL4

405nm(Y) vs 480nm(X)

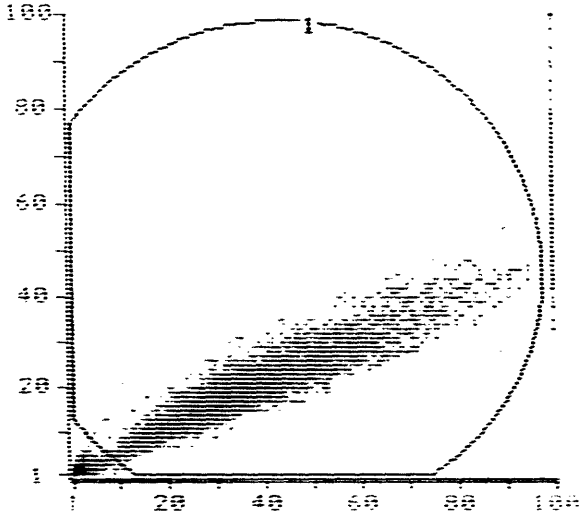

Phycoerythrin(Y) vs Ratio(X)

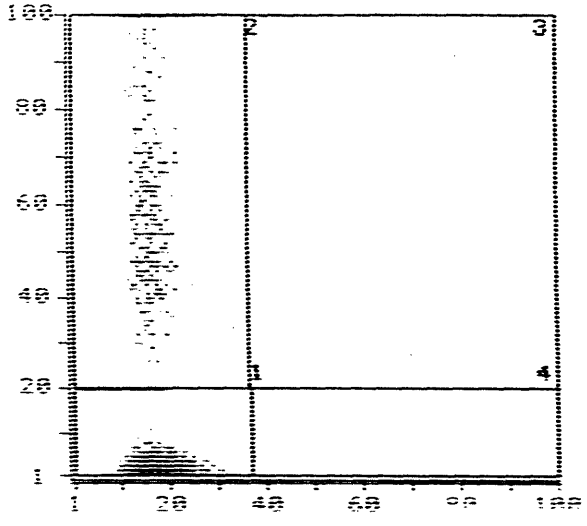

2C + EL4-1B2

405nm(Y) vs 480nm(X)

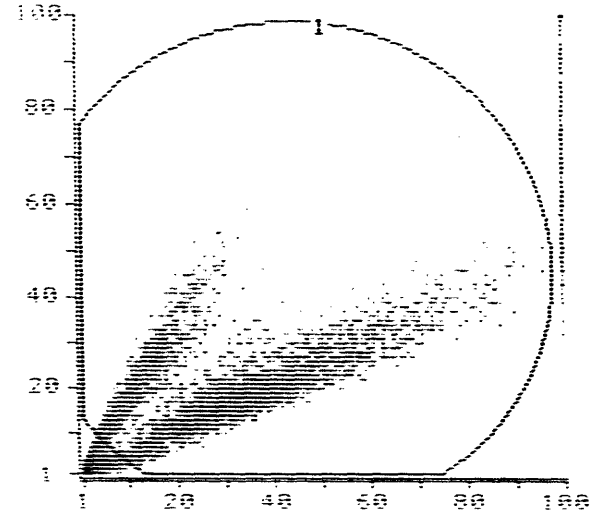

Phycoerythrin(Y) vs Ratio(X)

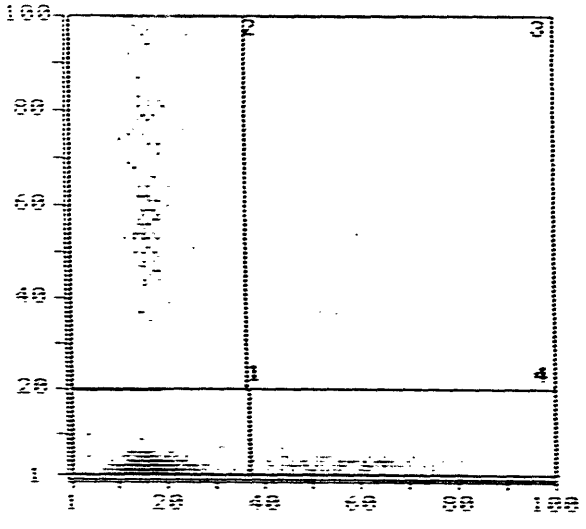

FIGURE 45

EL4 and EL4-1B2 cells were loaded with 5 uM indo-1 AM. The experiments and graphs are described in detail in the text in the section, "Double Label Conjugate Experiments."

normal ICF Ca++, 3. conjugated cells, elevated ICF Ca++, and 4. unconjugated cells, elevated ICF Ca++. Cells with a ratio greater than 1.25 were designated as having an elevated ICF Ca++ and those with less as having a normal ICF Ca++. The upper two graphs are the 15 minute time point for the 2C-PE + EL4-indo-1 mixture while the lower two graphs are the same time point for 2C-PE + EL4-indo-1-1B2 mixture. Both combinations of cells have clearly visible conjugates (box 2, ratio vs PE graph). The 2C-PE + EL4-indo-1-1B2 sample, however, also has a subpopulation of cells with an elevated calcium level (see the 405 vs 480 graph). It is also easily seen that the subpopulation of cells with an elevated Ca++ have a lower fluorescent intensity than the other cells, as though they are leaking dye. The decrease in intensity is not an artifact of an elevated Ca++ level since cells exposed to sublytic levels of granules do not undergo this fluorescent intensity decrease. At this time point (15 minutes), 22% of the conjugated EL4-indo-1-1B2 have an elevated Ca++, but this is not obvious from the ratio vs PE graph because box 3 occupies a large area and the dots do not reproduce well.

In this experiment measurements were taken at 0, 5, 15, 30, and 60 minutes. The percent of conjugated cells was slightly higher for EL4-indo-1-1B2 (20-37%) than for EL4-indo-1 alone (20-27%). In the control, 2C-PE + EL4-

indo-1 mixture, neither unconjugated nor conjugated EL4-indo-1 cells showed an increase in the intracellular free calcium. However, in the 2C-PE + EL4-indo-1-1B2 samples there was a striking increase in the percent of EL4-indo-1-PE cells with an elevated intracellular calcium in both the conjugated and unconjugated populations. At 30 minutes 33.5% of the target cells in the 2C-PE + EL4-indo-1-1B2 mixture had an elevated calcium whereas in the controls e.g. EL4-indo-1 alone, EL4-indo-1-1B2 alone, and 2C-PE + EL4-indo-1, only 1.3%, 1.5%, and 1.6% respectively of the indo-1 loaded cells had an elevated ICF Ca++. Also, at 30 minutes the 2C-PE + EL4-indo-1-1B2 mixture had a mean ratio of 1.09 whereas the EL4-indo-1, EL4-indo-1-1B2, and 2C-PE + EL4-indo-1 controls had mean ratios of 0.62, 0.63, and 0.64 respectively (Tables 11-14 and Figure 46). It is clear that an elevated intracellular calcium level was detectable within 5 minutes in the appropriate targets of 2C cells.

Double Label Conjugate Experiments (with EL4-1B2)

Table 11- Mean Ratio With 5uM Ionomycin (Control Cells)

Samples	5mM EGTA	1mM Ca++
EL4-indo-1	0.33	2.56
EL4-indo-1-1B2	0.37	2.53

Table 12- Mean Ratio of All Cells

	Minutes 0	5	15	30	60
Samples					
EL4-indo-1	0.46	0.54	0.58	0.62	0.68
EL4-indo-1 1B2	0.50	0.54	0.60	0.64	0.68
EL4-indo-1 + 2C-PE	0.48	0.53	0.59	0.63	0.68
EL4-indo-1-1B2 + 2C-PE	0.54	0.67	0.87	1.09	1.01

Table 13- % of Cells as Conjugates

	Minutes 0	5	15	30	60
Samples					
EL4-indo-1 + 2C-PE	22.8%	23.7%	27.1%	27.1%	20.9%
EL4-indo-1-1B2 + 2C-PE	21.1%	36.7%	36.7%	31.6%	21.9%

Table 14- % of Conjugates With an Elevated Ca++ in the Target Cell (R>1.25)

	Minutes 0	5	15	30	60
Samples					
EL4-indo-1 + 2C-PE	1.3%	0.5%	1.1%	1.3%	1.4%
EL4-indo-1-1B2 + 2C-PE	8.6%	17.8%	22.9%	14.9%	9.1%

FIGURE 46

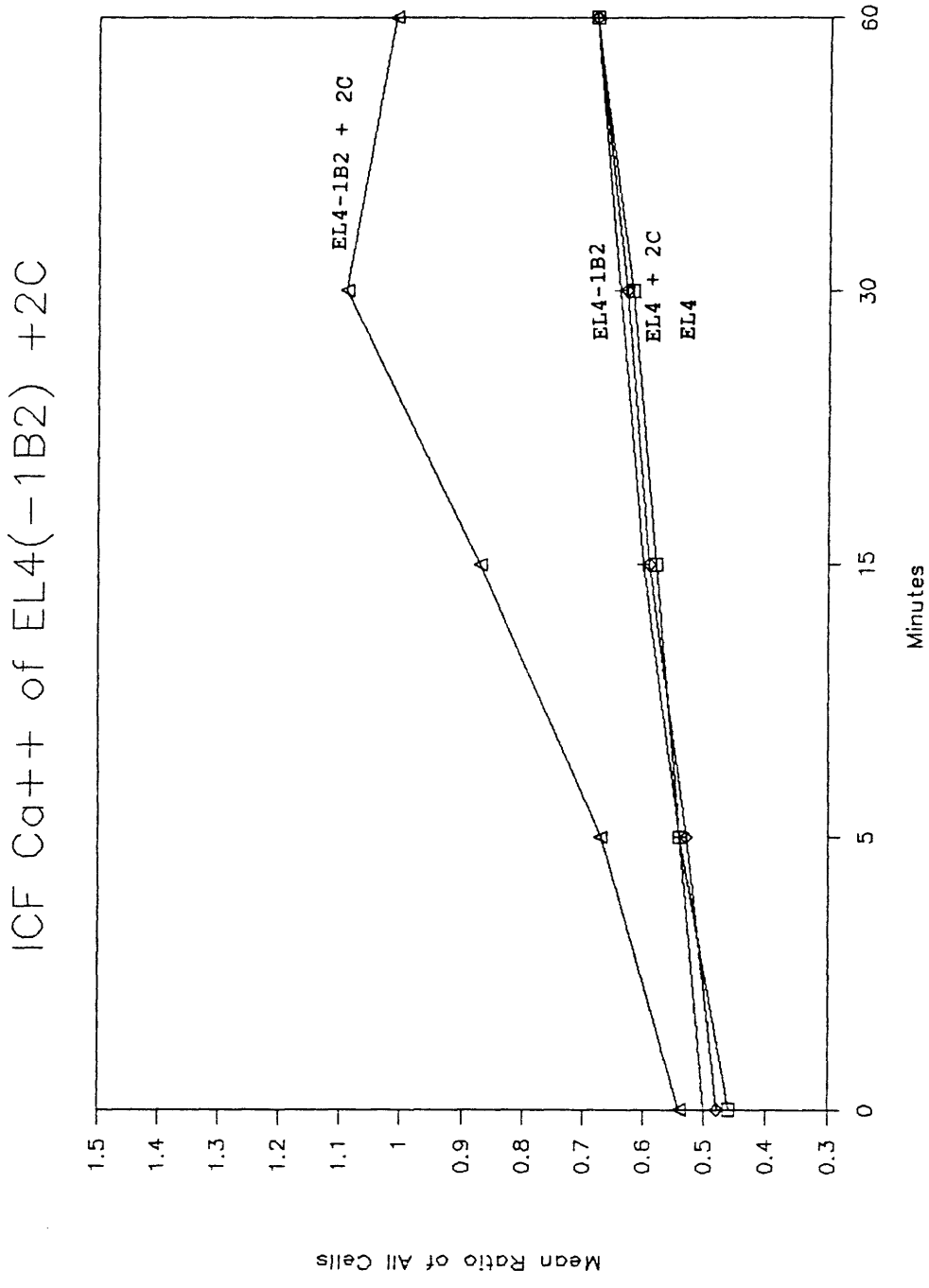
ICF Ca++ of EL4(-1B2) +2C
EL4-1B2 + 2C
EL4-1B2
EL4 + 2C
EL4
Mean Ratio of All Cells
Minutes
1.5
1.4
1.3
1.2
1.1
1
0.9
0.8
0.7
0.6
0.5
0.4
0.3
0
5
15
30
60

FIGURE 46

EL4 with and without 1B2 were loaded with 5 uM indo-1 AM and then mixed with 2C as described in the text ("Double Label Conjugate Experiments"). Figure 46 shows the mean ratio of the indo-1 loaded EL4 populations over time.

We were interested in establishing when in relation to conjugation the Ca++ level rose in target cells: an increase during conjugation could mean that an increase in ICF Ca++ is an early event in target cell death. Table 13 shows that a Ca++ increase is clearly correlated with cell death since it occured in conjugated target cells, EL4-indo-1-1B2, that could be killed by 2C but not in those that could not be killed by 2C. Figures 47 and 48 show three populations of cells; 1. conjugated target cells with a normal calcium (R<1.25), 2. conjugated target cells with an elevated calcium (R>1.25), and 3. unconjugated target cells with an elevated calcium. The peaks in these populations occurred sequentially in time in the EL4-indo-1-1B2 + 2C-PE mixture (Figure 47). This order suggests that conjugation occurs first, followed by a lytic attack producing an increased intracellular calcium in the target cells, and finally by deconjugation. In contrast, in the control mixture (EL4-indo-1 + 2C-PE) the populations of cells with elevated ICF Ca++ levels remained unchanged throughout the experiment (Figure 48).

The experiment with P815 cells as targets in place of EL4-indo-1-1B2 was carried out in exactly the same way. The results are similar but not as definitive as the EL4-indo-1-1B2 experiment, due to a drift in the calcium level of the control P815 cells. The results with P815 cells are presented in Figures 49, 50 and Tables 15-19.

FIGURE 47

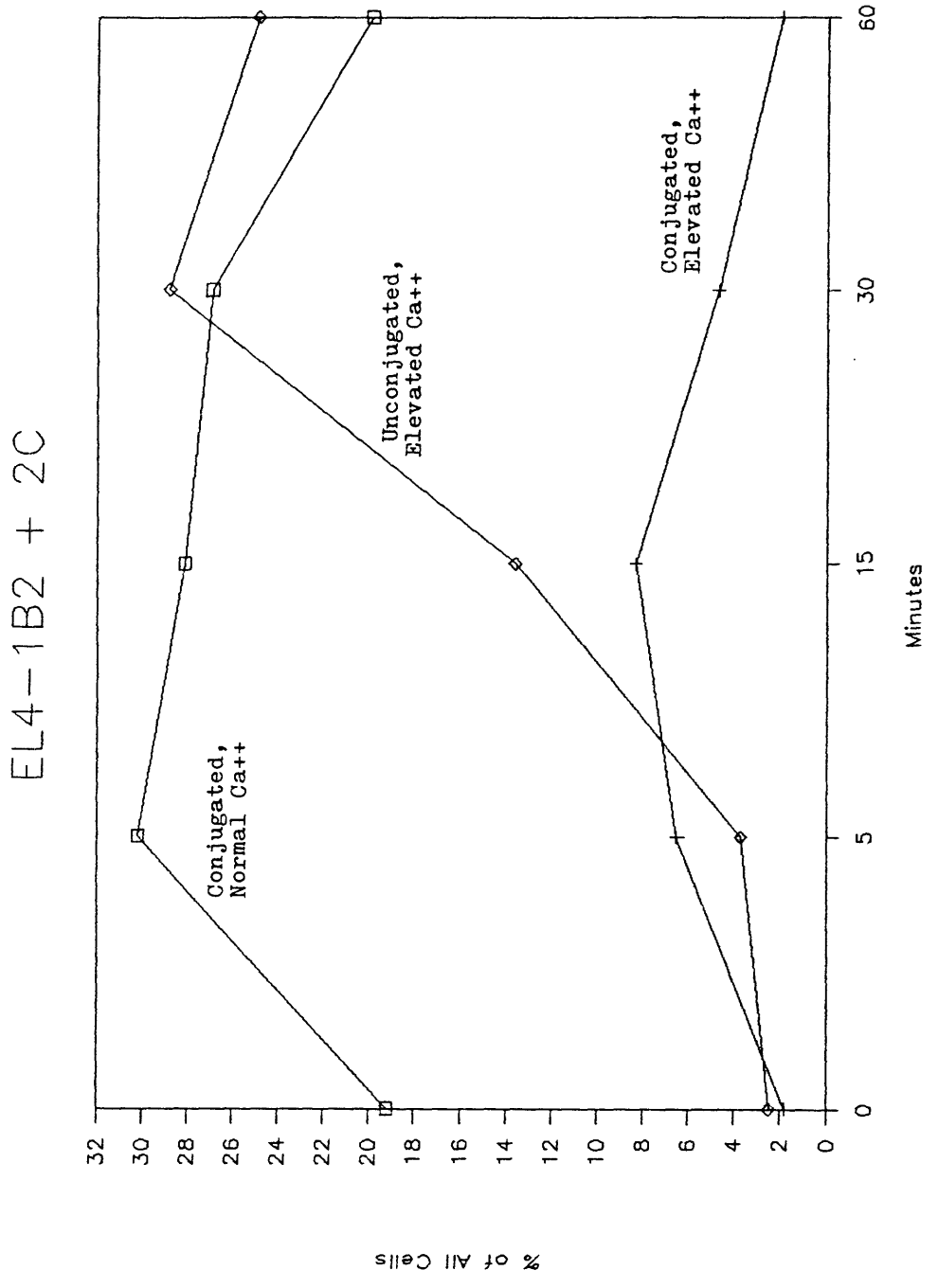
EL4-1B2 + 2C
Conjugated, Normal Ca++
Unconjugated, Elevated Ca++
Conjugated, Elevated Ca++
% of All Cells
Minutes
0
2
4
6
8
10
12
14
16
18
20
22
24
26
28
30
32
0
5
15
30
60

FIGURE 47

EL4 cells with and without 1B2 were loaded with 5 uM indo-1 AM while the 2C cells were labelled with PE. This figure and experiment are described in detail in the text.

FIGURE 48

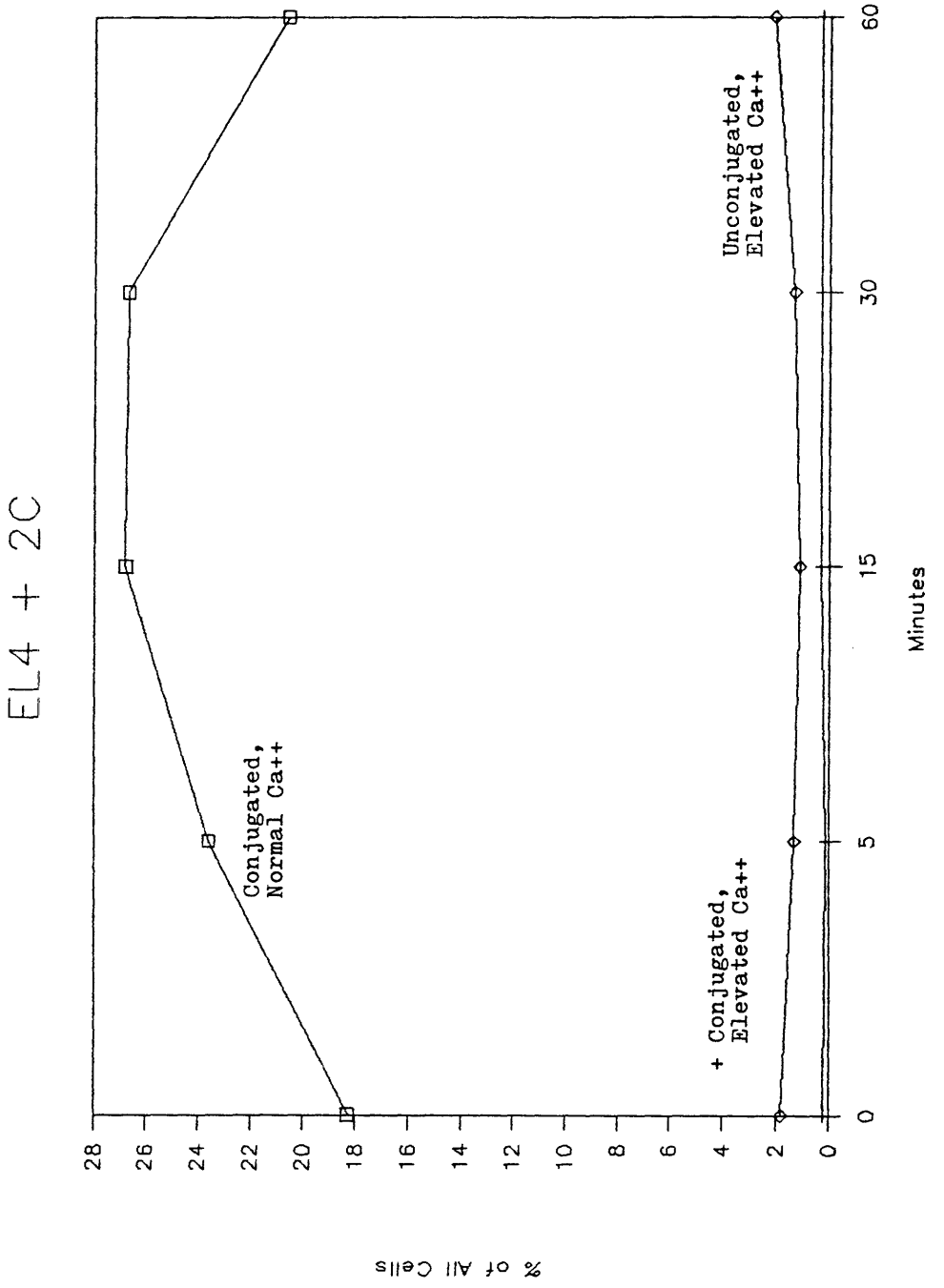
EL4 + 2C
Conjugated, Normal Ca++
Unconjugated, Elevated Ca++
+ Conjugated, Elevated Ca++
% of All Cells
Minutes
0
2
4
6
8
10
12
14
16
18
20
22
24
26
28
0
5
15
30
60

FIGURE 48

Figure 48 is identical to Figure 47 except that EL4 cells are used instead of EL4-1B2 cells.

Double Label Conjugate Experiments (with P815)

Table 15- Controls

Samples	Objects Staining Positive for Phycoerythrin	Counts on Ratio Cytogram	Counts on Ratio Cytogram that Are Positive for PE
2C	0.09%	0.17%	0.06%
2C+PE	97.6%	0.16%	0.07%
EL4	0.01%	0.01%	0.00%
EL4+indo-1	0.81%	76.6%	0.64%
P815	0.05%	0.05%	0.00%
P815+indo-1	0.94%	83.1%	0.78%

Table 16- Mean Ratio With 5uM Ionomycin (Control Cells)

Samples	5mM EGTA	1mM Ca++
EL4-indo-1	0.41	2.81
P815-indo-1	0.32	2.86

Table 17- Mean Ratio of All Cells

	Minutes 0	15	30	60	90
Samples					
P815-indo-1 +2C-PE	1.03	1.21	1.23	1.30	1.30
P815-indo-1	0.72	0.93	1.01	1.07	1.10
EL4-indo-1 + 2C-PE	0.74	0.75	0.79	0.85	0.89
EL4-indo-1	0.75	0.72	0.79	0.83	0.88

Table 18- % of Cells as Conjugates

	Minutes 0	15	30	60	90
Samples					
P815-indo-1 + 2C-PE	50%	52%	46%	34%	30%
EL4-indo-1 + 2C-PE	24%	29%	29%	25%	23%

Table 19- % of Conjugates With an Elevated Ca++

	Minutes 0	15	30	60	90
Samples					
P815-indo-1 + 2C-PE	20%	27%	25%	27%	29%
EL4-indo-1 + 2C-PE	8%	3%	5%	9%	14%

FIGURE 49

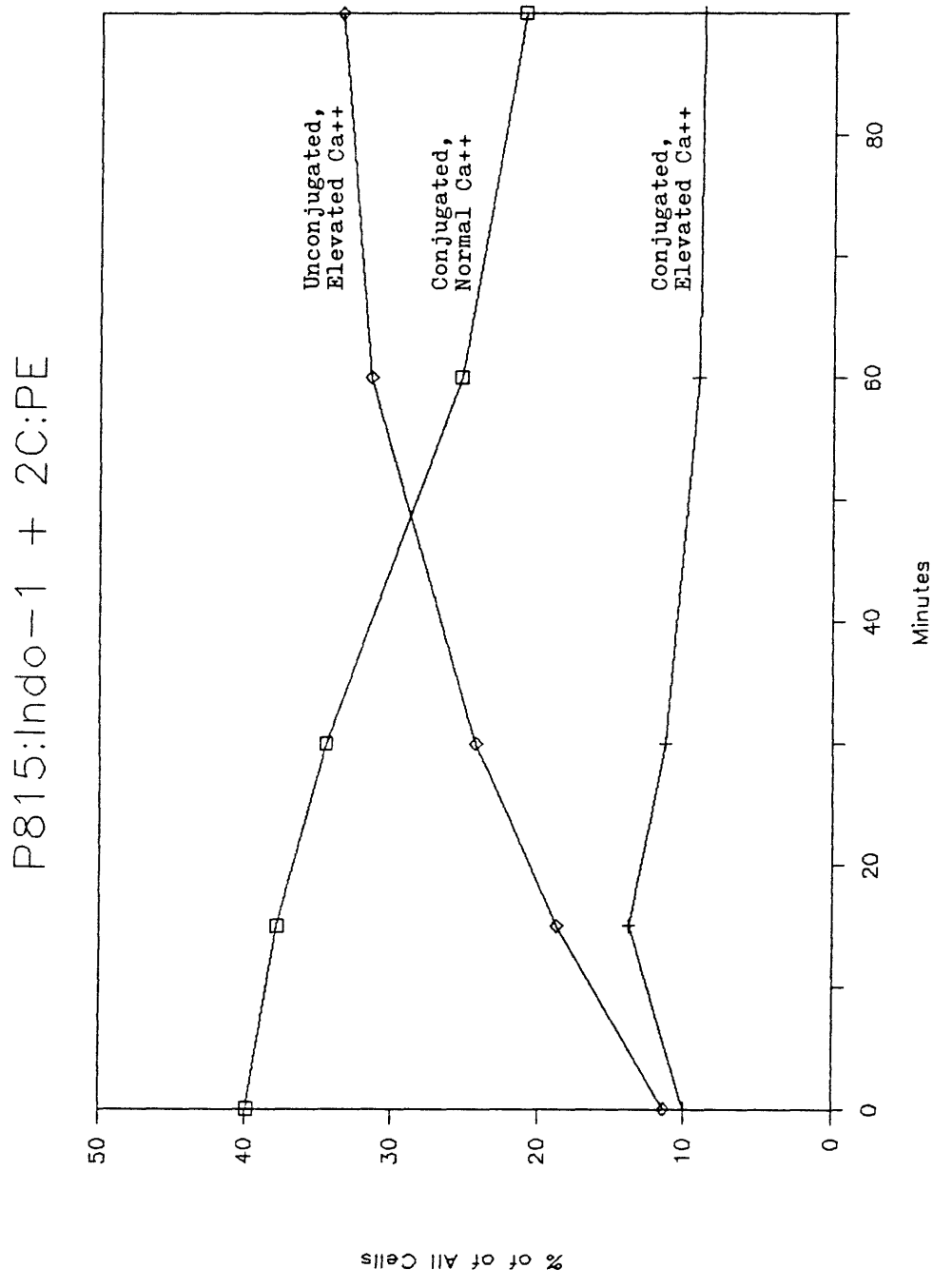
P815:Indo-1 + 2C:PE
Unconjugated, Elevated Ca++
Conjugated, Normal Ca++
Conjugated, Elevated Ca++
% of of All Cells
Minutes
0
10
20
30
40
50
0
20
40
60
80

FIGURE 49

Figure 49 was constructed in the same way as Figures 47 and 48. P815 cells loaded with 5 uM indo-1 AM were used in place of EL4 cells.

FIGURE 50

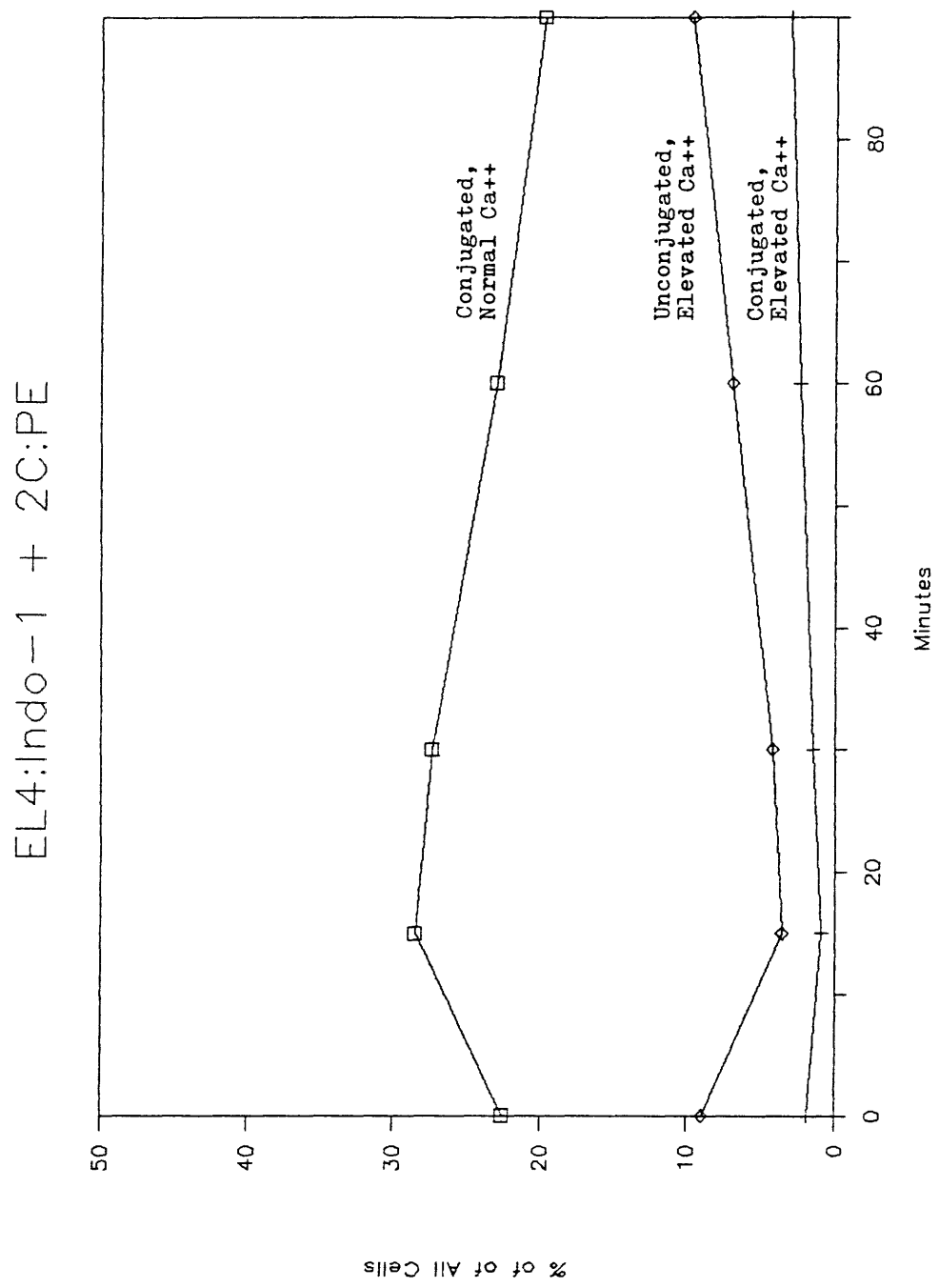
EL4:Indo-1 + 2C:PE
Conjugated, Normal Ca++
Unconjugated, Elevated Ca++
Conjugated, Elevated Ca++
% of of All Cells
Minutes
0
10
20
30
40
50
0
20
40
60
80

FIGURE 50

Figure 50 was constructed in the same way as Figures 47-49. EL4 cells loaded with 5 uM indo-1 AM were used as targets.

Toxicity of Increased Intracellular Free Calcium

A. Introduction

Perforin is thought to kill target cells by forming nonselective ion channels in cell membranes[42-46,49]. Of the common ions in cells, Na^+, K^+, and Ca^{++} are maintained at the highest concentration gradients across the plasma membrane. To determine the effects of equilibrating each of these ions, we examined whether selective Na^+-K^+, K^+, and Ca^{++} ionophores can cause cells to die.

Ionophores, which allow selective ions to flow down concentration gradients across permeability barriers such as lipid membranes, are composed of a back-bone structure that is capable of bending and placing strategically located oxygen groups about a central cavity[134]. This cavity with is hydrophilic and can bind cations while the outer backbone is hydrophobic, allowing membrane insertion. Properties of the central cavity determine ion selectivity. Cations bind to the ionophore on the outer surface of the membrane, displacing water. Then the ionophore crosses the membrane where the cation is released. This process is repeated as the ionophore shuttles back and forth across the membrane moving cations in or out of cells.

Many cytotoxic agents are dependent on the quantity of Ca++ in the extracellular medium e.g. glucocorticoids, A23817, lysolecithin, mellitin, and amphotericin B[81,85,86,98-100,102-105,135]. Most of these agents damage the membrane nonspecifically i.e. they do not create a specific ion leak across the membrane. A23817 is a carboxylic divalent cation ionophore[134,136]. In the deprotonated form, two A23817 molecules complex with a divalent cation and transport it as a zwitter ion through solvent barriers down concentration gradients[134]. Calcium-dependent lysis of cells by A23817 is well documented[81,105]. It has, however, roughly equal selectivities for Mg++ and Ca++[136,137]. In contrast ionomycin, also a carboxylic ionophore, is much more selective for Ca++ than Mg++[136,137]. It transports predominantly Ca++ in a 1:1 ratio across membranes[136]. Their different affinities for Mg++ vs Ca++ have been exploited in the past to discriminate between the effects of Ca++ and Mg++ on physiologic systems[137].

Gramicidin D is a polypeptide which creates membrane channels selective for Na^+ and K^+ [134,165]. It is a quasi-ionophore because it forms spiral dimers which insert into the membrane and extend the full length of the membrane. It functions as an ion conductor or pore rather than a mobile ion carrier. Upon addition to cells, gramicidin causes membrane depolarization[138,166].

Valinomycin is a neutral ionophore with a repeating backbone[134]. It is highly selective for K^+ and causes hyperpolarization of the plasma membrane[134,138,139]. Gramicidin and valinomycin have been used in the past to study mitochondrial and red blood cell ion transport and as a means to calibrate membrane potential sensitive dyes. The cellular toxicity of valinomycin and gramicidin is presented in the next section with the DNA degradation results.

All of these ionophores act primarily by transporting particular cations. However it must be kept in mind that they also induce many secondary effects intracellularly as the cell attempts to reestablish an equilibrium. For example the Ca++ ionophores can cause Ca++ activated K+ channels to open with subsequent membrane hyperpolarization, while valinomycin indirectly causes anion channels of the membrane to open resulting in Cl^- loss from cells[146,147,160,161].

B. Ionomycin Toxicity

Since both isolated granules and intact CTLs induce an increase in the intracellular free calcium of target cells, it is important to know whether the increase is sufficient by itself, to cause cell death. Because ionomycin is a selective Ca++ ionophore, we examined its effect on cell viability with and with out ECF Ca++

present. P815, Yac-1, RDM4, and 2C cells were tested for ionomycin toxicity using Cr^{51} release assays. In the presence of 1 mM Ca++ and 5 uM ionomycin, all cell lines exhibited a 40% or greater specific release of Cr^{51}. But the substitution of 5 mM EGTA for 1 mM Ca++ decreased the percent specific release markedly, usually by a factor of 50% or more. Figures 51 and 52 show typical Cr^{51} release curves with 1 mM Ca++ or 5 mM EGTA for P815 and 2C cells with varying concentrations of ionomycin (mean of 2 experiments). Thus it appears that a selective increase in ICF Ca++, if high enough and sustained for a long enough time, may well be sufficient to set off the sequence of events that lead inexorably to cell lysis.

Some cell death (i.e. Cr^{51} release) occurred in the 5 mM EGTA solutions probably because under these circumstances the ionophore acts to transport Ca++ out of the cell and into the extracellular media, thereby lowering the intracellular Ca++ below normal values. Since cells have only a limited store of intracellular calcium and require small amounts to function normally, it is not surprising that some cells die. Figure 53 shows the effect of ECF Ca++ levels on the ionomycin toxicity of Yac-1 and P815 cells. At low ECF Ca++ levels there was no toxicity. This is not surprising in light of Figure 23 (presented in the flow cytometry standards section), which showed that cells were capable of maintaining normal ICF

Ca++ levels in spite of the presence of ionomycin providing the ECF Ca++ levels were low (<39 uM). Cells show tremendous ability to regulate ICF Ca++, probably because of the ability of organelles (mitochondria, endoplasmic reticulum) to buffer large amounts of Ca++ and because of the cell's ability to pump Ca++ across the cytoplasmic membrane[96,97].

FIGURE 51

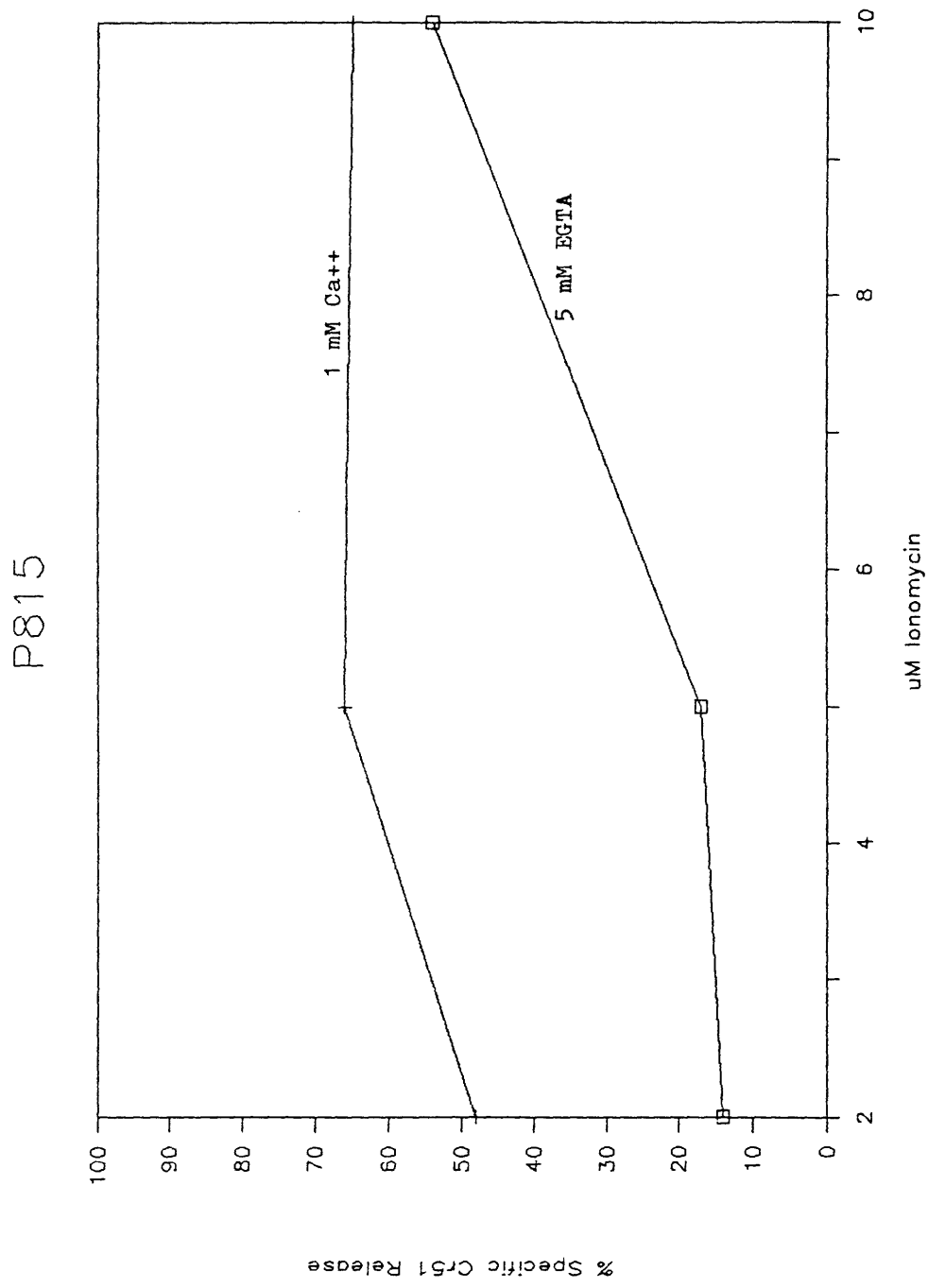
P815
1 mM Ca++
5 mM EGTA
% Specific Cr51 Release
uM Ionomycin
100
90
80
70
60
50
40
30
20
10
0
2
4
6
8
10

FIGURE 51

P815 cells were loaded with Cr^{51} and placed in ECBS with either 1 mM Ca++ or 5 mM EGTA. Figure 51 shows the cell death occurring an hour after addition of 2, 5, or 10 uM ionomycin.

FIGURE 52

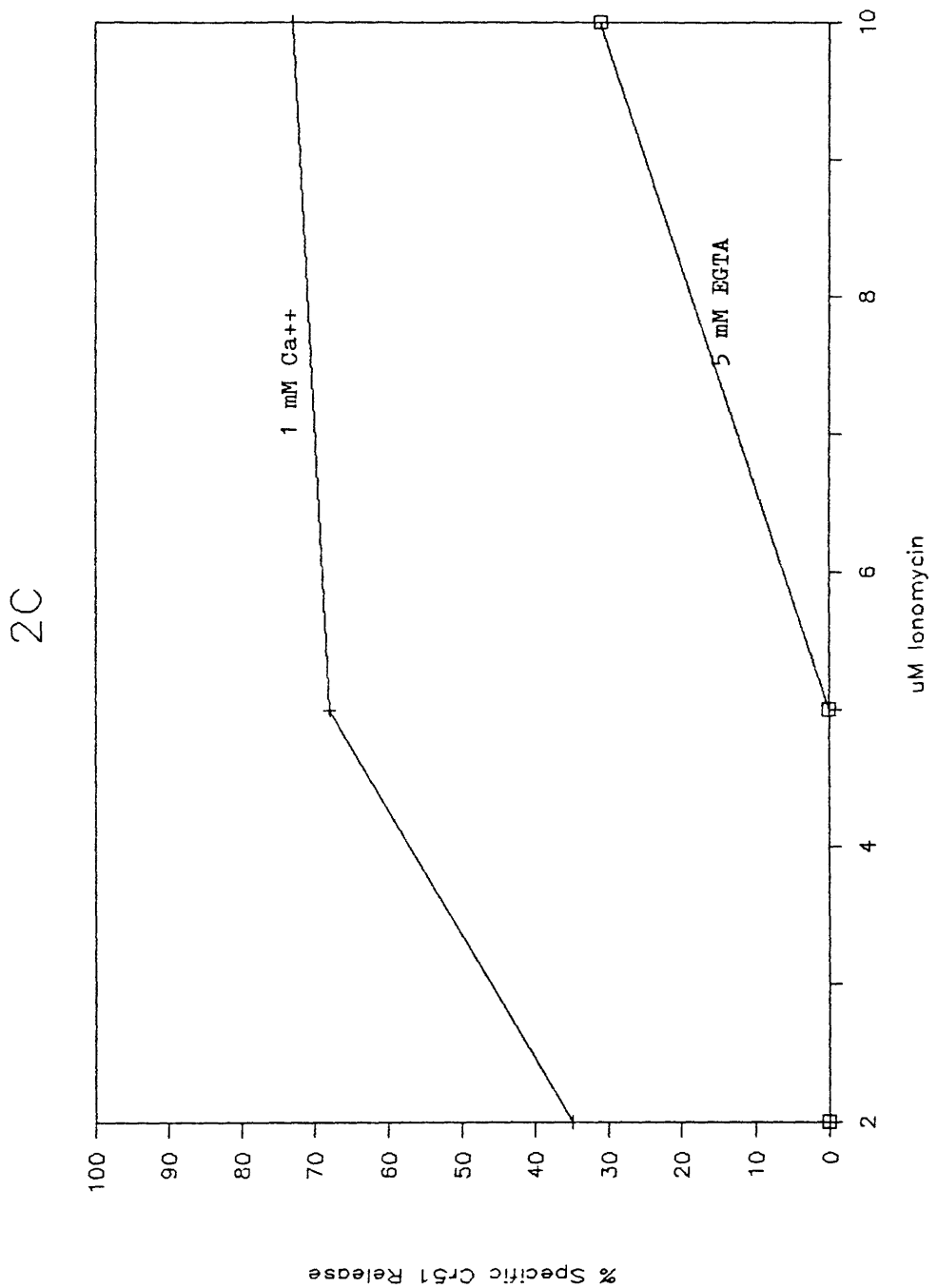
2C
% Specific Cr51 Release
100
90
80
70
60
50
40
30
20
10
0
2
4
6
8
10
uM Ionomycin
1 mM Ca++
5 mM EGTA

FIGURE 52

2C cells were loaded with Cr^{51} and placed in ECBS with either 1 mM Ca++ or 5 mM EGTA. Figure 52 shows the cell death occurring an hour after addition of 2, 5, or 10 uM ionomycin.

FIGURE 53

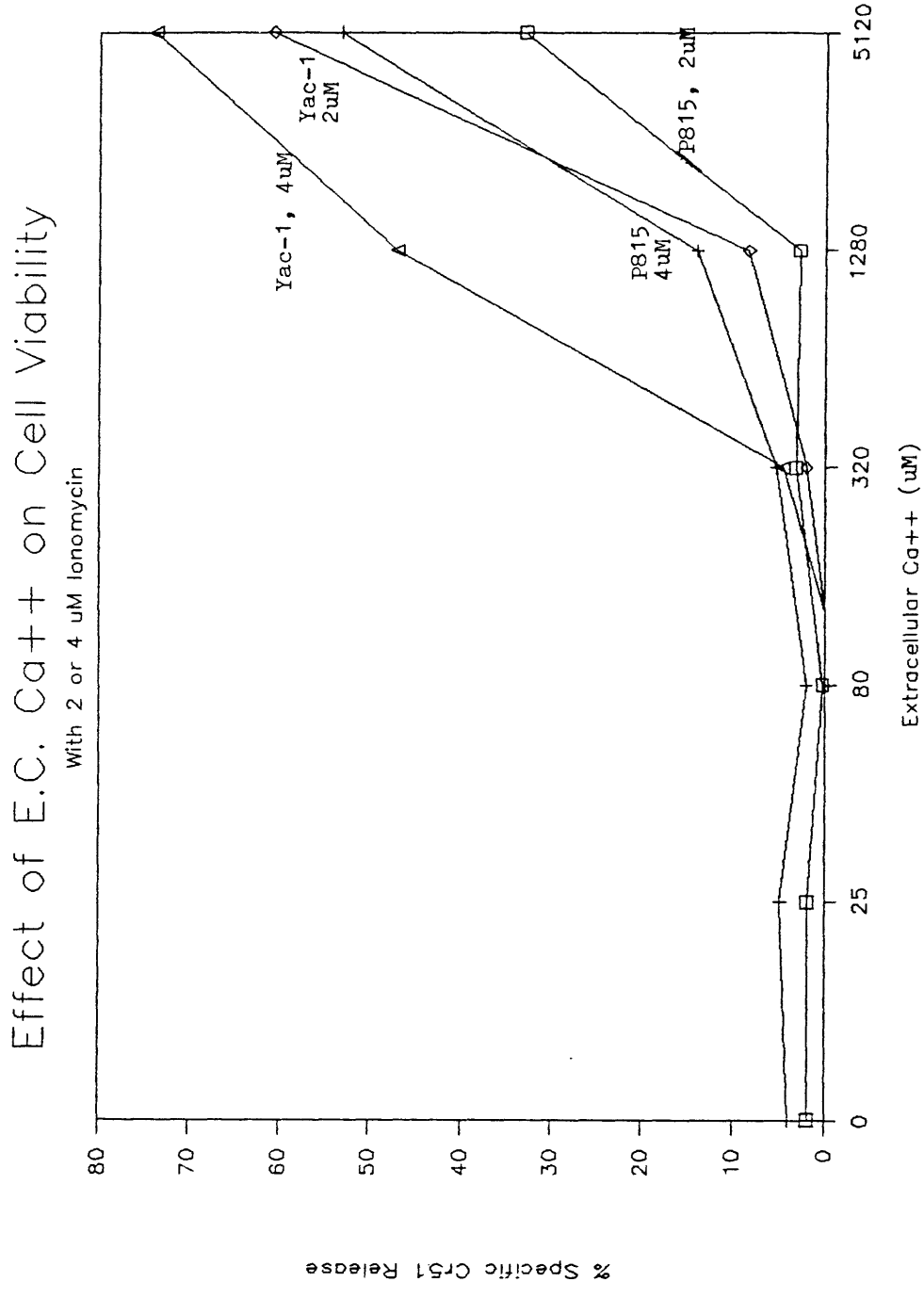
Effect of E.C. Ca++ on Cell Viability
With 2 or 4 uM Ionomycin
% Specific Cr51 Release
Extracellular Ca++ (uM)
Yac-1, 4uM
Yac-1
2uM
P815
4uM
P815, 2uM
0
10
20
30
40
50
60
70
80
0
25
80
320
1280
5120

FIGURE 53

Yac-1 and P815 cells were loaded with Cr^{51} and resuspended in ECBS with 0, 25, 80, 320, 1280, or 5120 uM of free Ca++. An hour after addition of 2 or 4 uM ionomycin, the percent specific Cr^{51} release was measured.

VIII. DNA Degradation

A. Introduction

When targets are killed by CTLs, some of their DNA is degraded[83,91-93,140]. The degradation is detectable as early as 5 minutes after CTLs and target cells are mixed[91-92]. In murine target cells, the chromatin is fragmented into multiples of 200 base pairs, the breaks in the DNA presumably occurring in the exposed linker region between nucleosomes[91]. Similar degradation of DNA is also seen in cells that are killed by glucocorticoids, interleukin 2 deprivation, lymphotoxin, irradiation and other means[65,87,90]. Human target cells that are killed by CTLs show single-stranded rather than double stranded DNA breaks[89]. The difference between human and murine target cells is maintained in situations where human cells are killed by murine CTLs and vice versa; hence it is likely that CTL-induced degradation is due to the activation of intracellular enzymes of the target cell. Ca++/Mg++ activated endonucleases have been described in thymocytes, spleen cells, lymph node cells, liver, and epithelial cells[141,142]. The endonuclease activity accompanying glucocorticoid-induced death is reduced in the absence of Ca++ and Mg++ and inhibited by Zn++[87]. CTL-induced DNA degradation is also inhibited by Zn++[92]. Since these endonucleases are Ca++/Mg++ activated, the

endonuclease activity in damaged target cells might also be Ca++/Mg++ activated. Since this paper has shown that Ca++ increases in cells being killed by intact CTLs, isolated granules, and ionomycin, it was of interest to determine if the Ca++ rise is correlated with DNA degradation. Hence, we looked for DNA degradation in target cells that were treated with granules and ionophores.

Since perforin, which appears to be primarily responsible for target cell death, forms nonselective ion channels in cell membranes, we were particularly interested in knowing whether ionophores for Na^{+}, K^{+}, and Mg^{++}, in addition to Ca^{++}, cause DNA degradation.

B. DNA Degradation Produced by Ionophores and Cytolytic Granules

Yac 1 was used as a target cell to study DNA degradation since it is very susceptible to granules and can be killed by 2C cells (Figure 54). The 10X (10 ul) concentration of a granule preparation from 3H2 cells (a CD8+, CTL cell line) and the concentration of G4 granules used in the DNA degradation assays caused a 70% or greater Cr^{51} release from Yac-1 cells. Figure 55 shows the DNA degradation in Yac-1 cells that were exposed to intact 2C cells, isolated granules, ionomycin, A23817 (a Ca++ and

FIGURE 54

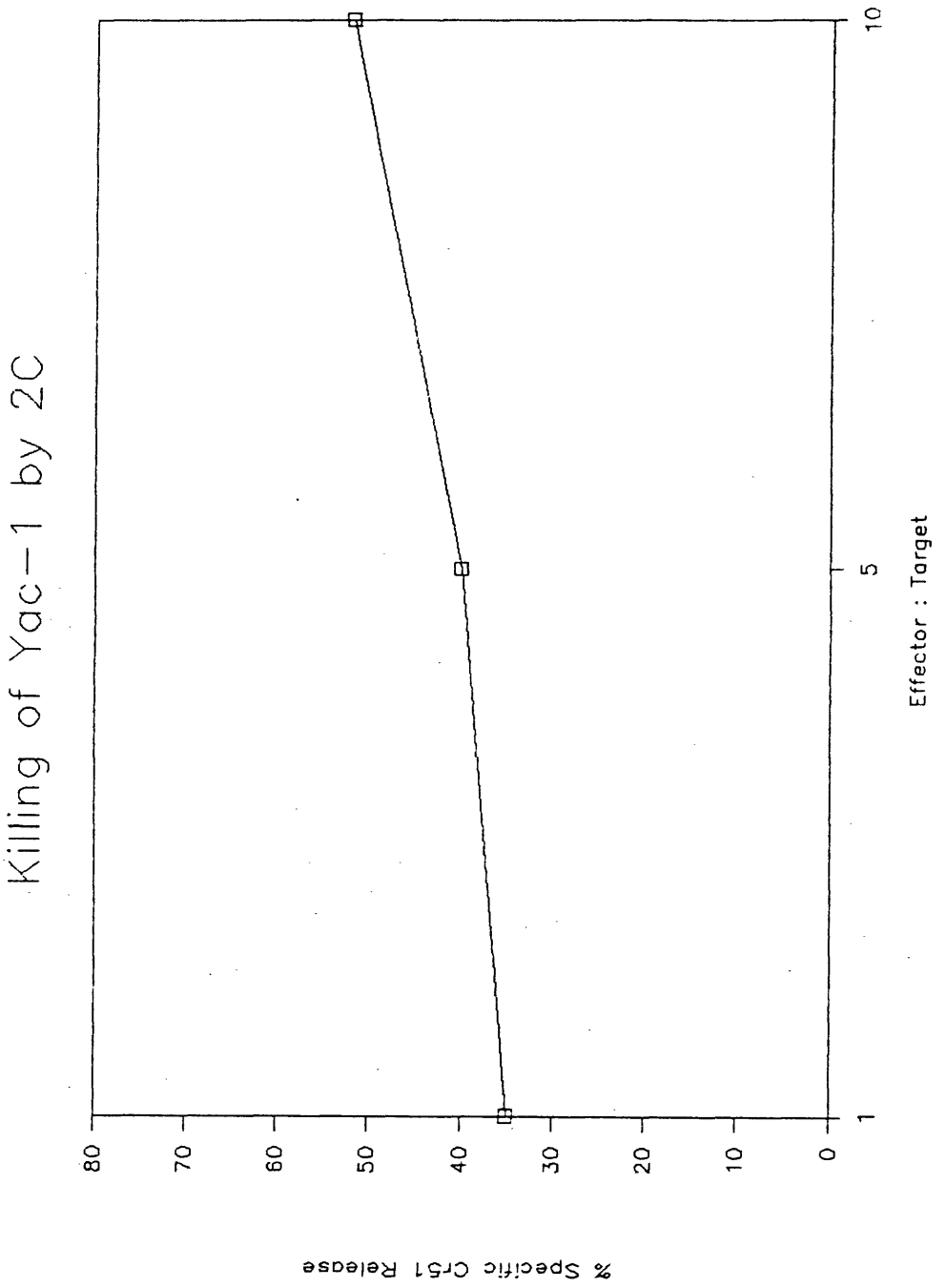
Killing of Yac-1 by 2C
% Specific Cr51 Release
0
10
20
30
40
50
60
70
80
1
5
10
Effector : Target

FIGURE 54

Figure 54 shows the ability of 2C to kill Yac-1 targets. Mg++ ionophore), valinomycin and gramicidin. Degradation of Yac-1 cell DNA was clearly caused by 2C cells (E:T=10:1), by isolated granules (10X 3H2 or about 6.5 ug granule protein/ml), and, surprisingly, by valinomycin (1.5 uM and 15 uM) but not by ionomycin, A23817, or gramicidin.

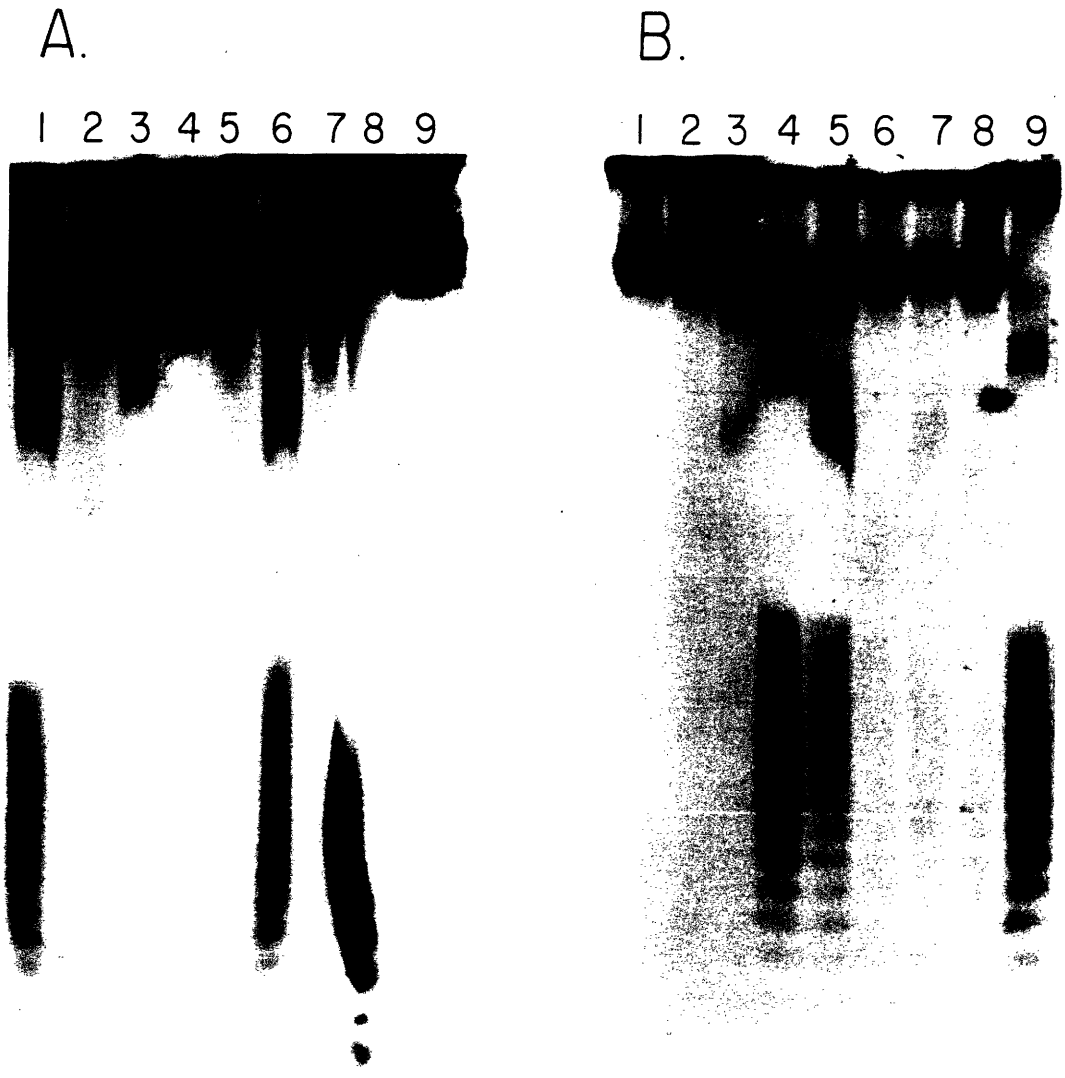
A.
1 2 3 4 5 6 7 8 9
B.
1 2 3 4 5 6 7 8 9

FIGURE 55

Yac 1 cells were loaded with I125-deoxyuridine as described in the methods section. The Yac 1 cells were exposed to CTLs (2C), cytolytic granules, or ionophores for one hour. Figure 55 shows the total DNA after electrophoresis on a 0.8% agarose gel. The lanes are as follows:

A

1. 10X 3H2 granules (caused ~70% lysis in a Cr^{51} release assay)
2. ECBS (Extracellular Buffered Salt Solution)
3. 1 uM ionomycin
4. 10 uM ionomycin
5. 1X 3H2 granules
6. 10X 3H2 granules (caused ~70% lysis in a Cr^{51} release assay)
7. ECBS
8. 2C (E:T = 10:1)
9. K medium

FIGURE 55 (continued)

B.

1. 10 uM A23817
2. 10 uM ionomycin
3. 30 uM gramicidin
4. 15 uM valinomycin
5. 1.5 uM valinomycin
6. 0.15 uM valinomycin
7. relaxation buffer
8. 10X 3H2 granules (repeatedly frozen and thawed)
9. G4 granules (caused ~70% lysis in a Cr^{51} release assay)

The mechanisms responsible for DNA degradation in target cells are unknown. It seems most unlikely that an enzyme or macromolecular enzyme activator could enter the cell from without, penetrating through perforin channels to gain access to the cell nucleus and degrade DNA. A more reasonable possibility is that intracellular perturbations, due to perforin channels, activate an endogenous target cell endonuclease. It is of some interest, however, that other toxic ion channels, such as those formed by activated complement do not trigger DNA degradation in affected cells.

It is also not clear why valinomycin causes DNA degradation. It could be due to either its ionophoric behavior or to an effect of valinomycin unrelated to K^+ transit[134,139,143-145]. It is possible that K^+ leakage or a secondary effect of that leakage results in endonuclease activation. In red blood cells, K^+ leakage results in hyperpolarization but no pH change, at least within 10 minutes[146,147]. A pH change does not occur because loss of Cl^- from the red blood cell (through anion channels) is simultaneous with K^+ leakage. The red cell responds to this decrease in osmolality by shrinking i.e. loosing water. This leaves the concentration of intracellular and extracellular Cl^- ions unchanged and consequently the pH is constant (Intracellular pH is regulated by the Donnan equilibrium of the negatively charged ions). Valinomycin

is a powerful uncoupler of mitochondrial oxidative phosphorylation so presumably at some later time the cell would begin to acidify and die[134]. It could be these early stages of "metabolic exhaustion" that are responsible for endonuclease activation.

Valinomycin has been observed at low concentrations (<1 uM) to have effects that are probably unrelated to its ionophoric properties[143-145]. Davidson et al have shown that valinomycin appears to bind directly to the (Ca^{++}, Mg^{++})-ATPase of skeletal muscle sarcoplasmic reticulum, inhibiting calcium transport[143]. Such an effect on a plasma membrane ATPase could raise the ICF calcium to a level sufficient to activate an endonuclease.

Valinomycin at low doses (0.1 uM) in lymphocytes has been shown to inhibit mitogenesis, decrease cellular ATP, and increase steady-state Na^+ exchange, but cause no increase in steady-state K^+ exchange[144]. These unexpected effects of valinomycin appear to be measurable only at low doses; at higher doses the K^+ leakage becomes the predominant effect[134,139]. However the nonionophoric properties of valinomycin at low doses cannot be ruled out as a direct or indirect cause of the DNA breakdown. It is notable that the amount of DNA degradation increases with the dose of valinomycin.

C. Cell Lysis By Gramicidin and Valinomycin

To determine whether the nonselective leakage of ions through the transmembrane channels due to perforin and/or other granule components was sufficient to cause cell death, we tested the effects of several ionophores on target cells, using Cr^{51}-release from the cell as an assay. Gramicidin and valinomycin were tested at the same concentrations used for studies of DNA degradation (Figure 56). 1.5 uM and 15 uM valinomycin caused a 3.0% and a 12.8% Cr^{51} release in Yac-1 targets while gramicidin caused a 2.1% release at 3.0 uM and 11.0% at 30 uM (average of two experiments). Higher concentrations of valinomycin and gramicidin precipitated out of aqueous solutions. Ionomycin caused much more cell death than valinomycin or gramicidin at similar molar concentrations. Thus while valinomycin caused significant DNA degradation, it caused far less Cr^{51} release in one hour than the isolated granules and the Ca++ ionophores.

Reynold Verret, postdoctoral fellow at MIT, and Mark Pasternack, Massachusetts General Hospital, provided the Cr^{51} release data for 3H2 and G4 granules, respectively (section VIII.B.).

FIGURE 56

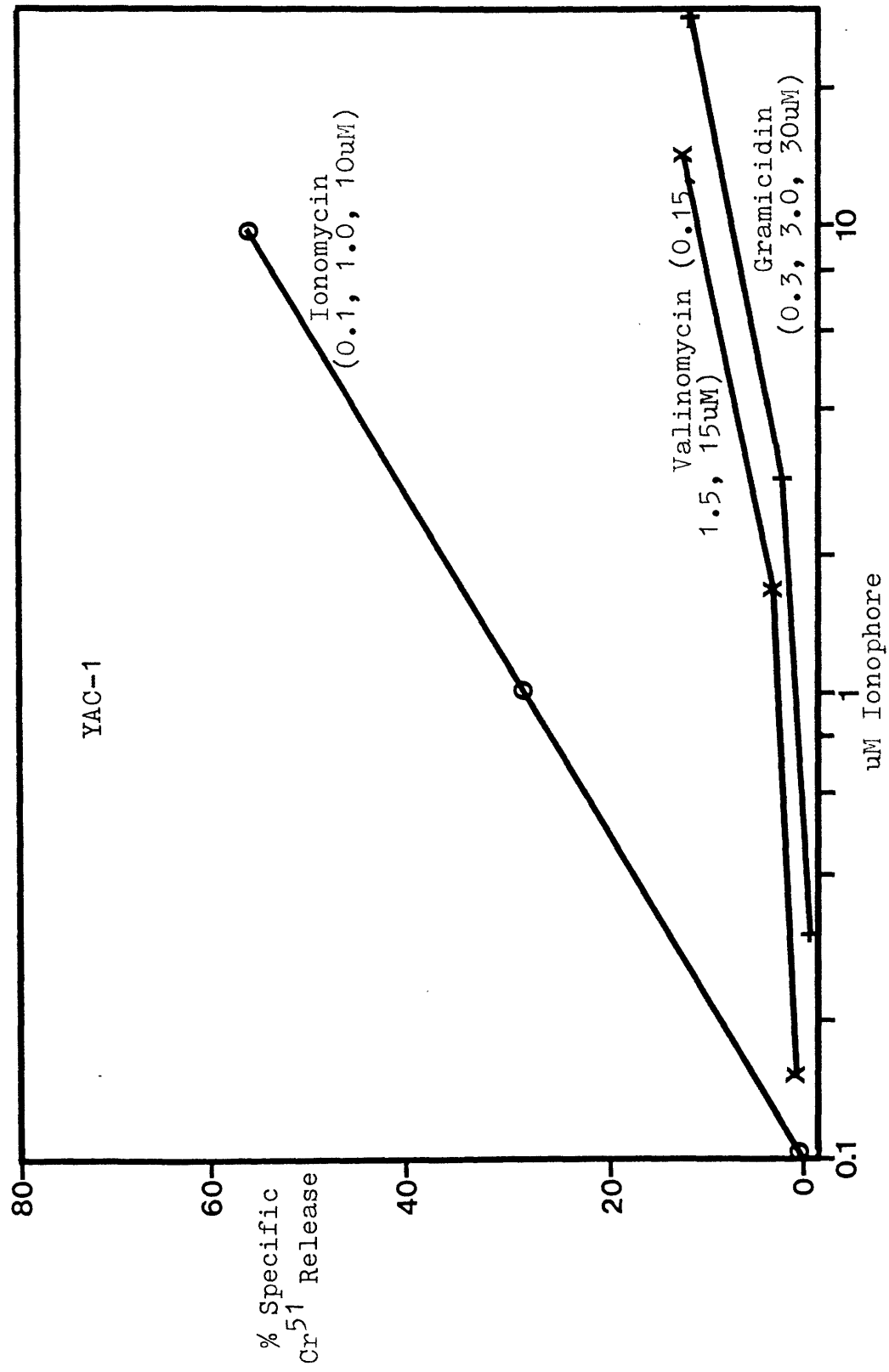
YAC-1
% Specific Cr^{51} Release
80
60
40
20
0
0.1
1
10
uM Ionophore
Ionomycin (0.1, 1.0, 10uM)
Valinomycin (0.15, 1.5, 15uM)
Gramicidin (0.3, 3.0, 30uM)

FIGURE 56

Yac 1 cells were loaded with Cr^{51} and resuspended in ECBS with 1 mM Ca++. Cell lysis was measured after exposure to the indicated concentration of ionophore for 1 hour.

IX. Discussion

This thesis is composed of two parts: 1. the development of a technique to measure the ICF Ca++ concentration in living cells and, 2. the application of this technique to a biologic problem (the mechanism of target cell destruction).

1.

The experiments presented show that indo-1 with flow cytometry can be used to measure the ICF Ca++ concentration in cells. This result is not trivial since the properties of new dyes must be carefully evaluated in biologic systems. All cell lines tested took up indo-1 AM and deesterified it to the Ca++-sensitive molecule, indo-1, although in some cell lines (some tumors) a significant amount of indo-1 AM remained unmetabolised in the cytoplasm. While this Ca++-insensitve dye can effect the 405/480 ratio and hence the calculated ICF Ca++ concentration, it does not prevent the measurement of changes in the ICF Ca++ level or the calculation of an approximate ICF Ca++ value. We have also shown that indo-1 can be used at intracellular concentrations that do not effect cellular functions or blunt changes in the ICF Ca++ concentration. In addition to providing measurements of the ICF Ca++ level, the indo-1 dye also behaves as a vital

dye, so that measurements are made only on "living" cells. We have shown that filters and excitation sources currently available for flow cytometry can be used for fluorescent measurements of indo-1 and a second label such as PE. Thus measurements of ICF Ca++ may be made on selected subpopulations of cells (others also have shown this recently)[114]. While flow cytometry with indo-1 is a sensitive indicator of changes in the ICF Ca++ concentration, measurement of the exact ICF Ca++ level is difficult because calibration constants cannot be determined precisely. We attempted to measure these constants but were not successful (as judged by comparison of our Ca++ concentrations with values measured in a spectrofluorimeter and reported in the literature). This calibration method does provide an estimate of the ICF Ca++ level (within a factor of ~2) although it is easier and possibly as accurate to use estimates of the constants obtained with a spectrofluorimeter. We conclude that measurements of the ICF Ca++ concentration with flow cytometry and indo-1 is a powerful technique which can be applied to the study of many cellular processes.

2.

The experiments described here suggest that the changes in target cell ICF Ca++ concentration resulting from exposure to cytotoxic granules, or intact CTLs,

determine whether cells are killed or survive. High concentrations of the isolated granules (about 130 ug protein/ml) cause representative tumor target cells, such as Yac-1 or P815 cells, to rapidly loose intracellular indo-1, preventing measurement of the ICF Ca++ concentration for greater than a few minutes. At lower concentrations of granules (~10 ug protein/ml) the dye is retained and these cells exhibited within 1-2 minutes after exposure to the granules a dramatic increase of ICF calcium (> 2 uM), followed over the next 5 to 10 minutes by a return of the calcium to the normal level. However when, cloned CTL lines, which are strikingly resistant to granule-mediated lysis[67], were tested as target cells they showed no increase in ICF Ca++ even at the highest concentrations of granules (130 ug/ml). After the CTLs were first exposed to azide and and cyanide for one hour (conditions that greatly enhance the susceptibility to lysis of all other cell lines tested), these cells still showed no increase in ICF Ca++ in response to granules (~10 ug protein/ml).

All of these findings are in accord with evidence that the principal (or only) cytolytic component of the toxic granules is perforin, a protein that forms transmembrane ion-channels in cell membranes[42-46,49]. Hence our findings are consistent with the view that an early event following insertion of perforin into the

target cell membrane is a large influx of calcium from the extracellular medium (about 1 mM) into cells whose normal ICF Ca++ is about $1X10^{-4}$ mM. It appears that if the resulting great increase in ICF Ca++ cannot be restored to the normal level, the cells will die, whereas they will survive if their calcium can be restored to normal levels (e.g. by clearing the affected membranes by endocytosis and/or activating Ca++ pumps). In the granule-resistant CTLs, no increase in ICF Ca++ was detected at all, perhaps because these cells have evolved a mechanism for preventing the binding of perforin (or other cytolytic components) to their plasma membrane.

To determine whether the increased intracellular calcium concentration is sufficient to cause cell lysis, we tested the effects of ionomycin, a calcium ionophore. In the presence of 1 mM extracellular calcium, the ionomycin caused marked lysis of cells (Yac-1, P815 and 2C) and concomittantly a marked increase in ICF Ca++ (>10 uM). But when the Ca++ in the extracellular medium was replaced by 5 mM EGTA, the same concentration of ionomycin caused a much lower level of cell lysis and no increase in ICF Ca++. The small amount of lysis in the presence of EGTA was probably due to ionomycin-induced leakage of intracellular calcium from cells. Thus the results with ionomycin support the view that a sustained high ICF calcium level is sufficient to trigger the intracellular changes that end as cell death.

That all these findings are relevant to the lysis of target cells by intact CTLs seems evident from the changes observed in the ICF Ca++ of indo-1-labelled target cells over time during their incubation with CTLs. Since the CTLs were labelled with PE it was possible to distinguish between indo-1 labelled target cells that were or were not conjugated with the CTLs and to follow the changes in intracellular calcium in each of these target cell populations. The results showed that the ICF Ca++ increase (to 2-4 uM) was evident in target cells only if they formed specific conjugates with CTLs; if they formed only antigen-nonspecific conjugates no increase in their ICF Ca++ was seen (Ca++ = 200-300 nM). Moreover, the sequences of changes in ICF Ca++ in these target cells indicated that their increase in calcium came about initially while the cells were conjugated with CTLs. It is not at all surprising that the time-course of the target cell calcium changes induced by intact CTLs was very much slower than the changes elicited by the isolated granules, because the CTLs have to move around and find their targets, become activated, and then deliver their granules to the target cell membrane; whereas with isolated granules all of these preliminary steps are by-passed.

Studies following voltage changes across artificial membranes induced by perforin indicate that the channels

formed by this protein do not discriminate between various ions and small molecules[42,46]. Accordingly, it is expected that when the toxic granules (or intact CTLs) attack a target cell, the resulting perturbations in ionic equilibria within the target cell are not limited to calcium. To examine the effects on target cells of changes in intracellular Na+ and K+ concentration we used ionophores that are selective for these ions and we looked at the degradation of DNA in the target cells as an indicator of cell death. DNA degradation was chosen as an indicator because one of the conspicuous early events in the destruction of target cells by CTLs is a characteristic cleavage of target cell DNA into fragments that vary in size by multiples of 200 nucleotides. We asked, therefore, which selective ionic perturbations, if any, can duplicate this type of DNA degradation. Surprisingly, valinomycin, a K^+-specific ionophore, induced the characteristic DNA degradation pattern, that is elicited by the toxic granules and the CTLs. But ionomycin, the Ca++ ionophore, and also gramicidin (a Na^+/K^+ ionophore) did not bring about such changes.

Although valinomycin caused DNA degradation within 1 hour, in the same time interval it did not induce significant Cr^{51}-release from the target cells. Thus the effects of this ionophore were, in effect, the reciprocal of those elicited by ionomycin, which caused marked Cr^{51}-

release but no obviuos DNA degradation. All of these results are consistent with the evidence that CTLs, via their released toxic granules, kill target cells by means of nonselective ion-channels formed by perforin. The resulting calcium influx is probably primarily responsible for cell death and the changes in potassium (or some other events triggered by valinomycin) are responsible for DNA degradation, probably by activating an endogenous nuclease in the target cell. That a sustained high ICF Ca++ level is the key event in target cell destruction by CTLs has precedent of several other cytotoxic agents, such as steroids, etc[81,98,101,105].

It has long been known that target cell destruction by CTLs is dependent upon adequate extracellular Ca++ concentration. It has been shown that the Ca++ is required for polymerization of perforin in its target cell membrane[42,46]. Our results strongly suggest that, in addition, the calcium is also essential to trigger the chain of events that determined death or survival of target cells.

Footnotes

1 Fathman CG, Frelinger JG. 1983. T-Lymphocyte Clones. In Annual Review of Immunology. eds, Paul WE, Fathman CG, Metzger H. Annual Reviews, Inc. Palo Alto. 1: 633.

2 Nabholz M, MacDonald HR. 1983. Cytolytic T Lymphocytes. In Annual Review of Immunology. eds, Paul WE, Fathman CG, Metzger H. Annual Reviews, Inc. Palo Alto. 1: 273.

3 Henkart PA. 1985. Mechanism of Lymphocyte-Mediated Cytotoxicity. In Annual Review of Immunology. eds. Paul WE, Fathman CG, Metzger H. 3:31.

4 Berke G. 1985. How T Lymphocytes Kill Infected Cells. Microbiol. Sci. 2:44.

5 Berke G. 1980. Interaction of Cytotoxic T Lymphocytes and Target Cells. Prog. Allergy 27:69.

6 Berke G. 1983. Cytotoxic T-Lymphocytes How Do They Function? Immunological Rev. 72: 5.

7 Hiserodt JC, Britvan LJ, Targan SR. 1982. Characterization of the Cytolytic Reaction Mechanism of the Human Natural Killer (NK) Lymphocyte: Resolution into Binding, Programming, and Killer Cell-Independent Steps. J. Immunol. 129: 1782.

8 Kranz DM, Tonegawa S, Eisen HN. 1984. Attachment of an Anti-receptor Antibody to Non-target Cells Renders Them Susceptible to Lysis by a Clone of Cytotoxic T Lymphocytes. Immun. 81:7922.

9 Krensky AM, Sanchez-Madrid F, Robbins E, Nagy JA, Springer TA, Burakoff SJ. 1983. J. The Functional Significance, Distribution, and Structure of LFA-1, LFA-2, and LFA-3: Cell Surface Antigens Associated With CTL-Target Interactions. Immunol. 131: 611.

10 Rothlein R, Dustin ML, Marlin SD, Springer TA. 1986. A Human Intercellular Adhesion Molecule (ICAM-1) Distinct From LFA-1. J. Immunol. 137: 1270.

11 Shaw S, Luce GEG, Quinones R, Gress RE, Springer TA, Sanders ME. 1986. Two Antigen-Independent Adhesion Pathways Used by Human Cytotoxic T-Cell Clones. Nature. 323: 262.

12 Sung KP, Sung LA, Crimmins M, Burakoff SJ, Chien S. 1986. Determination of Junction Avidity of Cytolytic T Cell and Target Cell. Science. 234: 1405.

13 Krensky AM, Robbins E, Springer TA, Burakoff SJ. 1984. LFA-1, LFA-2, snd LFA-3 Antigens Are Involved in CTL-Target Conjugation. J. Immunol. 132: 2180.

14 Sanchez-Madred F, Krensky AM, Ware CF, Robbins E, Strominger JL, Burakoff SJ, Springer TA. 1982. Three Distinct Antigens Associated With Human T-Lymphocyte-Mediated Cytolysis: LFA-1, LFA-2, LFA-3. P.N.A.S. 79: 7489.

15 Platsoukas CD. 1984. Human T Cell Antigens Involved in Cytotoxicity Against Allogeneic or Autologous Chemically Modified Targets: Association of the Leu-2a/T8 Antigen with Effector-Target Cell Binding and of the Leu-4/T3 Antigen with Triggering. Eur. J. Immunol. 14: 566.

16 Landegren UU, Ramstedt U, Axberg I, Ullberg M, Jondal M, Wigzell H. 1982. Selective Inhibition of Human T Cell Cytoxicity at Levels of Target Recognition or Initiation of Lysis by Monoclonal OKT3 and Leu-2a Antibodies. J. Exp. Med. 155: 1579.

17 Perez P, Bluestone JA, Stephany DA, Segal DM. 1985. Quantitative Measurements of the Specificity and Kinetics of Conjugate Formation Between Cloned Cytotoxic T Lymphocytes and Splenic Target Cells by Dual Parameter Flow Cytometry. J. Immun. 134: 478.

18 Berke G. 1985. Enumeration of Lymphocyte-Target Cell Conjugates by Cytofluorometry. Eur. J. Immun. 15: 337.

19 Meuer SC, Acuto O, Hercend T, Schlossman SF, Reinherz EL. 1984. The Human T-Cell Receptor. In Annual Review of Immunology. eds, Paul WE, Fathman CG, Metzger H. Annual Reviews, Inc. Palo Alto. 2: 23.

20 Haskins K, Kappler J, Marrack P. 1984. The Major Histocompatibility Complex-Restricted Antigen Receptor on T Cells. In Annual Review of Immunology. eds, Paul WE, Fathman CG, Metzger H. Annual Reviews, Inc. Palo Alto. 2: 51.

21 MacDonald HR, Nabholz M. 1986. T-Cell Activation. In Annual Review of Cell Biology. eds, Palade GE, Alberts BM, Spudich JA. Annual Reviews, Inc. Palo Alto. 2: 231.

22 Dembic Z, von Boehmer H, Steinmetz M. 1986. The Role of T Cell Receptor Alpha and Beta Genes in MHC-Restricted Antigen Recognition. Immunol. Today. 7: 308.

23 Isakov N, Scholz W, Altman A. 1986. Signal Transduction and Intracellular Events in T-Lymphocytes. Immunol. Today. 7: 271

24 Saito T, Weiss A, Miller J, Norcross MA, Germain RN. 1987. Specific Antigen-Ia Activation of Transfected Human T Cells Expressing Murine Ti alpha, beta- Human T3 Receptor Complexes. Nature. 325: 125.

25 Gray LS, Gnarra JR, Engelhard VH. 1987. Demonstration of a Calcium Influx in Cytolytic T Lymphocytes in Response to Target Cell Binding. J. Immunol. 138:63.

26 Weissman AM, Samelson LE, Klausner RD. 1986. A New Subunit of the Human T-Cell Antigen Receptor Complex. Nature 324: 480.

27 Cantrell D, Davies AA, Londei M, Feldman M, Crumpton MJ. 1987. Association of Phosphorylation of the T3 Antigen With Immune Activation of T Lymphocytes. Nature. 325: 540.

28 Imboden JB, Weiss A, Stobo JD. 1985. Transmembrane Signalling by the T3-Antigen Receptor Complex. Immunol. Today. 6: 328.

29 Weiss A, Stobo JD. 1984. Requirements for the Coexpression of T3 and the T Cell Antigen Receptor on A Malignant T Cell Human Line. J. Exp. Med. 160: 1284.

30 Droge W. 1986. Protein Kinase C in T-Cell Regulation. Immunol. Today. 7: 340.

31 Tsien RY. 1981. A Non-disruptive Technique for Loading Calcium Buffers and Indicators into Cells. Nature. 290: 527.

32 Hesketh TR, Smith GA, Moore JP, Taylor MV, Metcalfe JC. 1983. Free Cytoplasmic Calcium Concentration and the Mitogenic Stimulation of Lymphocytes. J. Biol. Chem. 258: 4876.

33 Kikkawa U, Nishizuka Y. 1986. The Role of Protein Kinase C in Transmembrane Signalling. In Annual Review of Cell Biology. eds, Palade GE, Alberts BM, Spudich JA. Annual Reviews, Inc. Palo Alto. 2: 149.

34 Rasmussen H. 1986. The Calcium Messenger System, Part 1. N.E.J.M. 314: 1094

35 Rasmussen H. 1986. The Calcium Messenger System, Part 2. N.E.J.M. 314: 1164.

36 Havran WL, Fitch FW. 1987. Characterization of Murine Cytolytic-Helper Hybrid T Cell Clones. Nature. 325: 65.

37 Henkart PA, Yue CC, Yang J, Rosenberg SA.1986. Cytolytic and Biochemical Properties of Cytoplasmic Granules of Murine Lymphokine-Activated Killer Cells. J. Immunol. 137: 2611.

38 Young JD, Nathan CF, Podack ER, Palladino MA, Cohn ZA. 1986. Functional Channel Formation Associated with Cytotoxic T Cell Granules. P.N.A.S. 83: 150.

39 Herberman RB, Reynolds CW, Ortaldo J. 1986. Mechanisms of Cytotoxicity by Natural Killer (NK) Cells. In Annual Review of Immunology. eds. Paul WE, Fathman CG, Metzger H. Annual Reviews Inc. 4: 651.

40 Henkart PA, Yue CC, Yang J, Rosenberg SA. 1986. Cytolytic and Biochemical Properties of Cytoplasmic Granules of Murine Lymphokine-Activated Killer Cells. J. Immunol. 137: 2611.

41 Podack ER. 1985. The Molecular Mechanism of Lymphocyte Mediated Tumor Cell Lysis. Immunol. Today. 6: 21.

42 Young JD, Podack ER, Cohn ZA. 1986. Properties of a Purified Pore-forming Protein (Perforin-1) Isolated From H-2 Restricted Cytotoxic T Cell Granules. J. Exp. Med. 164: 144.

43 Young DJ, Leong LG, Liu C, Damiano A, Wall DA, Cohn ZA. 1986 Isolation and Characterization of a Serine Esterase from Cytolytic T Cell Granules. Cell. 47: 183.

44 Liu C, Perussia B, Cohn ZA, Young JD. 1986. Identification and Characterization of a Pore-Forming Protein of Human Peripheral Blood Natural Killer Cells. J. Exp. Med. 164: 2061.

45 Tschopp J, Masson D. 1985. Isolation of a Lytic Pore-Forming Protein (Perforin) from Cytolytic T Lymphocytes. J. Biol. Chem. 260: 9069.

46 Podack ER, Young JD, Cohn ZA. 1985. Isolation and Biochemical and Functional Characterization of Perforin 1 from Cytolytic T Cell Granules. P.N.A.S. 82: 8629.

47 Pasternack MS, Verret CR, Liu MA, Eisen HN. 1986. Serine Esterase in Cytolytic T Lymphocytes. Nature. 322: 740.

48 Pasternack MS, Eisen HN. 1985. A Novel Serine Esterase Expressed by Cytotoxic T Lymphocytes. Nature. 314: 743.

49 Blumenthal R, Millard PJ, Henkart MP, Reynolds CW, Henkart PA. 1984. Liposomes as Targets for Granule Cytolysin from Cytotoxic Large Granular Lymphocyte Tumors. P.N.A.S. 81: 5551.

50 Koren HS, Ferber E, Fischer H. 1971. Changes in Phospholipid Metabolism of a Tumor Target Cell During a Cell-Mediated Cytotoxic Reaction. Biochim. Biophys. Acta. 231: 520.

51 Yannelli JR, Sullivan JH, Mandell GL, Engelhard VH. 1986. Reorientation and Fusion of Cytotoxic T Lymphocyte Granules After Interaction with Target Cells as Determined by High Resolution Cinemicrography. J. Imuunol. 136: 377.

52 Bykovskaja SN, Rytenko AN, Rauschenbach MO, Bykovsky AF. 1978. Ultrastructural Alteration of Cytolytic T Lymphocytes Following Their Interaction With Target Cells. II. Morphogenesis of Secretory Granules and Intracellular Vacuoles. Cell Immunol. 40: 175.

53 Bykovskaja SN, Rytenko AN, Rauschenbach MO, Mykovsky AF. 1978. Ultrastructural Alteration of Cytolytic T Lymphocytes Following Their Interaction With Target Cells. I. Hypertrophy and Change of Orientation of the Golgi Apparatus. Cell Immunol. 40: 164.

54 Geiger B, Rosen D, Berke R. 1982. Spatial Relationships of Microtubule-Organizing Centers and the Contact Area of Cytotoxic T Lymphocytes and Target Cells. J. Cell Biol. 95: 137.

55 Ryser JE, Rungger-Brandle E, Chaponnier C, Gabbiani G, Vassalli P. 1982. The Area of Attachment of Cytolytic T Lymphocytes to Their Target Cells Shows High Motility and Polarization of Actin but not Myosin. J. Immunol. 128: 1159.

56 Zagury D. 1982. Direct Analysis of Individual Killer T Cells: Susceptibility of Target Cells to Lysis and Secretion of Hydrolytic Enzymes by CTL. Adv. Exp. Med. Biol. 146: 149.

57 Brondz BD, Snegirova AE, Rassulin YA, Shamborant OG. 1973. Modification of In Vitro Immune Lymphocyte-Target Cell Interaction by Some Biologically Active Drugs. Immunochem. 10: 175.

58 Creutz CE. 1984. The Roles of Ca++ in the Regulation and Mechanism of Exocytosis. In Metal Ions in Biological Systems. Calcium and Its Role in Biology. ed, Sigel H. Marcel Dekker, Inc. New York. 17: 319.

59 Young JD, Leong LG, Liu C, Damiano A, Cohn ZA. 1986. Extracellular Release of Lymphocyte Cytolytic Pore-Forming Protein (Perforin) After Ionophore Stimulation. P.N.A.S. 83: 5668.

60 Cantor CR, Schimmel PR. 1980. Biophysical Chemistry, Part II: Techniques for the Study of Biological Structure and Function. W.H. Freeman and Co. San Francisco. p433-451.

61 Berke G, Clark WR. 1982. T Lymphocyte-Mediated Cytolysis - A Comprehensive Theory I. The Mechanism of CTL-Mediated Cytolysis. In Mechanisms of Cell Mediated Cytotoxicity. Eds. Clark, Goldstein. Plenum Publishing Corp. p57.

62 Berke G. 1987. An Appraisal of Some Current Thoughts on Cytolytic T Lymphocyte Killing Mechanisms. Annals de l'Institute Pasteur/Immunology. In Press.

63 Deem RL, Niederlehner A, Targan SR. 1986. Active Target Cell Processes, Possibly Involving Receptor-Mediated Endocytosis, Are Critical for Expression of Cytotoxicity by Natural Killer Cell-Derived Cytolytic Factor. Cell. Immuno. 102: 187.

64 Ortaldo JR, Ransom JR, Sayers TJ, Herberman RB. 1986. Analysis of Cytostatic/Cytotoxic Lymphokines: Relationship of Natural Killer Cytotoxic Factor to Recombinant Lymphotoxin, Recombinant Tumor Necrosis Factor, and Leukoregulin. J.Immunol. 137: 2857.

65 Schmid DS, Ruddle NH. 1986. Production and Function of Lymphotoxin Secreted by Cytolytic T Cells. In Handbook, Chemical Rubber Co. (CRC), Cleveland. In Press.

66 Green LM, Reade JL, Ware CF, Devlin PE, Liang C, Devlin JJ. 1986. Cytotoxic Lymphokines Produced by Cloned Human Cytotoxic T Lymphocytes II. A Novel CTL-Produced Cytotoxin That Is Antigenically Distinct from Tumor Necrosis Factor and Alpha-Lymphotoxin. J. Immunol. 137: 3488.

67 Verret R, Firmenich A, Kranz D, Eisen HE. On the Resistance of Cytotoxic T Lymphocytes to Cytolytic Effects of Their Toxic Granules. In Preparation.

68 Kranz D, Eisen HE. 1987. Resistance of Cytotoxic Lymphocytes to Lysis by a Clone of Cytotoxic Lymphocytes. P.N.A.S. In Press.

69 Simone CB, Henkart P. 1980. Permeability Changes Induced in Erythrocyte Ghost Targets by Antibody-Dependent Cytotoxic Effector Cells Cytotoxic Effector Cells: Evidence for Membrane Pores. J. Immunol. 124: 954.

70 Zalman LS, Brothers MA, Chiu FJ, Muller-Eberhard HJ. 1986. Mechanism of Cytotoxicity of Human Large Granular Lymphocytes: Relationship of the Cytotoxic Lymphocyte Protein to the Ninth Component (C9) of Human Complement. P.N.A.S. 83: 5262.

71 Zalman LS, Brothers MA, Chiu FJ, Muller-Eberhard HJ. 1986. Mechanism of Cytotoxicity of Human Large Granular Lymphocytes: Relationship of the Cytotxic Lymphocyte Protein to the Ninth Component (C9) of Human Complement. P.N.A.S. 83: 5262.

72 Tschopp J, Masson D, Stanley KK. 1986. Structural/Functional Similarity Between Proteins Involved in Complement- and Cytotoxic T-Lymphocyte-Mediated Cytolysis. Nature. 322: 831.

73 Mayer M. 1982. Membrane Attack by Complement (With Comments on Cell- Mediated Cytotoxicity). In Mechanisms of Cell Mediated Cytotoxicity. Clark, Golstein eds. Plenum Publishing Corp. 193.

74 Muller-Eberhard HJ. 1986. The Membrane Attack Complex of Complement. In Annual Review of Immunology. eds. Paul WE, Fathman CG, Metzger H. Annual Reviews Inc. 4: 503.

75 Bashford CL, Alder GM, Menestrina G, Micklem KJ, Murphy JJ, Pasternak CA. 1986. Membrane Damage by Hemolytic Viruses, Toxins, Complement, and Other Cytotoxic Agents. J. Biol. Chem. 261: 9300.

76 Henney CS. 1974. Estimation of the Size of a T Cell-Induced Lytic Lesion. Nature. 249: 456.

77 Ferluga J, Allison AC. 1974. Observations on the Mechanism by Which T Lymphocytes Exert Cytotoxic Effects. Nature. 250: 673.

78 Kurt EA, Lindquist RR. 1981. Failure of Dextran to Osmotically Protect CTL-"Hit" Target Cells. Transplant. Proc. 8: 1178.

79 Sanderson CJ. 1976. The Mechanism of T Cell Mediated Cytotoxicity II. Morpholgic Studies of Cell Death by Time-Lapse Microcinematography. Proc. R. Soc. Lond. 192: 241.

80 Duvall E, Wyllie AH. 1986. Death and the Cell. Immunol. Today. 7: 115.

81 Tirosh R, Berke G. 1985. T-Lymphocyte-Mediated Cytolysis as an Excitatory Process of the Target. I. Evidence That the Target Cell May Be the Site of Ca^{++} Action. Cell. Immuno. 95: 113.

82 Tirosh R, Berke G. 1985. Immune Cytolysis Viewed as a Stimulatory Process of the Target. In Mechanisms of Cell Mediated Cytotoxicity II. eds. Henkart P, Martz E. Plenum Press. p473.

83 Russell JH, Masakowski VR, Dobos CB. 1980. Mechanisms of Immune Lysis I. Physiological Distinction Between Target Cell Death Mediated by Cytotoxic T Lymphocytes and Antibody Plus Complement. J. Immunol. 124: 1100.

84 Farber JL, Chien KR, Mittnacht S. 1981. The Pathogenesis of Irreversible Cell Injury in Ischemia. Amer. J. Pathol. 102: 271.

85 Trump BF, Berezesky IK, Osornio-Vargas AR. 1981. Cell Death and the Disease Process. The Role of Calcium. In Cell Death in Biology and Pathology. eds. Bowen ID, Lockshin RA. Chapman and Hall. p209.

86 Duvall E, Wyllie AH. 1986. Death and the Cell. Immunol. Today. 7: 115.

87 Cohen JJ, Duke RC. 1984. Glucocorticoid Activation of a Calcium-dependent Endonuclease in Thymocyte Nuclei Leads to Cell Death. J. Immunol. 132: 38.

88 Deleted in Proof.

89 Gromkowski SH, Brown TC, Cerutti PA, Cerottini J. 1986. DNA of Human Raji Target Cells Is Damaged Upon Lymphocyte Mediated Lysis. J. Immunol. 136: 752.

90 Duke RC, Cohen JJ. 1986. IL-2 Addiction: Withdrawal of Growth Factor Activates a Suicide Program in Dependent T Cells. Lymphokine Res. 5: 289.

91 Russell JH, Masakowski V, Rucinsky T, Phillips G. 1982. Mechanisms of Immune Lysis III. Characterization of the Nature and Kinetics of the Cytotoxic T Lymphocyte-Induced Nuclear lesion in the Target. J. Immunol. 128: 2087.

92 Duke RC, Chervenak R, Cohen JJ. 1983. Endogenous Endonuclease-Induced DNA Fragmentation: An Early Event in Cell-Mediated Cytolysis. Immunol. 80: 6361.

93 Cohen JC, Duke RC. 1985. DNA Fragmentation in Targets of CTL: An Example of Programmed Cell Death in the Immune System. In Mechanisms of Cell-Mediated Cytotoxicity II. eds. Henkart P, Martz E. Plenum Press. p493.

95 Cox JA, Comte M, Malnoe A, Burger A, Stein EA. 1984. Mode of Action of the Regulatory Protein Calmodulin. In Metal Ions in Biological Systems. Calcium and Its Role in Biology. ed, Sigel H. Marcel Dekker, Inc. New York. 17: 215.

96 Carafoli E, Inesi G, Rosen BP. 1984. Calcium Transport Across Biological Membranes. In Metal Ions in Biological Systems. Calcium and Its Role in Biology. ed, Sigel H. Marcel Dekker, Inc. New York. 17: 129.

97 Fiskum G. 1984. Physiological Aspects of Mitochondrial Calcium Transport. In Metal Ions In Biological Systems. Calcium and Its Role in Biology. ed. Sigel H. Marcel Dekker, Inc. New York 17: 1.

98 Schanne FAX, Kane AB, Young EE, Farber JL. 1979. Calcium Dependence of Toxic Cell Death: A Final Common Pathway. Science. 206: 700.

99 Farber JL. 1982. Membrane Injury and Calcium Homeostasis in the Pathogenesis of Coagulative Necrosis. Lab. Invest. 47: 114.

100 Campbell AK, Luzio JP. 1981. Intracellular Free Calcium as a Pathogen in Cell Damage Initiated by the Immune System. Experientia. 37: 1110.

101 Martz E, Parker WL, Gately MK, Tsoukas CD. 1982. The Role of Calcium in the Lethal Hit of T Lymphocyte-Mediated Cytolysis. In Mechanisms of Cell-Mediated Cytotoxicity. eds. Clark WR. Plenum Press. p121.

102 Snowdowne KW, Freudenrich CC, Borle AB. 1985. The Effects of Anoxia on Cytosolic Free Calcium, Calcium Fluxes, and Cellular ATP Levels in Cultured Kidney Cells. J. Biol. Chem. 260: 11619

103 Thor H, Hartzell P, Orrenius S. 1984. Potentiation of Oxidative Cell Injury in Hepatocytes Which Have Accumulated Ca^{++}. J. Biol. Chem. 259: 6612.

104 Kaiser N, Edelman IS. 1977. Calcium Dependence of Glucocorticoid-induced Lymphocytolysis. Cell Biol. 74: 638.

105 Kaiser N, Edelman IS. 1978. Calcium Dependence of Ionophore A23187-induced Lymphocyte Cytotoxicity. Cancer Res. 38: 3599.

106 Kranz DM, Sherman DH, Sitkovsky MV, Pasternak MS, Eisen HN. 1984. Immunoprecipitation of Cell Surface Structures of Cloned Cytotoxic T Lymphocytes by Clone-Specific Antisera. P.N.A.S. 81: 573.

107 Grabstein K, Chen YU. 1980. Cell Mediated Cytolytic Responses. In Selected Methods in Cellular Immunology. eds. Mishell BB, Shiigi SM. W.H. Freeman and Co. San Francisco. p124.

108 Oi VT, Glazer AN, Stryer L. 1982. Fluorescent Phycobiliprotein Conjugates for Analyses of Cells and Molecules. J. Cell Biol. 93: 981.

109 Maniatis T, Fritsch EF, Sambrook J. 1982. Molecular Cloning, A Laboratory Manual. Cold Spring Harbor Laboratories. Cold Spring Harbor.

110 Rink TJ, Pozzan T. 1985. Using Quin 2 in Cell Suspensions. Cell Calcium. 6: 133.

111 Martell, Smith. 1974. Critical Stability Constants. Plenum Press. 1: 269.

112 Moisescu DG, Pusch H. 1975. A pH-Metric Method for the Determination of the Relative Concentration of Calcium to EGTA. Pflugers Arch. 355: R122.

113 Grynkiewicz G, Poenie M, Tsien R. 1985. A New Generation of Ca^{++} Indicators with Greatly Improved Flourescence Properties. J. Biol. Chem. 260: 3440.

114 Rabinovitch PS, June CH, Grossman A, Ledbetter JA. 1986. Heterogeneity Among T Cells in Intracellular Free Calcium Responses After Mitogenic Stimulation With PHA or Anti-CD3. Simultaneous Use of Indo-1 and Immunofluorescence With Flow Cytometry. J. Immunol. 137: 952.

115 Wier WG, Cannell MB, Berlin JR, Marban E, Lederer WJ. 1987. Cellular and Subcellular Heterogeneity of Ca^{++} in Single Heart Cells Revealed by Fura-2. Science. 235: 325.

116 Tsien RY, Pozzan T, Rink TJ. 1982. Calcium Homeostasis in Intact Lymophocytes: Cytoplasmic Free Calcium Monitored With A New, Intracelluarly Trapped Fluorescent Indicator. J. Cell Biol. 94: 325.

117 Lazzari KG, Proto PJ, Simons ER. 1986. Measurement of Stimulus-induced Changes in Cytoplasmic Ca++ and in Membrane Potential of Human Neutrophils. J. Biol. Chem. 261:9710.

118 Ashley CC, Moisescu DG. 1977. Effect of Changing the Composition of the Bathing Solutions Upon the Isometric Tension-pCa Relationship in Bundles of Crustacean Myofibrils. J. Physiol. 270: 627.

119 Moisescu DG, Thieleczek R. 1978. Calcium and Strontium Concentration Changes Within Skinned Muscle Preparations Following A Change in the External Bathing Solution. J. Physiol. 275: 241.

120 Luckhoff A. 1986. Cytosolic Free Calcium Concentration in Endothelial Cells With Indo-1: The Pitfall of Using the Ratio of Two Fluorescence Intensities Recorded at Different Wavelengths. Cell Calcium. 7: 233.

121 Carney DF, Hammer CH, Shin ML. 1986. Elimination of Terminal Complement Complexes in the Plasma Membrane of Nucleated Cells: Influence of Extracellular Ca^{++} and Association with Cellular Ca^{++}. J. Immunol. 137: 263.

122 Shapiro HS. 1986. Practical Flow Cytometry. Alan R. Liss, Inc. New York.

123 Dean PN. 1985. Methods of Data Analysis in Flow Cytometry. In Flow Cytometry: Instrumentation and Data Analysis. eds. Dilla MA, Dean PN, Laerum OD, Melamed MR. Academic Press, New York. p195.

124 Alabaster O, Bentley SA, Herman CJ. 1979. Quantitative Cytology: New Dimensions in Automation and Diagnosis. Path. Annual. 14 pt2: 1.

125 Herzenberg LA, Sweet RG, Herzenberg LA. 1976. Fluorescence-Activated Cell Sorting. Sci. Am. 234: 108.

126 Aubin JE. 1979. Autofluorescence of Viable Cultured Mammalian Cells. J. Histochem. Cytochem. 27: 36.

127 Benson RC, Meyer RA, Zaruba ME, McKhann GM. 1979. Cellular Autofluorescence - Is It Due to Flavins? J. Histochem. Cytochem. 27: 44.

128 Thorell B. 1981. Flow Cytometric Analysis of Cellular Endogenous Fluorescence Simultaneously with Emission from Exogenous Fluorochromes, Light Scatter and Absorption. Cytometry. 2: 39.

129 Good AH, Wofsky L, Kimura J, Henry C. Purification of Immunoglobulins and Their Fragments. In Selected Methods in Cellular Immunology. eds. Mishell BB, Shiigi SM. W.H. Freeman and Co. San Francisco.

130 Valet G, Raffael A, Russman L. 1985. Naturwissenschaften. Determination of Intracellular Calcium in Vital Cells by Flow Cytometry. 72: 600.

131 O'Flynn K, Zanders ED, Lamb JR, Beverley PCL, Wallace DL, Tatham PER, Tax WJM, Linch DC. 1985. Investigation of Early T Cell Activation: Analysis of the Effect of Specific Antigen, Interleukin 2 and Monoclonal Antibodies on Intracellular Free Calcium Concentration. Eur. J. Immunol. 15: 7.

132 Young JD, Liu C, Leong LG, Cohn ZA. 1986. The Pore-Forming Protein (Perforin) of Cytolytic T Lymphocytes Is Immunologically Related to the Components of Membrane Attack Complex of Complement Through Cysteine-Rich Domains. J. Exp. Med. 164: 2077.

133 Young JD, Cohn ZA. 1986. Cell Mediated Killing: A Common Mechanism. Cell. 46: 642.

134 Pressman BC. 1976. Biological Applications of Ionophores. In Annual Review of Biochemistry. eds Snell EE, Boyer PD, Meister A, Richardson CC. Annual Reviews, Inc. Palo Alto. 45: 501.

135 Kaiser N, Edelman IS. 1978. Further Studies on the Role Calcium in Glucorticoid-induced Lymphocytolysis. Endocr. 103: 936

136 Liu C, Hermann TE. 1978. Characterization of Ionomycin as a Calcium Ionophore. J. Biol. Chem. 253: 5892.

137 Nakashima RA, Dordick RS, Garlid KD. 1982. On the Relative Roles of Ca^{++} and Mg^{++} in Regulating the Endogenous K^{+}/H^{+} Exchanger of Rat Liver Mitochondria. J. Biol. Chem. 257: 12540.

138 Rosenthal KS, Shapiro HM. 1983. Cell Membrane Potential Changes Follow Epstein-Barr Virus Binding. J. Cell Physiol. 117: 39.

139 Bramhall JS, Morgan JI, Perris AD, Britten AZ. 1976. The Use of a Fluorescent Probe to Monitor Alterations in Trans-Membrane Potential in Single Cell Suspensions. Biochem. Biophys. Res. Commun. 72: 654.

140 Sears DW, Christiansen JW. 1985. Mechanism of Rapid Tumor Lysis by Human ADCC: Mediation by Monoclonal Antibodys and Fragmentation of Target Cell DNA. In Mechanisms of Cell- Mediated Cytotoxicity II. eds. Henkart P, Martz E. Plenum Press. p509.

141 Nakamura M, Sakaki Y, Watanabe N, Takagi Y. 1981. Purification and Characterization of the Ca^{++} Plus Mg^{++} Dependent Endodeoxyribonuclease from Calf Thymus Chromatin. 89: 143.

143 Davidson GA, Berman MC. 1985. Interaction of Valinomycin and Monovalent Cations With the (Ca++, Mg++)-ATPase of Skeletal Muscle Sarcoplasmic Reticulum. J. Biol. Chem. 260: 7325.

144 Negendank W, Shaller C. 1982. Effects of Valinomycin on Lymphocytes Independent of Potassium Permeability. Bioch. Biophys. Acta. 688: 316.

145 Dise CA, Goodman DBP. 1985. The Relationship Between Valinomycin-Induced Alterations in Membrane Phospholipid Fatty Acid Turnover, Membrane Potential, and Cell Volume in the Human Erythrocyte. J. Biol. Chem. 260: 2869.

146 Hladky SB, Rink TJ. 1976. Potential Difference and the Distribution of Ions Across the Human Red Blood Cell Membrane: A Study of the Mechanism by Which the Fluorescent Cation, dis-C_3-(5) Reports Membrane Potential. J. Physiol. 263: 287.

147 Jennings ML. 1978. Characteristics of CO_2-Independent pH Equilibration in Human Red Blood Cell. J. Membr. Biol. 40: 365.

148 Zalman LS, Wood LM, Muller-Eberhard HJ. 1986. Isolation of a Human Erythrocyte Membrane Protein Capable of Inhibiting Expression of Homologous Complement Transmembrane Channels. P.N.A.S. 83: 6975.

149 Tschopp J, Masson D, Schafer S. 1986. Inhibition of the Lytic Activity of Perforin by Lipoproteins. J. Immunol. 137: 1950.

150 Kupfer A, Singer SJ, Dennert G. 1986. On the Mechanism of Unidirectional Killing in Mixtures of Two Cytotoxic T Lymphocytes. J. Exp. Med. 163: 489.

151 Stephenson DG, Williams DA. 1981. Calcium-Activated Force Resonses in Fast- and Slow-twitch Skinned Muscle Fibres of the Rat at Different Temperatures. J. Physiol. 317: 281.

152 Horan PK, Wheeless LL. 1977. Quantitative Single Cell Analysis and Sorting. Sci. 198: 149

153 Nisbet-Brown E, Cheung RK, Lee JWW, Gelfand EW. 1985. Antigen-Dependent Increase in Cytosolic Free Calcium in Specific Human T-Lymphocyte Clones. Nature. 316: 545.

154 Tsien RY, Pozzan T, Rink TJ. 1984. Measuring and Manipulating Cytosolic Ca++ With Trapped Indicators. T.I.B.S. June, 263.

155 Scarpa A. 1985. Measurements of Intracellular Calcium. Cell Calcium. 6: 1.

156 Tsien RY, Rink TJ, Poenie M. 1985. Measurement of Cytosolic Free Ca++ in Individual Small Cells Using Fluorescence Microscopy With Dual Excitation Wavelengths. Cell Calcium. 6: 145.

157 Pozzan T, Rink TJ, Tsien RY. 1981. Intracellular Calcium in Intact Lymphocytes. Proc. Physiol. Soc. April, 12P.

158 Dilla MA, Dean PN, Laerum OD, Melamed MR. 1986. Flow Cytometry: Instrumentation and Data Analysis. Academic Press, New York. p195.

159 Martin RB. 1984. Bioinorganic Chemistry of Calcium. In Metal Ions in Biological Systems. Calcium and Its Role in Biology. ed. Sigel H. Marcel Dekker, Inc. New York 17: 1.

160 Freedman JC, Novak TS. 1983. Membrane Potentials Associated With Ca-Induced K Conductance in Human Red Blood Cells: Studies With A Fluorescent Oxonal Dye, WW 781. J. Membr. Biol. 72: 59.

161 Vestergaard-Bogind B, Bennekou P. 1982. Calcium-Induced Oscillations in K+ Conductance and Membrane Potential of Human Erythrocytes Mediated By the Ionophore A23187. Biochim. Biophys. Acta. 688: 37.

162 Alcover A, Weiss MJ, Daley JF, Reinherz EL. 1986. The T11 Glycoprotein Is Functionally Linked to a Calcium Channel in Precursor and Mature T-lineage Cells. P.N.A.S. 83: 2614.

163 Hood LE, Weissman IL, Wood WB,Wilson JH. 1984. Immunology. Benjamin Cummings Publishing Co., Inc. Reading, MA.

164 Kimball JW. 1986. Introduction to Immunology. Macmillan Publishing Co. New York. 2nd edition.

165 Anderson OS. 1984. Gramicidin Channels. Annual Review of Physiology. Annual Reviews, Inc. Palo Alto. 46: 531.

166 Rink TJ, Montecucco C, Hesketh TR, Tsien RY. 1980. Lymphocyte Membrane Potential Assessed With Fluorescent Probes. Bioch. Bioph. Acta. 595: 15.